EVAPORATION FROM THE ORANGE RIVER:

Quantifying open water resources

CS Everson

WRC Report No 683/1/99

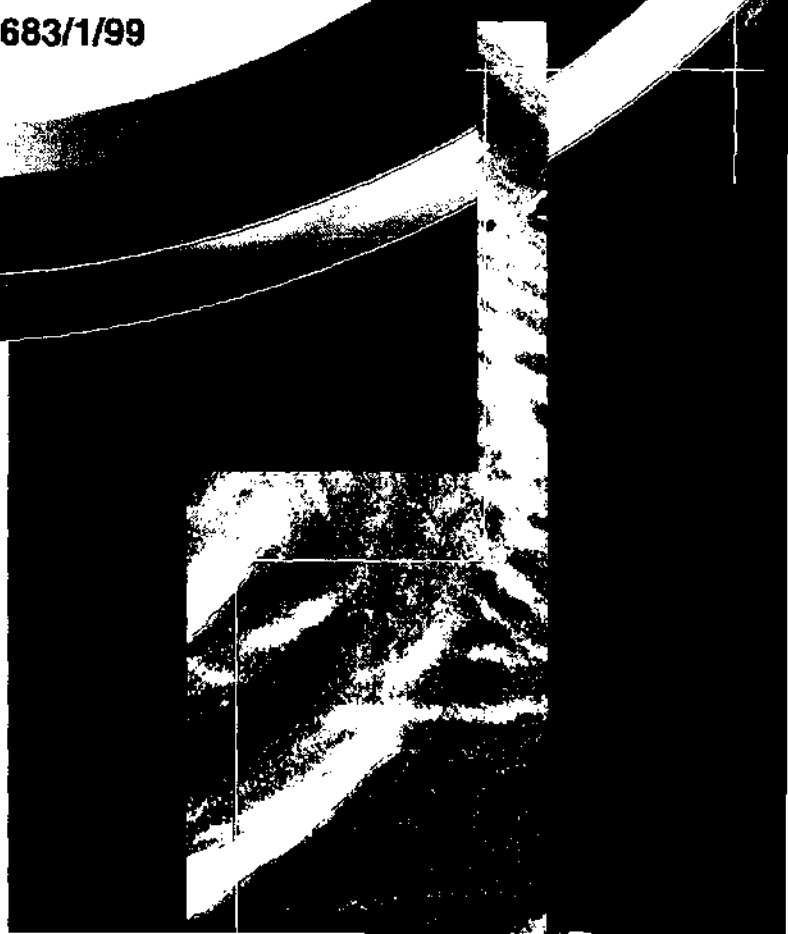

Water Research Commission

EVAPORATION FROM THE ORANGE RIVER: QUANTIFYING OPEN WATER RESOURCES

by

C.S. Everson
Environmentek, CSIR, Pietermaritzburg

Report to Water Research Commission

on the project

Evaporation from the Orange River: Quantifying open water resources

WRC Report No. 683/1/99
ISBN No. 1 86845 520 3

DEDICATION

This report is dedicated to Kraai Luus who passed away shortly after the completion of the field studies. Without the dedication and enthusiasm shown by Kraai, this project would not have been possible.

CONTENTS

Executive summary 5

Recommendations for future research 7

1. Introduction 9

1.1 Project objectives 10

2. Study area 11

2.1 The Orange River 11

2.1.1 *General* 11

2.1.2 *The Bowen ratio study site* 11

2.2 The land based weather stations 13

3. Methods 15

3.1 Bowen ratio energy balance technique 15

3.1.1 *Background and theory* 15

3.1.2 *Bowen ratio instrumentation* 16

3.2 Other estimation methods or models of evaporation 19

3.2.1 *A-pan estimates* 19

3.2.2 *Penman evaporation and other derived equations* 20

3.2.3 *The modelling of net radiation* 21

4. Results 24

4.1 General 24

4.2 Ambient air and surface water temperature 25

4.3 Energy budget 27

4.3.1 *Bowen ratio versus evaporation pan measurements* 30

4.3.1.1 August - September 1993 30

4.3.1.2 June to October 1994 36

4.3.2 *A comparison of the Bowen ratio with other measures of*

evaporation. 40

4.3.2.1 Radiation Modelling 40

4.3.3. *Bowen ratio, Penman, equilibrium and Priestley Taylor estimates of evaporation-(data from above the river)* 42

4.3.4 *Land based measurements* 44

4.3.4.1 Solar radiation 44

4.3.4.2 Temperature 47

4.3.4.3 Relative humidity 47

4.3.5 *Evaporation along the Orange River* 51

4.3.5.1 Rainfall 51

4.3.5.2 Solar radiation 51

4.3.5.3 Wind 56

4.3.5.4 Temperature 56

4.3.5.5 Relative humidity 56

4.3.5.6 Evaporation 56

5. **Conclusions** 63

5.1 **Acknowledgments** 64

5.2 **References** 65

Appendix 1 67

Appendix 2 68

Appendix 3 71

EVAPORATION FROM THE ORANGE RIVER: QUANTIFYING OPEN WATER RESOURCES

Executive Summary

The Orange River basin is one of the largest in southern Africa (1 million km^2) supporting agricultural, industrial and municipal demands, as well as hydro-electric power generation. There is growing concern that the Orange River will not be able to meet these demands when the Lesotho Highland Water Scheme becomes operational. The Orange River Losses study was therefore commissioned by the Department of Water Affairs and Forestry in 1988 and undertaken by BKS Inc. to assess the water resources of the Orange River system. The initial results of the BKS study estimated a 842 million m^3 $annum^{-1}$ deficit after implementation of the Lesotho Highland Water Scheme. These results were based on indirect estimates of water losses using pan evaporation data. However, the use of pan data to represent evaporation from a moving water surface may be seriously in error. The accuracy of these data need to be established if confident decisions on water resource allocation are to be made.

This study forms a component of the Orange River Losses study : Phase II (funded by the Water Research Commission) and aims to determine evaporation losses from the Orange River using the energy balance Bowen Ratio technique. A pilot study, initiated in 1993, indicated that this technique provided accurate and reliable estimates of evaporation from the flowing water surface.

Comparison between evaporation data collected from the Bowen ratio above the Orange River

and A-pan evaporation indicated that pan data were approximately 8% lower than the energy balance technique. Regression analysis between the A-pan and Bowen ratio showed that the A-pan can be used to predict transmission losses from the Orange River. However, the large scatter found in pan data, associated with the inherent problems that arise from poor installation and maintenance, make pan data potentially unreliable. If pan data are used they should be obtained from organisations which maintain high standards of meteorological observation.

Evaporation from the Orange River was modelled using the energy balance approach (Priestley Taylor and Penman formulations) from standard weather data measured along the extent of the river. The measurements used were dry bulb temperature, relative humidity (2 m height), wind speed and solar radiation. Comparison of the Priestley Taylor equation with direct measurements using the Bowen ratio energy balance approach showed small errors (approximately 3% or 0.2 mm day^{-1}). The Priestley Taylor model can therefore be used to estimate evaporation from the Orange River where advective conditions are extreme.

The Penman equation underestimated the river evaporation by about 9% (0.6 mm day^{-1}), while the equilibrium evaporation rate underestimated the Bowen ratio seasonal total by 23%. These differences therefore need to be accounted for when estimating river losses in arid environments.

Algorithms developed for adjusting the land based weather data to approximate the river conditions had little effect on the overall evaporation loss. Therefore adjusting the land based weather data to river conditions is not necessary. It was shown that the net radiation can be modeled very accurately from standard weather station data, an essential requirement when using the energy balance approach. Simple linear models are also proposed for predicting the surface albedo and net radiation.

There is a climatic gradient down the Orange River which resulted in a increase in the evaporation by 380 mm over 1 000 km (or 0.3 mm km^{-1}). The high annual evaporation measured from the Orange River (2500-2700 mm) in this study confirms that transmission losses are a major component of the water balance. These evaporation data translate into river losses that vary between 516 and 841 million m^3 $annum^{-1}$ for the low (60 m^3 s^{-1}) and high (400 m^3 s^{-1}) flows respectively. These findings are in agreement with A-pan based estimates of river losses determined by McKenzie and Craig (1997, in press).

Extent to which contract objectives have been met

The primary objectives of this project were to determine evaporation rates from the Orange River using the Bowen ratio technique and to relate meteorological variables measured on land (radiation, temperature, vapour pressure deficit, wind speed) to actual evaporation from the river. The evaporation monitoring using the Bowen ratio technique was successfully accomplished for a continuous period between June and December 1995. Although the intention was to continue until March 1996, the January 1996 floods necessitated the emergency removal of all the equipment from the river. At this point it was felt that sufficient data had been obtained to achieve the objectives of the project and monitoring was discontinued. The Bowen ratio evaporation data collected for the six month period from June to December 1995 were of a high quality and made the comparisons with land based weather stations easy to achieve.

Recommendations for future research

The study showed that the energy budget approach can be used to successfully predict the river evaporation from standard weather stations. A more elegant approach to the problem of predicting evaporation in real time is through a knowledge of the surface water temperature. This would allow for a Bowen ratio approach to the energy balance: the surface temperature being the lower part of the gradient (and the water vapor pressure being a saturated value

corresponding to the surface temperature). The air temperature and water vapor pressure at the upper level could be defined from the automatic weather stations or alternatively by a point measurement of temperature and humidity above the water surface. The following new research topics are recommended for future research:

- If a number of flow gauging stations are linked to telemetry along the Orange River, then it would be possible to design a system for monitoring the gradients in temperature and humidity above the water surface. These measurements, combined with solar radiation would allow real time estimates of evaporation at key points along the river.

- The use of infra-red thermal remote sensing to monitor surface water temperatures would provide a technique for measuring evaporation that could be used for all large water bodies in southern Africa.

- In the present study it was only possible to examine three stations over a two year period. A complete analysis of the historical weather data for evaporation modelling would provide useful insights into the variability of the annual evaporation total.

- Data gathered by McKenzie and Craig (1997, in press) show that the area of reeds and trees along the Orange River course can represent over 50 % of the total evaporating surface during low flow periods. Errors in the estimation of evaporation from these communities could lead to gross errors in predicting transmission losses. A knowledge of the evaporation processes in wetland communities would clearly be of great benefit to water resource managers and modellers.

CHAPTER 1

Introduction

The Orange River basin is one of the largest in southern Africa with a total catchment area of approximately 1 million km^2 (McKenzie, Roth & Stoffberg 1993). The water of the Orange River is utilized for agricultural, industrial and municipal demands, as well as hydroelectric power generation at two dams (Gariep and Van der Kloof). Until recently there has been sufficient water in the Orange River to meet these demands. However, there is growing concern that the Orange River will not be able to meet these demands when the Lesotho Highlands Water Project is fully operational. One of the unknown factors in the water budget is the amount of water lost directly by evaporation (transmission losses). An estimation of evaporation from the Orange River is therefore necessary for water management, particularly during low flow periods. An evaluation of river losses from the Orange River down stream of the Vanderkloof dam has been prepared by BKS (Mckenzie & Roth, 1994). In this study evaporation from the Orange River has been estimated indirectly using Symon's pan evaporation data. These data, multiplied by the appropriate pan factors, estimate that losses are very high (800 million cubic meters per annum). The use of pan data to represent evaporation from the Orange River may, however, be seriously in error. The accuracy of these data therefore need to be established if confident decisions on water resource allocation are to be made.

Routine estimates of open water evaporation are typically estimated using simple energy budget methods, such as the Penman equation. These methods generally give good results if suitable meteorological data are available for use in the calculations. One possibility is to use land-based weather stations. However, if conditions at the land surface are different to those above the water then large errors will occur. Because of these uncertainties, it is desirable to make direct measurement of evaporation over the water to enable the development and testing of suitable calculation methods.

Energy balance studies have been successful for estimating evaporation from water bodies

(Fricke 1972, Ryan, Harleman & Stolzenbach 1974). Accuracies to within 5%, have been obtained for periods of a week or more (Anderson, 1972). However, the technique was less accurate for shorter periods and was unacceptable for periods of a day or less. More recently, Stewart and Rouse (1976) successfully used this method to estimate evaporation for 30-minute periods at a shallow lake. With recent improvements in micrometeorological instrumentation, good estimates of evaporation should be attainable using the energy balance approach.

The techniques most frequently used in energy balance studies are the eddy correlation and Bowen ratio techniques. Although the eddy correlation technique may be more accurate, it cannot be easily left unattended at remote sites. The Bowen ratio energy technique, which can be used to monitor evaporation for extended periods is therefore the preferred choice.

This study examined the use of the Bowen ratio energy balance technique of measuring evaporation from the Orange River. Direct measurements were made using the Bowen ratio energy balance technique. The data are used to verify indirect methods of estimating evaporation from the river using historical data from nearby weather stations.

1.1 Project objectives

(i) To determine evaporation rates from the Orange River with Bowen ratio equipment.

(ii) To relate meteorological variables measured on land (radiation, temperature, vapour pressure deficit, wind speed) to evaporation from the Orange River.

(iii) To recommend the most cost-effective technique for estimation of evaporation from reservoirs and rivers.

CHAPTER 2

Study area

2.1. The Orange River

2.1.1. *General*

The Orange River rises in the mountains of Lesotho and flows into South Africa (Figure 2.1). It is the longest river in South Africa, winding west and northwest for about 2,100 kilometers. The river then flows across the plateaux of central South Africa to the town of Prieska. From Prieska to the Augrabies Falls, the elevation of the river drops steadily. The lower course of the river stretches from the Augrabies Falls to the western coast, flowing through rugged desert country eventually emptying into the South Atlantic Ocean at Alexander Bay. The river has two major branches, the Vaal and Caledon rivers.

In 1962, the South African government announced a development plan for the Orange River. Since then, the government has built dams on the river to provide hydroelectric power. It has also built canals and tunnels to irrigate nearby land and to provide flood control.

2.1.2 *The Bowen Ratio study site*

The study site was located at an altitude of 793 m at Gifkloof (28°27'S, 21°15'E), approximately 10 km upstream from Upington. The Bowen ratio apparatus was sited on a small rock outcrop in the centre of the river (Plate 2.1). During winter when the river was at its lowest, the area of exposed rock was approximately 5m long by 2m wide, providing an excellent platform from which to conduct the evaporation measurements. The water was > 2.5 m deep around the rock. The shortest distance from the site to each river bank was approximately 110 m. Access to the study site was only by boat.

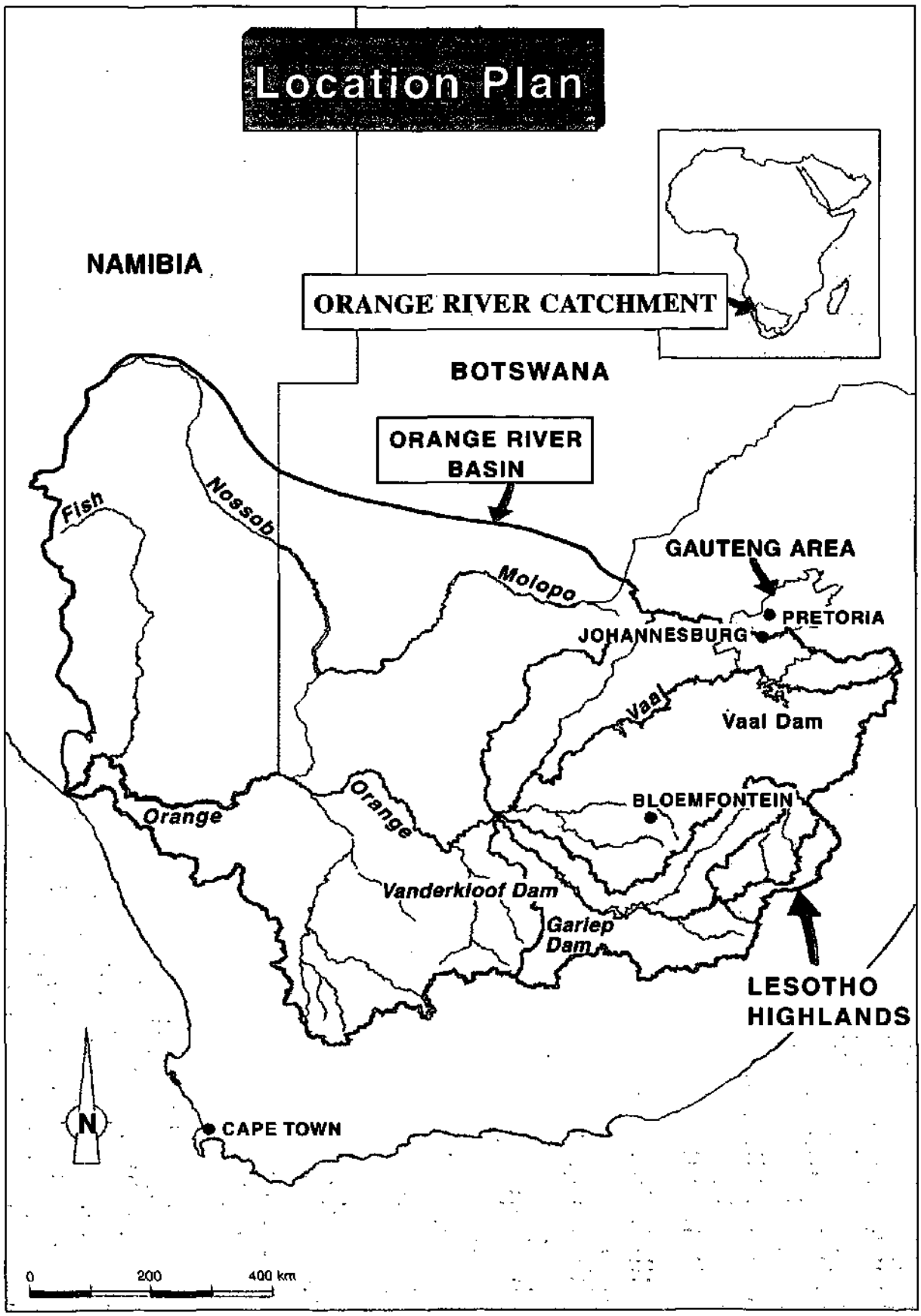

Figure 2.1. General map of the Orange River basin. (The master copy of this graph was kindly supplied by BKS Inc. and is reproduced with their permission).

2.2. The land based weather stations

An investigation by BKS in 1966 revealed a number of weather stations suitable for land based assessments of evaporation along the Orange River (River losses study: Phase 2. Interim report). The position of these stations is shown in Figure 2. Three stations representing the upper, middle and lower reaches of the Orange River were chosen. These were namely: Bleskop, Upington and Vioolsdrif. The down stream distance between Bleskop and Upington and Upington to Vioolsdrif is approximately 550 km and 465 km respectively.

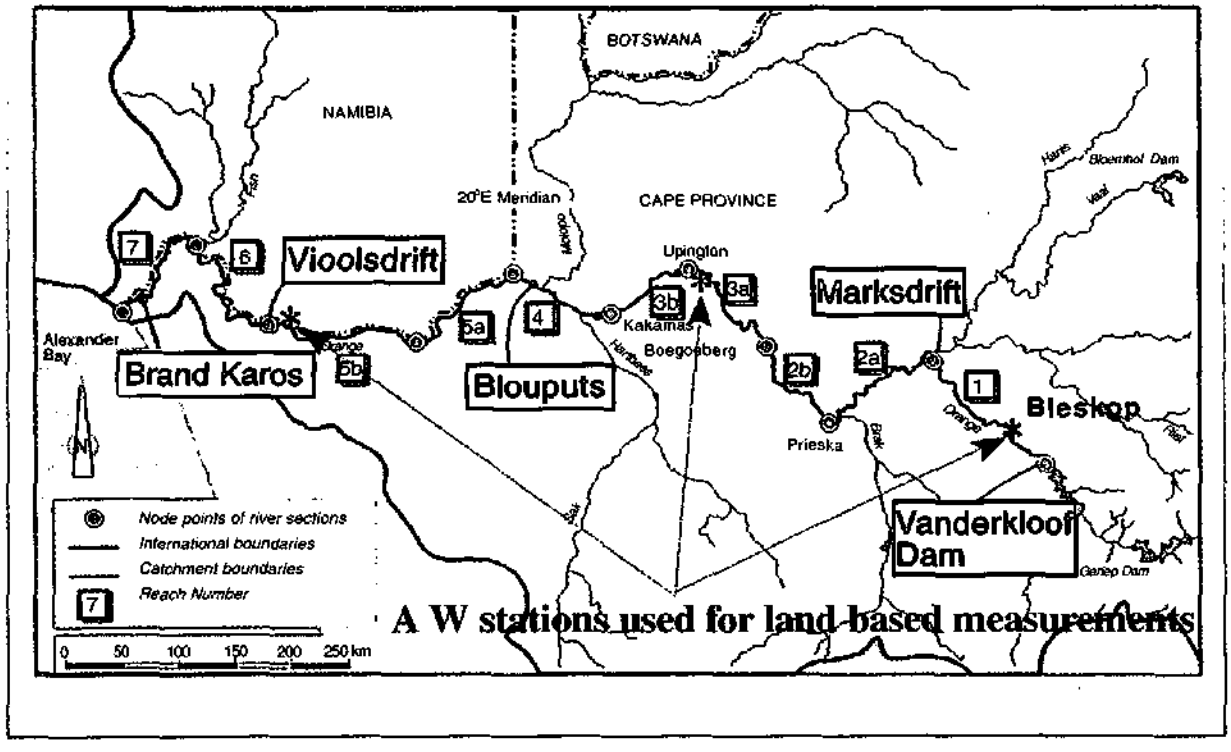

Figure 2.2. The position of the 3 weather stations along the Orange River. (The master copy of this graph was kindly supplied by BKS Inc. and is reproduced with their permission)

Plate 2.1. Aerial view of the Gifkloof study area. Extensive irrigation areas are visible on the northern bank of the river. The main irrigation canal is on the south bank.

CHAPTER 3

Methods

3.1 Bowen Ratio Energy balance technique.

3.1.1 *Background and Theory.*

Evaporation from the river was evaluated by the energy balance (Bowen ratio) approach. The energy balance method requires knowledge of the factors contributing to the thermal balance at the evaporating surface. The energy balance equation for a water body may be written as:

$$R_n = H + \lambda E + G_s + R_s + R_i \qquad (1)$$

where H is the sensible heat flux, E is the evaporation rate, λ is the latent heat of vaporization ($J\ kg^{-1}$), R_n is the net (all wave) radiation (Wm^{-2}), G_s is the soil heat flux, R_s is the heat stored in the water and R_i is the heat moved into or out of the system (eg by water inflow or outflow)(Wiesner, 1970). Over short periods R_i is not usually significant and can be ignored. R_s can be measured from the water temperature profile and G_s from the ground heat flux.

To permit the determination of evaporation by equation (1) the relationship established by Bowen (The Bowen ratio, β) can be used:

$$\beta = \frac{H}{\lambda E} \qquad (2)$$

The Bowen ratio may also be expressed in terms of the temperature (T) and specific humidity (q) gradients where z is the vertical height interval:

$$\frac{\partial T}{\partial z} \quad and \quad \frac{\partial q}{\partial z}$$

Using appropriate transfer coefficients K_h and K_w:

$$= \frac{H}{\lambda E} = \frac{\rho C_p K_h \frac{\partial T}{\partial z}}{\rho C_p K_w \frac{\partial q}{\partial z}} = \gamma \frac{\Delta T}{\Delta q} \text{ since } K_h \text{ and } K_w \text{ are assumed equ} \quad (3)$$

Equation (3) shows that β values are derived from measuring gradients in air temperature and vapour pressure over the same vertical height interval (Δz) and the thermodynamic value of the psychrometric constant $\gamma = c_p / \lambda$, where c_p is the specific heat of air at constant pressure.

From (1) and (2) β and (R_n-G - R_s) values are used to compute the latent heat flux from:

$$\lambda E = \frac{(R_n - G_s - R_s)}{(1 + \beta)} \quad (4)$$

The sensible heat flux is calculated from:

$$H = (R_n - G_s)(1 + \beta) \quad (5)$$

β can be estimated from both equations (2) and (3), by measuring the surface temperature of the water, and the temperature and vapour pressure gradients above the water.

3.1.2 Bowen Ratio Instrumentation

The dewpoint temperature (°C) of air drawn in from sensors situated at 0,5 m and 1,5 m above the water surface was measured with a dewpoint hygrometer. The dewpoint temperature was used to estimate the vapour pressure (kPa) of the air (e_a).

Air temperature at 0,5 m and the air temperature difference between 0,5 and 1,5 m were measured using two bare type E-thermocouples, each with a parallel combination of 76 μm diameter thermocouples. This combination functions even if one thermocouple is damaged. Measurements of the surface water temperature were also made. Thus the following vapour (and

temperature) gradients were estimated:

e_s to $e_{a\,0.5m}$: e_s to $e_{a\,1.5m}$ and $e_{a\,0.5m}$ to $e_{a\,1.5m}$.

All sensors were connected to a Campbell 21X datalogger. A frequent measurement period of 1 s for dewpoint and air temperatures was employed and 10 s for all other sensors. The dewpoint temperature was averaged over 80 s (after a mirror stabilization time of 20 s), converted to water vapour pressure and then the datalogger switched a solenoid to sample the other level. Every 20 minutes the datalogger converted an average of the output storage values to final storage. The data were transferred to an SM196 storage module. These data were transferred to a computer and the data checked for errors. The daily evaporation for the river was calculated from the sum of all the 20 minute data. An example of the output data is shown in appendix 1.

Net radiation was measured over the river with a Q*6 REBS net radiometer mounted 1 m above the water surface. The heat flux into the river was estimated from the equation:

$$G = F_s + C_w \frac{\Delta T_r}{\Delta t} \qquad (6)$$

F_s is the heat flux through the river bed, C_w the heat capacity of water (4181.59 J kg^{-1} K^{-1}) and $\Delta T_r / \Delta t$ is the average change in temperature of the river over time (20 minutes in this case). The heat flux in the water was estimated by two heat flux plates placed 1.0 m below the surface. The river temperature was monitored with shielded thermocouples mounted on two float systems. Each float was constructed from 150 mm diameter PVC piping (1.2 m long), sealed on both ends. By adding or removing water from the pipe it was possible for the pipe to float upright at a predetermined depth. The water surface temperature was measured with four thermocouples (two per float) mounted a few millimetres below the water surface. Thermocouples mounted at a depth of 1.0 m below the surface allowed the depth-averaged water temperature to be measured.

Because of the large number of sensors it was necessary to multiplex nine thermocouples and two heat flux plates to a single differential channel on the 21X data logger, using a Campbell AM 416 relay driver. Measurements of wind speed, wind direction, precipitation, air temperature, relative humidity and incoming solar radiation were recorded at 2 m above the water surface. The entire

Bowen ratio and weather station system are shown in Plate 3.1. The entire Bowen ratio apparatus and weather station were mounted on a mast. The base plate of the mast was attached by bolts grouted into a concrete slab.

The weather station instruments linked to the CR21X recorded the following measurements above the water:

I) Rain: an MCS 160 tipping bucket raingauge (0.2 mm tip) measured precipitation
ii) Solar radiation: A Kipp solarimeter measured radiation
iii) Wind speed: Wind speed was measured at a height of 2.0 m above the water with a cup anemometer.
iv) Wind direction was monitored with an MCS 176 wind direction sensor.
v) Temperature and relative humidity were measured with a PC207 temperature and humidity probe at 2m.
vi) Albedo was measured with a Middleton CN6 albedometer.

All sensors were averaged or totalled at 20 minute intervals.

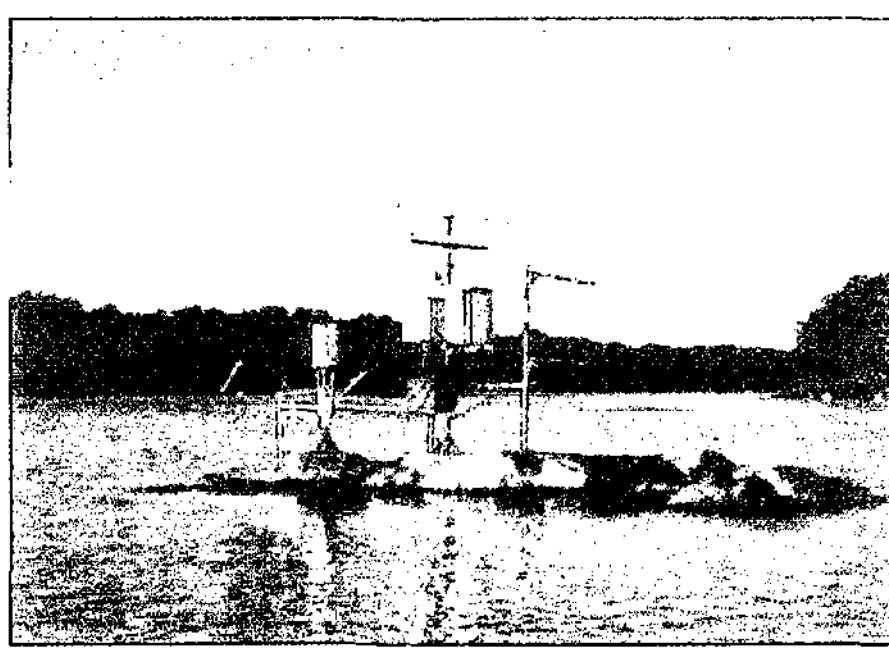

Plate 3.1. The Bowen ratio energy balance apparatus and weather station mounted in the Orange river.

3.2 **Other estimation methods or models of evaporation.**

An evaluation of the various indirect estimation methods was achieved by comparison with the actual evaporation measured from the river using the Bowen ratio technique. Meteorological data collected in the centre of the river were used for these calculations. From these comparisons the most suitable method(s) could be identified for investigating the suitability of using land based weather station data for estimating river evaporation.

3.2.1. *A-pan estimates.*

Evaporating pans have been widely used in South Africa for predicting reference evaporation and for estimating river losses along the Orange River. In the preliminary phase of the project an investigation into the suitability of using pan data was carried out. Evaporation was measured daily from an A-pan sited on the bank near the Bowen ratio apparatus. The installation details, as specified by the Department of Water Affairs were strictly adhered to. The pan was mounted on a wooden platform, over stone chips, with 15 mm wire-mesh over the top to prevent birds and animals from drinking. This site is referred to as the Gifkloof site.

Additional evaporation pan measurements enabling comparisons between the energy balance approach and pan coefficients method, were obtained from the airport (A-pan and S-tank), the agricultural research station (A-pan), Dept. of Water Affairs offices (A-pan), and SADOR farms (A-pan). Data from the latter was omitted due to too many inconsistencies in the data. In the second phase of the study daily evaporation from the A-pan at the Agricultural research station were compared with Bowen ratio and equilibrium estimates from June to October 1994.

3.2.2. *Penman evaporation and other derived equations*

One of the most widely used methods of approximating evaporation from open water surfaces is the Penman equation. The equation is derived from a combination of the energy balance and aerodynamic approaches.

The Penman equation is derived by combining equations (2) and (4) and by making two further assumptions in order to eliminate the variables describing conditions at the water surface. The first assumption is that the ratio:

$$\Delta = \frac{e_s - e_a}{T_s - T_a} \qquad (7)$$

is a reasonable approximation to the differential de/dT of the water vapour saturation curve at the air temperature T; the second is that the evaporation can be approximated by an empirical expression of the form:

$$E = f(U)(e_s - e)$$

where $f(U)$ is a measured function of the wind velocity.

Combining equations (7) and (8) with (2) and (4) gives the usual form of the Penman equation:

$$E_0 = \frac{\Delta}{\Delta + \gamma} \cdot \frac{R_n - G}{\lambda} + \frac{\Delta}{\Delta + \gamma} f(U)(e_s - e) \qquad (9)$$

where γ is the psycrometric constant and Δ the slope of the saturation pressure curve at the mean wet bulb temperature. The two terms in the expression are often termed the net radiation and the aerodynamic terms.

The aerodynamic term was calculated from the empirical relationship:

$$E_a = 2.6\,(e_s\,(T) - e)\,(1 + 0.537\,U_2) \qquad (10)$$

where U_2 is the wind speed (m s^{-1}) at 2 m height, and vapour pressure is in units of kPa.

Priestley and Taylor (1972) showed that, over a suitable averaging period (determined experimentally), the aerodynamic term can often be approximated as a fixed fraction (α) of the total evaporation, so that equation (9) can be rewritten:

$$E = \alpha \frac{\Delta}{\Delta + \gamma} \cdot \frac{R_n - G}{\lambda} \qquad (11)$$

The parameter α was found to have a value of 1.26 for a wide variety of saturated surfaces, oceans and lakes.

If one assumes a weak flow of air over a humid surface then the vapour pressure deficit ($e_s\,(T) - e$) and the wind speed U are small. Under these conditions the aerodynamic term in equation (9) or α in (11) becomes negligible, resulting in the so called equilibrium evaporation rate:

3.2.3 *The modelling of net radiation*

The isothermal net radiation is the sum of the net solar radiation and the net isothermal long-wave radiation:

$$R_{ni} = a_{st} + L_{ni}, \qquad (12)$$

where a_s is the albedo (absorptivity of water for solar radiation), S_t is the incident solar radiation measured by the datalogger, and L_{ni} is the atmospheric radiant emittance minus the water

emittance at air temperature. Under clear skies, L_{ni} closely approximated by

$$L_{nic} = 0.0003 T_a - 0.107 \ (kWm^{-2}) \tag{13}$$

where T_a (°C) is the air temperature. In cloudy conditions, L_{ni} increases (approaches zero). Cloudiness was estimated from the ratio of measured to potential solar irradiance: S_t/S_o. A cloudiness function was computed from:

$$f\left(\frac{S_t}{S_o}\right) = \frac{1}{[1+0.034 \exp(7.9\ S_t/S_o)]} \tag{14}$$

The net isothermal long-wave is then calculated as:

$$L_{ni} = f\left(\frac{S_t}{S_o}\right) L_{nic} \tag{15}$$

Equation 17 requires the computation of S_o, the potential solar radiation of a horizontal surface outside the earth's atmosphere. This is calculated from:

$$S_o = 1.36 \sin \phi \tag{16}$$

where 1.36 (kW m^{-2}) is the solar constant, and ϕ is the elevation angle of the sun. Sin ϕ is computed from

$$\sin \phi = \cos d \cos l + \sin d \sin l \cos [15\ (t-t_0)] \tag{17}$$

where d is the solar declination angle l is the latitude of the site, t is the datalogger clock time, and t_0 is the time of solar noon. Sin d was estimated from:

$$\sin d = -0.37726 - 0.10564J + 1.2458J^2 + 0.75478J^3 + 0.13627J^4 - 0.00572J^5 \tag{18}$$

where J is the day of the year. The cosine is computed from the trigonometric identity:

$$\cos d = (1 - \sin^2 d)^{1/2} \quad (19)$$

The time of solar noon was calculated from:

$$t_0 = 12 - L_c - E_t \quad \text{(hr)} \quad (20)$$

where L_c is a longitude correction and E_t is the "Equation of Time". The longitude correction was calculated from:

$$L_c = (L_s - L)/ 15 \quad (21)$$

L_s is the longitude of the standard meridian and L the longitude of the site.

The equation of time has an additional correction to the time of solar noon that depends on the day of the year. Two equations are used, one for the first half of the year and one for the second. For the first half :

$$E_t = -.0.04056 - 0.74503j + 0.08823j^2 + 2.0516j^3 - 1.8111j^4 + 0.42832j^5 \quad (22)$$

where j=J/100. For the second half of the year (J > 180),

$$E_t = -.0.05039 - 0.33954j + 0.04084j^2 + 1.8928j^3 - 1.7619j^4 + 0.4224j^5 \quad (23)$$

where j = (J- 180) / 100.

CHAPTER 4

Results

4.1 General

A preliminary 30 day investigation in October and September 1993 was undertaken to test the feasibility of using the Bowen ratio energy balance technique in the Orange River. The full study began on 14 June 1995 and continued until January 1996, when flooding of the river necessitated the removal of all the equipment from the river. During the five months prior to the study (January - May 1995) the agricultural research station recorded 112 mm of rainfall. Approximately 114 mm of rain was recorded during the study period (Figure 4.1), giving an annual total of ± 220 mm for 1995. Since this represented twice the mean annual rainfall (100 mm), the study was conducted in a relatively wet year.

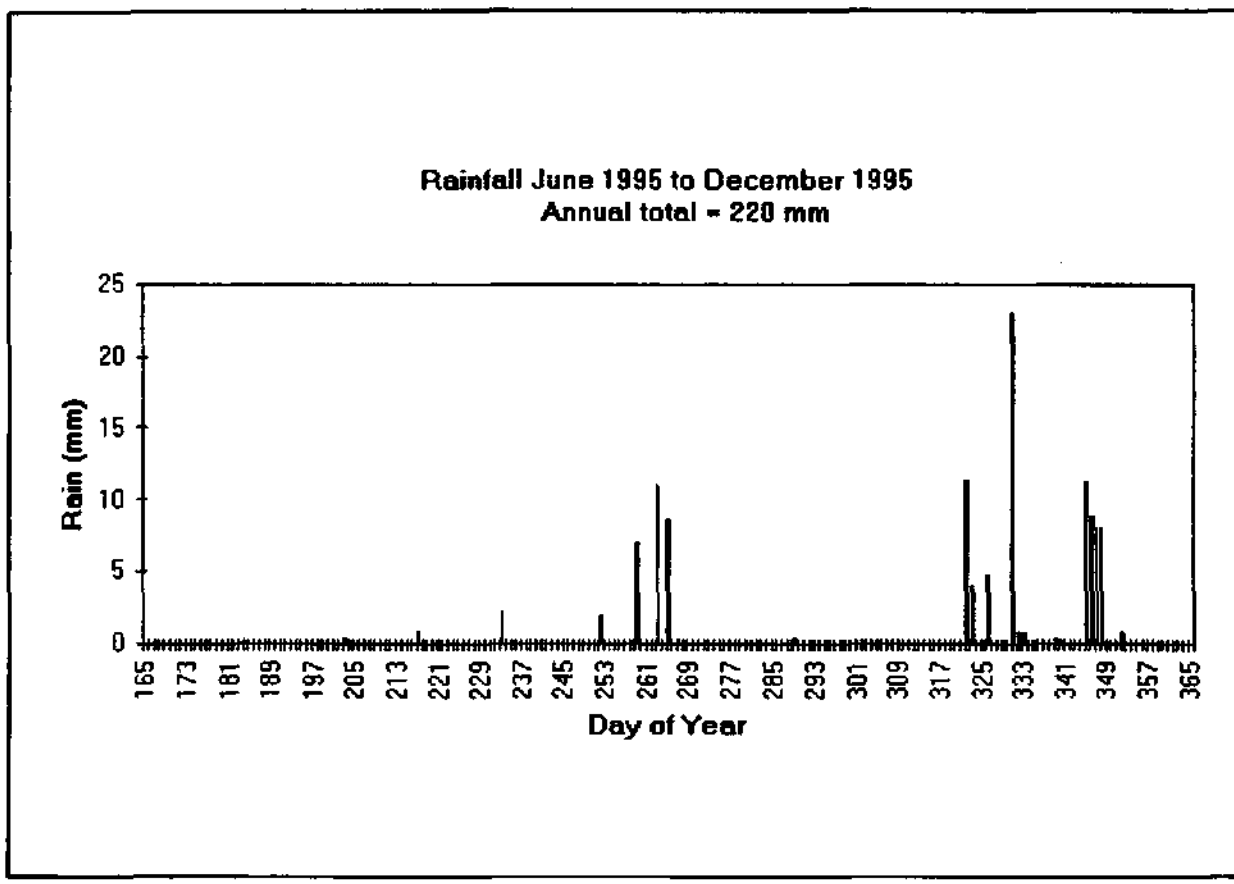

Figure 4.1. Daily rainfall at Upington during the study period.

4.2 Ambient air and surface water temperature

Mean daily air temperatures increased from 10 °C in mid-June (DOY 165) to 26 °C by the end of December (DOY 365). The pattern of mean temperature was characterized by significant daily fluctuations over short periods, with high average temperatures (>20 °C) being followed by days with temperatures below 10 °C (Figure 4.2).

Ambient air temperatures increased from daily maxima of approximately 25°C in mid-June to 40 °C by mid-November (DOY 318, Figure 4.3). Daily minimum air temperatures varied between 0 °C in July to 20 °C in December. The pattern of high daytime and low nighttime temperatures is typical of desert type environments. By contrast, the daily river water temperature was stable with little difference between the daily minimum and maximum temperatures (< 3 °C, Figure 4.3). The mean river temperature responded to changes in the daily air temperature very quickly, there being no significant lags in the system. The mean daily river temperature increased from 12 °C in June (DOY 165) to 27 °C by the end of December (DOY 365)(Figure 4.2). This is remarkably similar to the change in mean air temperature. Air temperature therefore had a marked influence on the mean river temperature during the study period.

The diurnal trend in the river temperature followed the cycle of ambient temperature (e.g. November 1995, Appendix 2 a-f). The diurnal daytime air temperatures were consistently higher (5-10°C) and nighttime air temperatures consistently lower (5-10°C) than the water temperature. These results contrast markedly with energy budget experiments from northern hemisphere lakes, where the diurnal temperature changes are small, and the lake is often warmer than the overlying air during the day.

The high air temperature during the day raises evaporation by increasing the vapour pressure deficit of the overlying air. A number of important features are evident in these data.

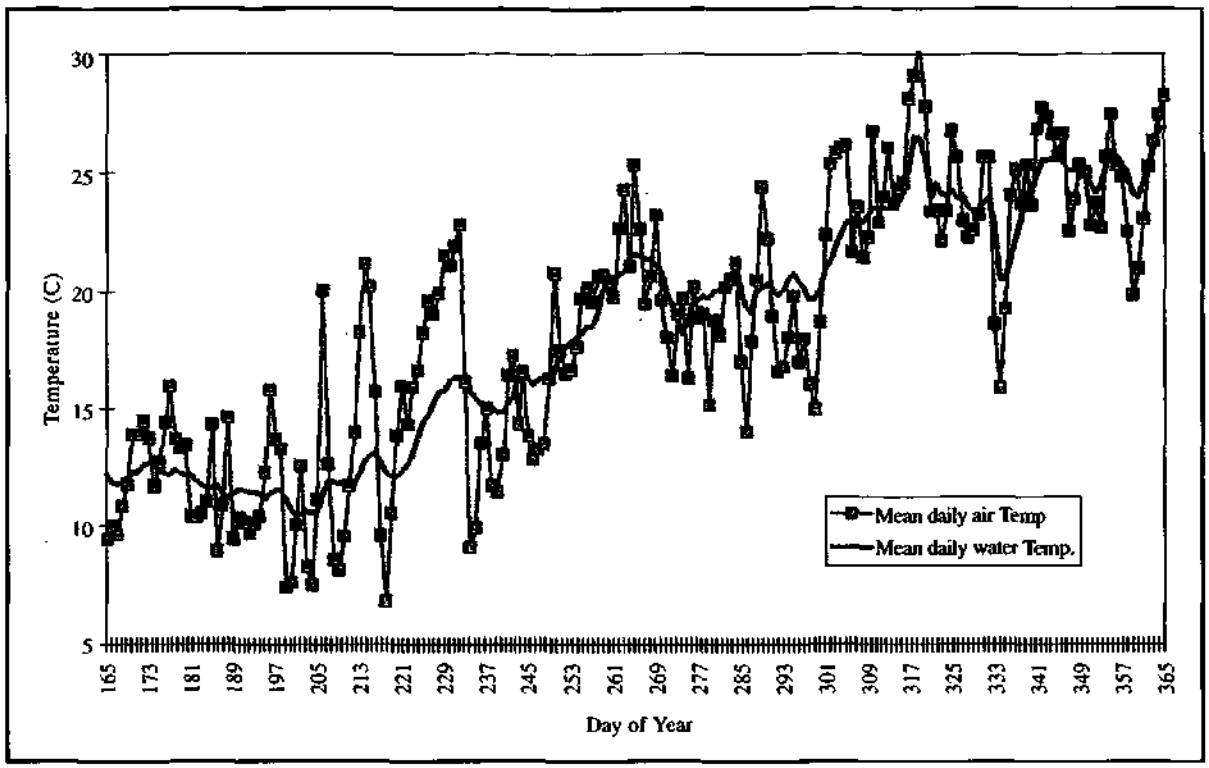

Figure 4.2. Average ambient air and surface water temperature. June to December 1995.

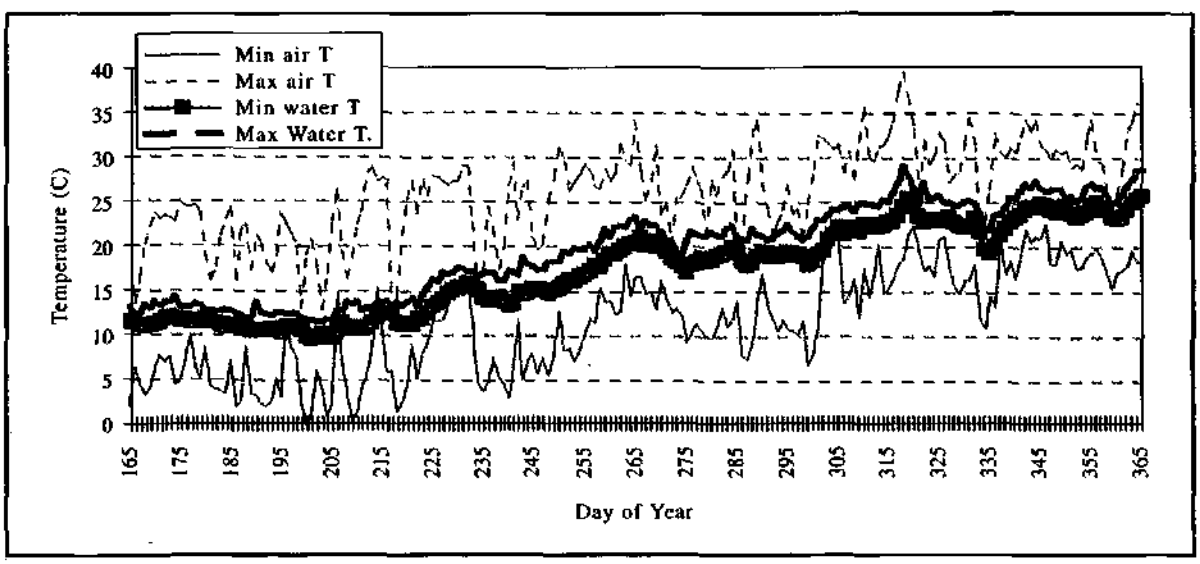

Figure 4.3. Ambient air and surface water temperature. June to December 1995.

Firstly, the river temperature responds fairly rapidly (within hours) to the changing ambient air temperature. This has important implications when using land based weather stations, as it is generally accepted that a major error in using land stations is through the heat stored in large water bodies causing substantial lags between the annual cycles of evaporation and solar radiation. This does not appear to be a problem in the present study. Secondly, there is a predictable and regular pattern between the air and surface temperatures. If this can be modelled then it would provide a more accurate and simpler approach to calculating open water evaporation, since the measurement or estimation of surface water temperature allows the saturation pressure of the water to be calculated at that temperature. If an automatic weather station is used to provide the ambient air and water vapour pressure estimate, then it is possible to use the Bowen ratio using equations (2) and (4) and hence solve the energy balance to obtain the evaporation rate. Time series analysis of the air and surface water temperature have been attempted in consultation with biometricians at the University of Natal. Due to complexities in the analyses the results are not available yet. A problem with this data series is that it only spans half a year. For these reasons considerable effort was spent on trying to use the equilibrium temperature concept to predict changes in the water temperature (Keijman, 1974). This technique requires the wet bulb temperature, which was not determined in the present study. The wet bulb temperature can be determined with a knowledge of the dry bulb temperature and vapour pressure, but the process is laborious, as it can only be done using iterative techniques. At the time of writing these results were not available.

Routine measurements of the surface water temperature could provide a way of monitoring the evaporation along the river. This could be done using thermocouples as in this study, or with infra-red thermometers. The use of remotely sensed data could also be considered. This is clearly an area for future research.

4.3 **Energy Budget**

During winter (Appendix 3 b.) midday net radiation values were approximately 500 W m^{-2} and increased steadily to nearly 900 W m^{-2} in summer (Appendix 3 t). A full series of the energy balance of the river during the study period (DOY 192 to 357) is given in Appendix 3 a-t.

Cloudless days dominated the study period and were characterized by typical bell shaped curves. Nighttime radiation values varied between -50 W m^{-2} and -75 W m^{-2} (Appendix 3 a-t)

In this study the value of the Bowen ratio was small, ranging from (-0.8 to 0.6, Appendix 3 a-t), indicating the absence of any surface control over evaporation. In general β was positive during periods when the air temperature was less than the surface water temperature, and negative when the air temperature was greater than the surface water temperature (Figure 4.4). The Bowen ratio showed a marked inverse relationship with air temperature. The average value of β for the entire study was -0.03. This is similar to other studies over oceans and lakes where a Bowen ratio of 0.1 for a water temperature of 25° C has been recorded (Priestley & Taylor, 1972).

The latent heat flux (evaporation) was high during the day >500 W m^{-2} and low at night. Night values increased towards summer, when values of 100 W m^{-2} were common. An example of a two day period is shown in Figure 4.5. In the hours between sunset and sunrise on DOY 356 and 357 the latent heat reached values of 250 W m^{-2}. The total evaporation for this night was approximately 2 mm which represents approximately 25% of daytime evaporation. Thus night time evaporation may represent a significant proportion of the daily evaporation total during the summer months. These data may explain why A-pan data may underestimate daily evaporation. The A-pan, being a small volume of exposed water, will cool much faster than the river water. Thus temperature gradients above the river will be much higher than those at the pan water interface.

Since the latent heat flux (λE) is calculated by dividing the available energy by $1+\beta$ (see equation 4), small negative values of β give a numerator less than unity, resulting in large latent heat fluxes during the day (Appendix 3 a-t). The latent heat was generally in excess of the net radiation during the hottest part of the day. The effect of hot dry winds from the surrounding land surface (advection), probably played a significant role in supplying the additional energy.

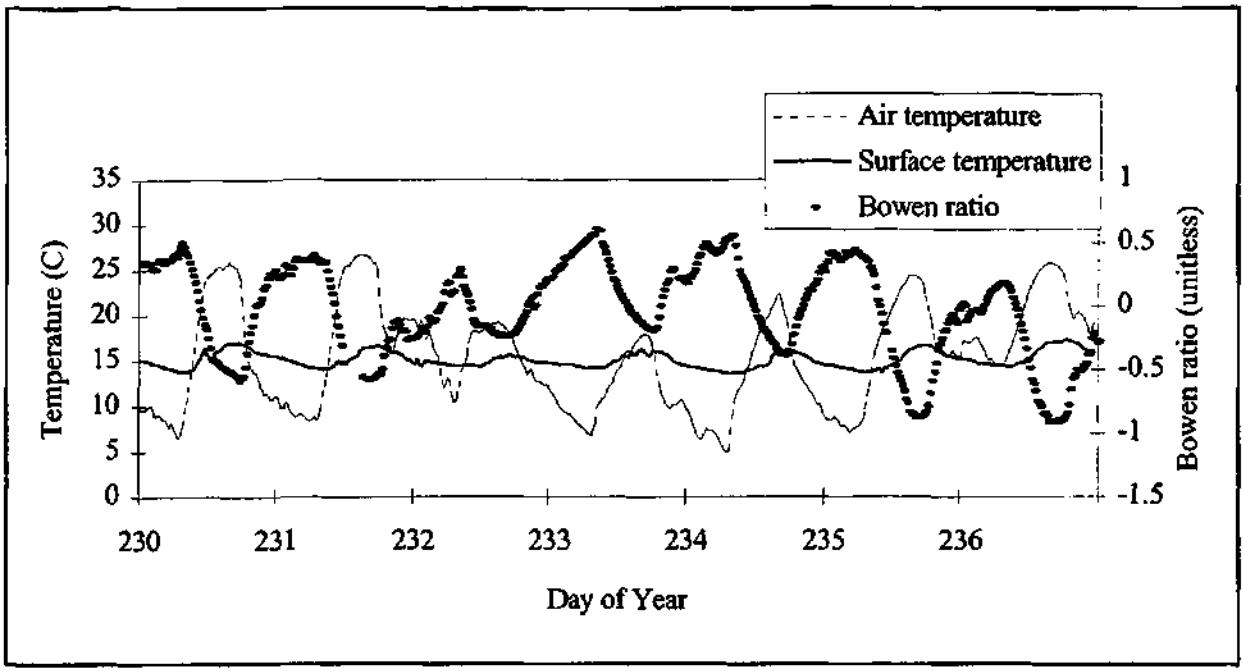

Figure 4.4. Variation in the surface temperature, air temperature and Bowen ratio, clearly showing the strong inverse relationship between the air temperature and Bowen ratio.

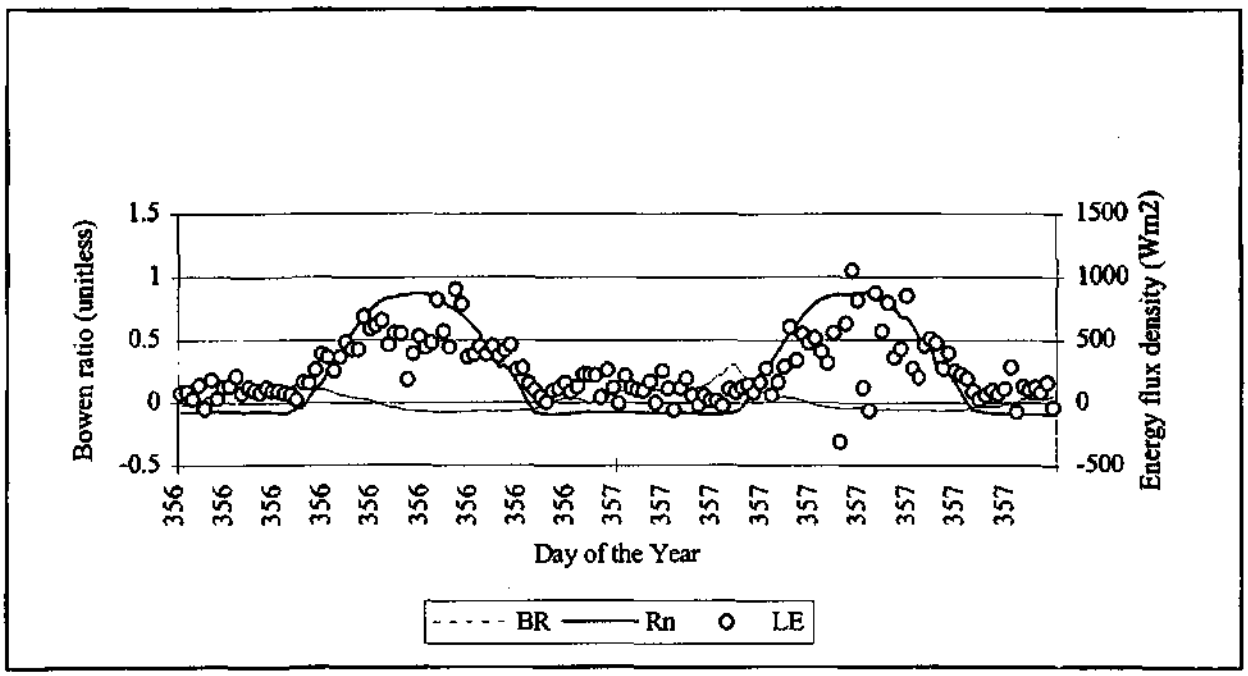

Figure 4.5. Diurnal variation in the net radiation, latent heat flux density and Bowen ratio for two days in December 1995.

The heat flux at the surface (G_s) was generally negative at night indicating that the river was losing energy to the surrounding atmosphere (Figure 4.6). By contrast, G_s fluctuated widely during the day between positive and negative values. In this way large amounts of energy (600-800 Wm^{-2}) were absorbed and then released for driving the evaporation process (Figure 4.6). The mechanism which was causing these 'overturns' in the water column is unclear (wind did not appear to play a significant role), but is most likely due to turbulence created by the flow of the river. These data indicate that changes in heat storage in the river cannot be neglected, over short periods.

Estimates of the daily heat content of the river were obtained by summing the 20 minute data for each day (01h00 to 24h00). During winter (DOY 165 to 200), the changes in heat storage were small (Figure 4.7). Similarly, the pilot study in 1993 showed that G_s was not a significant proportion of the energy balance during winter. However, as the summer progressed, G_s significantly increased indicating that large amounts of radiation are used to heat up the water (Figure 4.7). This trend was interrupted by cold frontal systems (DOY 270 and DOY 320) when the river lost large amounts of energy as it cooled. The total incoming radiation for the study period was 2413 MJ. The sum of the daily changes in heat energy content in the river was +83 MJ and represents only 3.4% of the total energy balance. This suggests that in a daily evaporation model, G_s could be ignored with little loss of accuracy.

4.3.1 *Bowen ratio versus evaporation pan measurements*

4.3.1.1 August - September 1993

The daily estimates of evaporation from the Bowen ratio technique and the various evaporation pans for the study period, showed large discrepancies between all the estimates of evaporation (Figure 4.8). The Bowen ratio estimates were generally 2-3 mm higher than the A-pan estimates. Of most concern is the high variability between the four A-pans, which could be as high as 80% on any particular day. There were also no consistent trends in the data. For example, the airport A-pan was initially higher than the others from DOY 230 to 247 and then became lower for the rest of the study period.

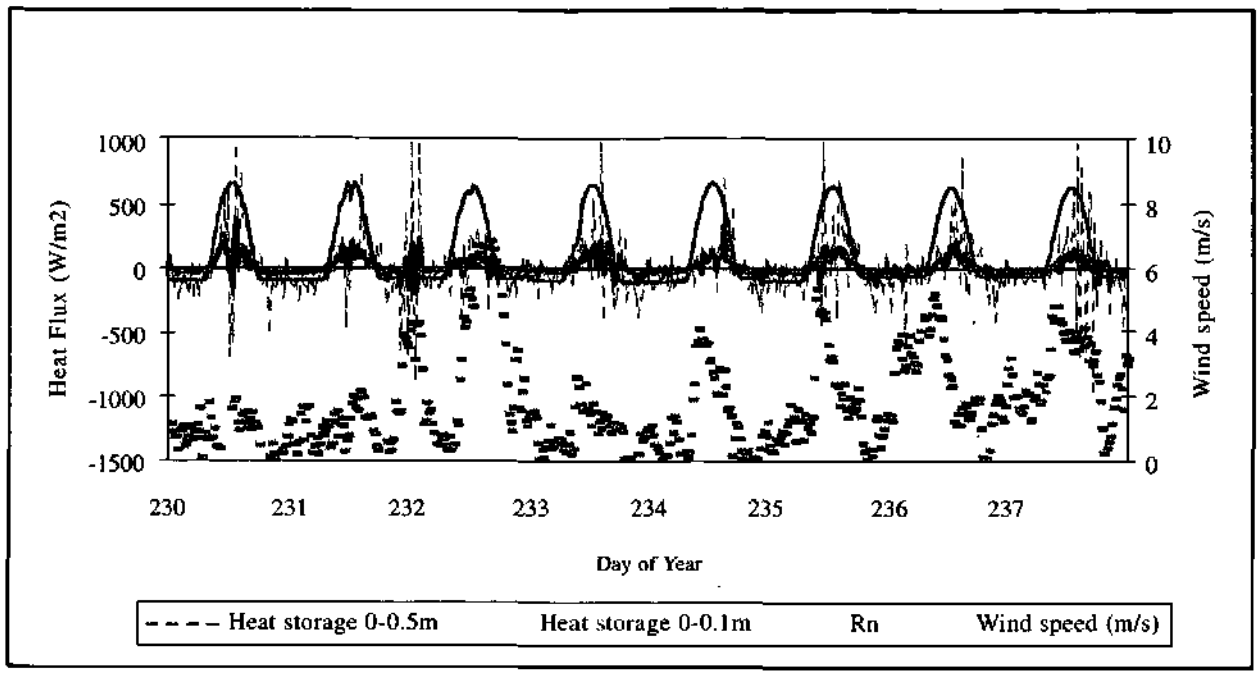

Figure 4.6. Variation in the heat flux at the surface (G) for 0-0.1 and 0.7m depths, net radiation and windspeed for DOY230 to 237.

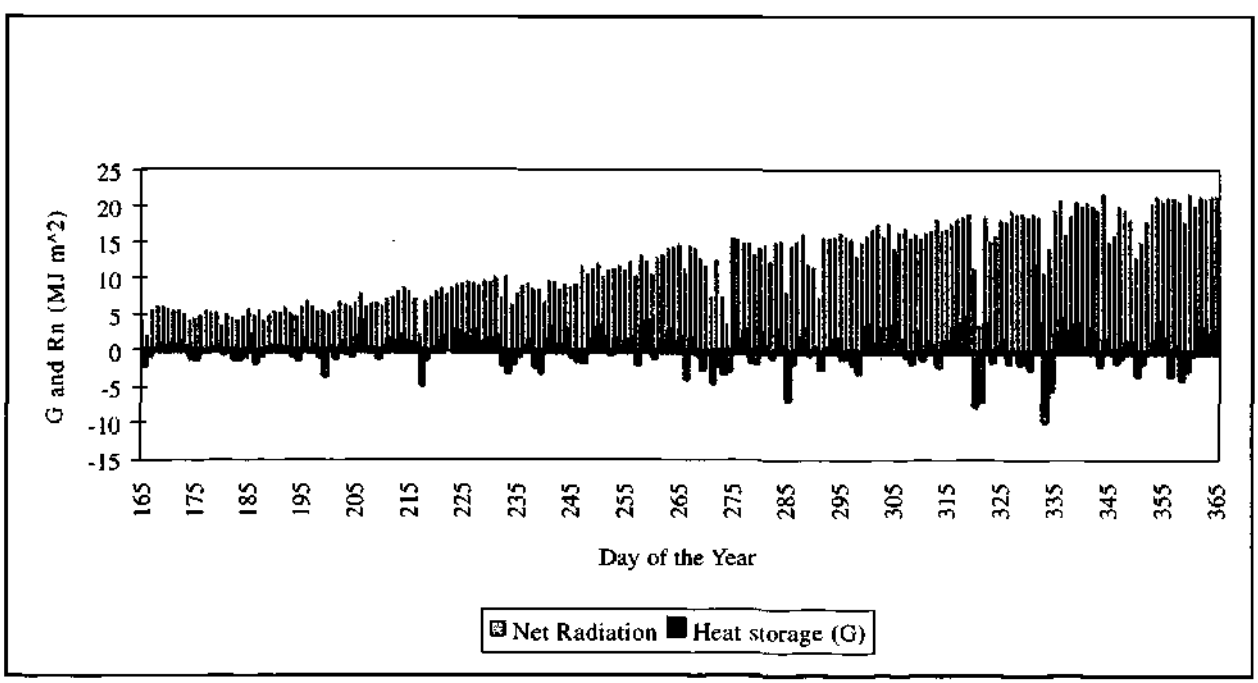

Figure 4.7. Daily variation in the heat storage (G) and net incoming radiation during the study period.

The large variation in the evaporation data from the different A-pans is partly due to variations in their set-up. For example, the pan at Gifkloof (Plate 4.1a) has been set to CSIR specifications and allows free air flow under the pan. By contrast the DWA pan is mounted on wood with no allowance made for air flow beneath the pan (Plate 4.1b). Evaporation from the SADOR farm pan (Plate 4.1c) is likely to be highly inaccurate since the pan is mounted on metal and is painted red on the inside. Pans at the airport (Plate 4.1d and 4.1e) were well maintained, but the water was full of algae. Weeds growing along the far side of the A-pan at the agricultural research station prevented free air flow below the pan (Plate 4.1f).

Another factor that varied between pans was the mesh size of the screens. The data were corrected to allow for these differences, using reductions recommended by Schulze (1989). Another variable was observer accuracy in reading the evaporation from the pans. Some observers read the scale only to the nearest millimetre, while others read the scale to the nearest half millimetre. This variability highlights the difficulty of using A-pan data to estimate river evaporation, particularly if the condition of the pan is unknown. The regression analyses between the Bowen ratio and evaporation pans (Figure 4.9 and Table 4.1) indicate that the best fit was against the A-pan at Gifkloof ($r=0.81$). The DWA ($r=0.62$) and Agricultural research station (0.52) showed some degree of correlation.

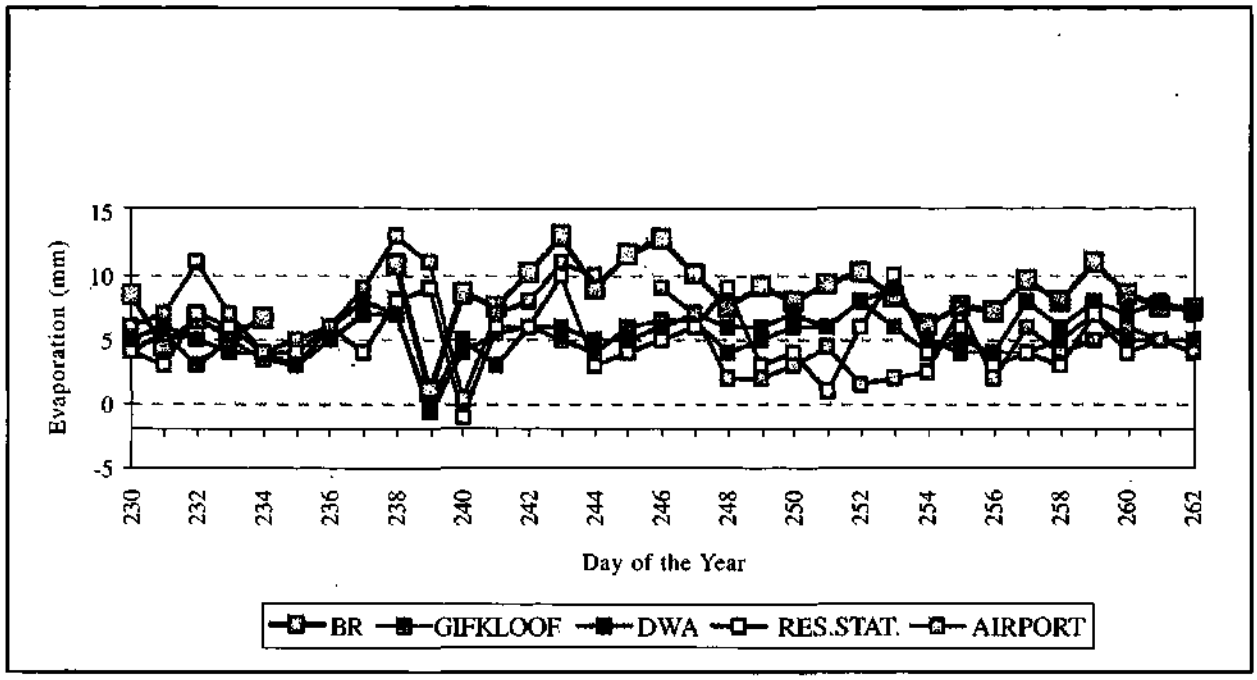

Figure 4.8. Daily estimates of A-pan and Bowen ratio evaporation during the study period.

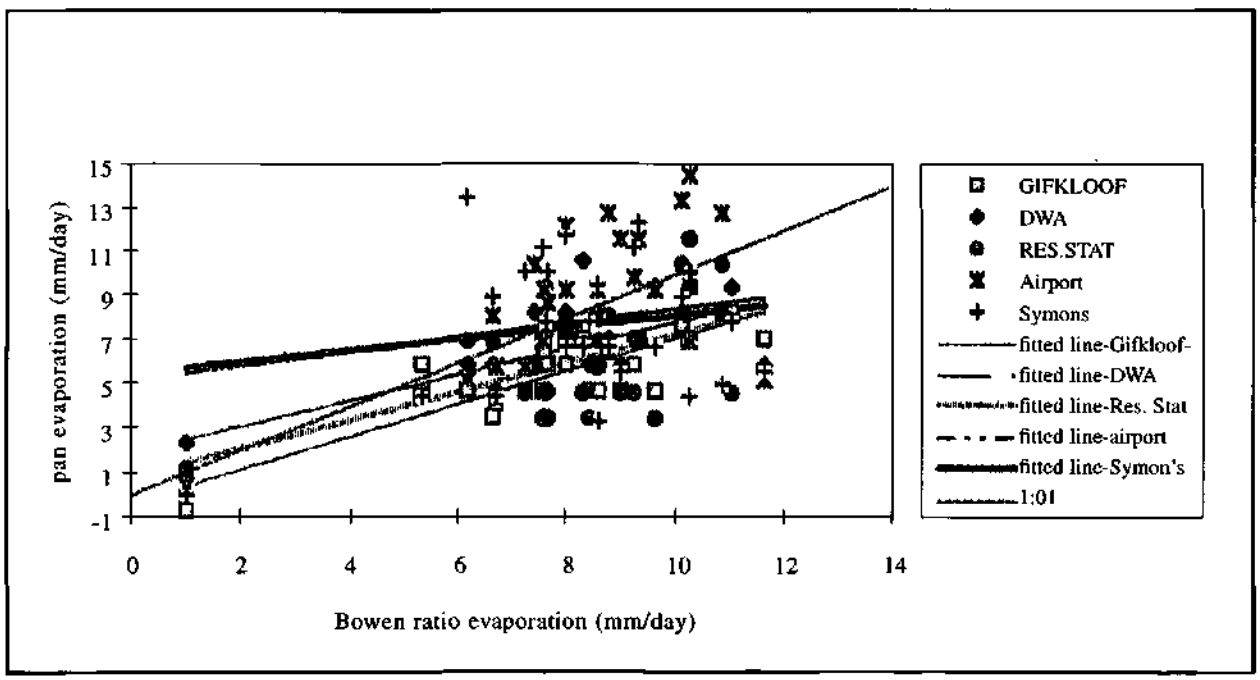

Figure 4.9. Regression of the Bowen ratio evaporation data against the various pan data.

Table 4.1. Regression analysis of the Bowen ratio evaporation against the various A-pans ans 1 Symon's pan evaporation in Upington during August/September 1993.

A -pan - Gilldoof (next to the river near Bowen ratio instrument)

Regression Statistics	
	0.81661619
R Square	0.666965266
Adjusted R Square	0.653539679
Standard Error	1.13366122
Analysis of Variance	

Multiple R	*df*	*Sum of Squares*	*Mean Square*	*F*	*Significance F*	
Regression	1	64.31571662	64.31571662	50.04471	2.04E-07	
Residual	25	32.12912723	1.285165089			
Total	26	96.44484385				
	Coefficients	*Standard Error*	*t Statistic*	*P-value*	*Lower 95%*	*Upper 95%*
Intercept	-0.325718099	0.897104864	-0.36307695	0.719463	-2.173339	1.521903
x 1	0.74525329	0.105347699	7.074226714	1.64E-07	0.5282859	0.962221

A-pan - DWA (office site)

Regression Statistics	
Multiple R	0.624932108
R Square	0.39064014
Adjusted R Square	0.366181745
Standard Error	1.592017871
Analysis of Variance	

	df	*Sum of Squares*	*Mean Square*	*F*	*Significance F*	
Regression	1	40.60284414	40.60284414	16.01993	0.0004923	
Residual	25	63.36302253	2.534520901			
Total	26	103.9658667				
	Coefficients	*Standard Error*	*t Statistic*	*P-value*	*Lower 95%*	*Upper 95%*
Intercept	1.826710681	1.259629258	1.450342702	0.159256	-0.667954	4.321376
x 1	0.592136874	0.147942613	4.002490313	0.000484	0.2874458	0.896832

A-pan - Agricultural research station

Regression Statistics	
Multiple R	0.523489058
R Square	0.274041736
Adjusted R Square	0.245003405
Standard Error	2.285047299
Analysis of Variance	

	df	*Sum of Squares*	*Mean Square*	*F*	*Significance F*	
Regression	1	49.2780007	49.2780007	9.437241	0.0050755	
Residual	25	130.5360289	5.221441157			
Total	26	179.8120296				
	Coefficients	*Standard Error*	*t Statistic*	*P-value*	*Lower 95%*	*Upper 95%*
Intercept	0.755511006	1.808251685	0.417612905	0.679514	-2.968851	4.479873
x 1	0.652323571	0.212344287	3.072009344	0.004938	0.2149027	1.089654

A-pan - Airport

Regression Statistics	
Multiple R	0.217188192
R Square	0.047170711
Adjusted R Square	0.009057539
Standard Error	3.143699116
Analysis of Variance	

	df	*Sum of Squares*	*Mean Square*	*F*	*Significance F*	
Regression	1	12.23304393	12.23304393	1.237649	0.2765063	
Residual	25	247.1025413	9.88410165			
Total	26	259.3355852				
	Coefficients	*Standard Error*	*t Statistic*	*P-value*	*Lower 95%*	*Upper 95%*
Intercept	5.17805992	2.487896752	2.080496273	0.047475	0.0521442	10.29998
x 1	0.325021691	0.292155419	1.112496533	0.276106	- 0.276083	0.926727

Symon's pan - Upington airport

Regression Statistics	
Multiple R	0.218534736
R Square	0.047757431
Adjusted R Square	0.009667728
Standard Error	2.599347112
Analysis of Variance	

	df	*Sum of Squares*	*Mean Square*	*F*	*Significance F*	
Regression	1	8.471531491	8.471531491	1.253815	0.273468	
Residual	25	168.9151352	6.756605407			
Total	26	177.3866867				
	Coefficients	*Standard Error*	*t Statistic*	*P-value*	*Lower 95%*	*Upper 95%*
Intercept	5.454766604	2.056970341	2.651846502	0.013457	1.2183629	9.691170
x 1	0.27047449	0.241551436	1.119739865	0.273063	-0.22701	0.767959

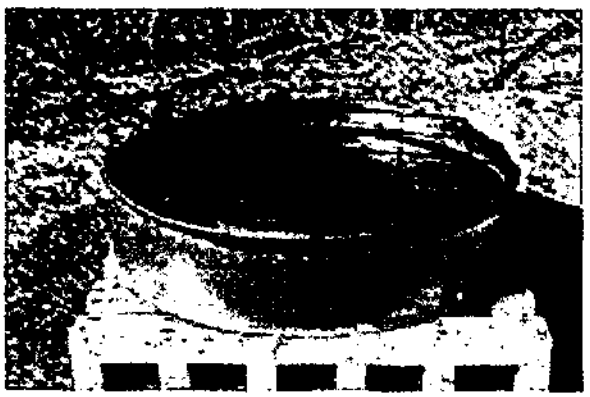

Plate 4.1a. The Gifkloof A-pan.

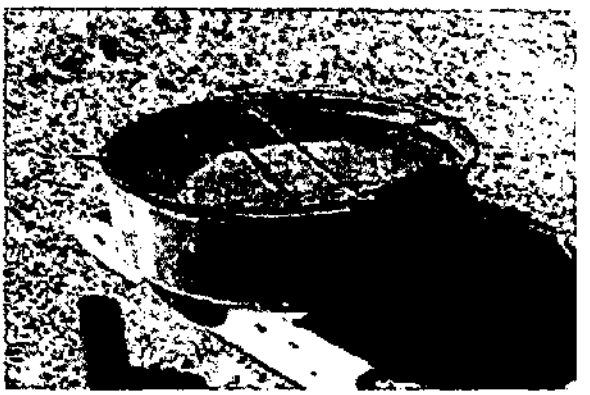

Plate 4.1b. The DWA A-pan.

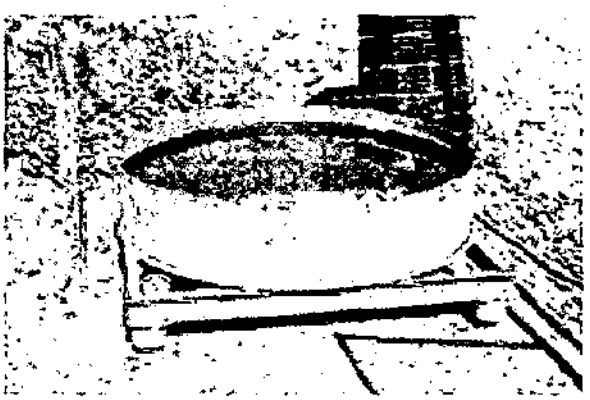

Plate 4.1c. The SADOR farm A-pan.

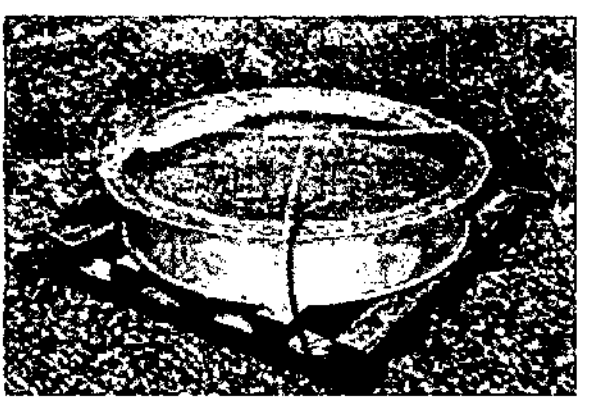

Plate 4.1d. The Airport A-pan.

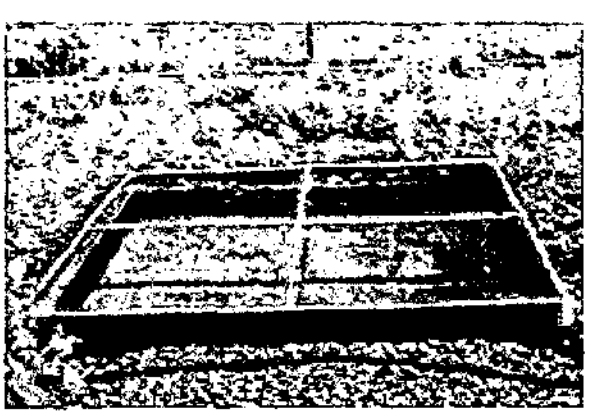

Plate 4.1e. The Airport Symon's-pan.

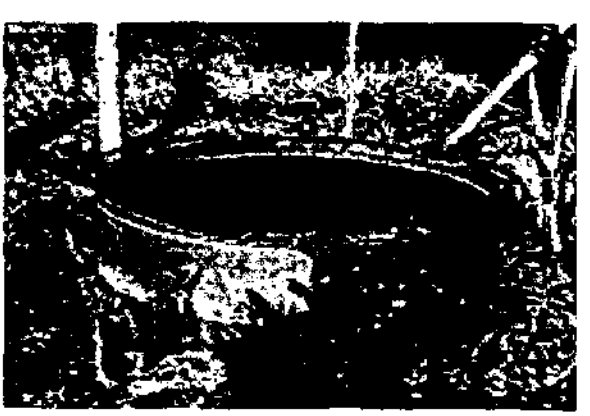

Plate 4.1f. The Research Station A-pan.

Plate 4.1 a-f. The various evaporation pans for which data were obtained during the study.

There was no significant relationship between the Bowen ratio versus the airport A-pan (r=0.21) and the Bowen ratio versus the Symon's pan (r=0.21). The coefficient of x, was 0.75 for Gifkloof, implying that the A-pan would on average underestimate the evaporation from the river by 25%. This value increased as the r value decreased for the comparisons with the other pans (Table 4. 1). The poor relationship between estimates of evaporation from the Bowen ratio and the well-maintained airport pans may be due to the fact that the airport is situated away from the river and irrigation areas, and is subjected to extreme advection from the surrounding desert. In spite of this poor relationship, the total evaporation recorded from this pan (220 mm, Table 4.2) was close to the Bowen ratio estimate of evaporation (230 mm). In contrast, total evaporation from the pan with the highest correlation to the Bowen ratio (Gifkloof) was significantly lower (163 mm). The location of this pan in the humid environment next to the river, may account for these low values.

Table 4.2. Monthly totals of evaporation (mm) from the Bowen ratio and evaporation pans.

Data type	Bowen ratio	Gifkloof A-pan	DWA A-pan	Res. station A-pan	Airport A-pan	Airport Symon's pan
uncorrected	230	138	163	148	224	197
corrected	230	163	192	171	260	220

4.3.1.2 June to October 1995

Daily estimates of evaporation from the Bowen ratio technique, the equilibrium evaporation rate and the A-pan at the Agricultural Research Station for DOY 165 to 305 (June to October 1995) are illustrated in Figure 4.10. Daily evaporation from the Bowen ratio method increased from 2-4 mm/day in June, reaching a maximum of 10 mm by the end of October (DOY 305). The total evaporation for this period was 658 mm. The A-pan evaporation (corrected by +16% for 20 mm mesh) showed similar trends to the Bowen ratio technique, but the seasonal total was 607 mm (approximately 8%) lower than the energy balance technique. These data indicate that uncorrected A-pan data would underestimate evaporation from the river by 25%.

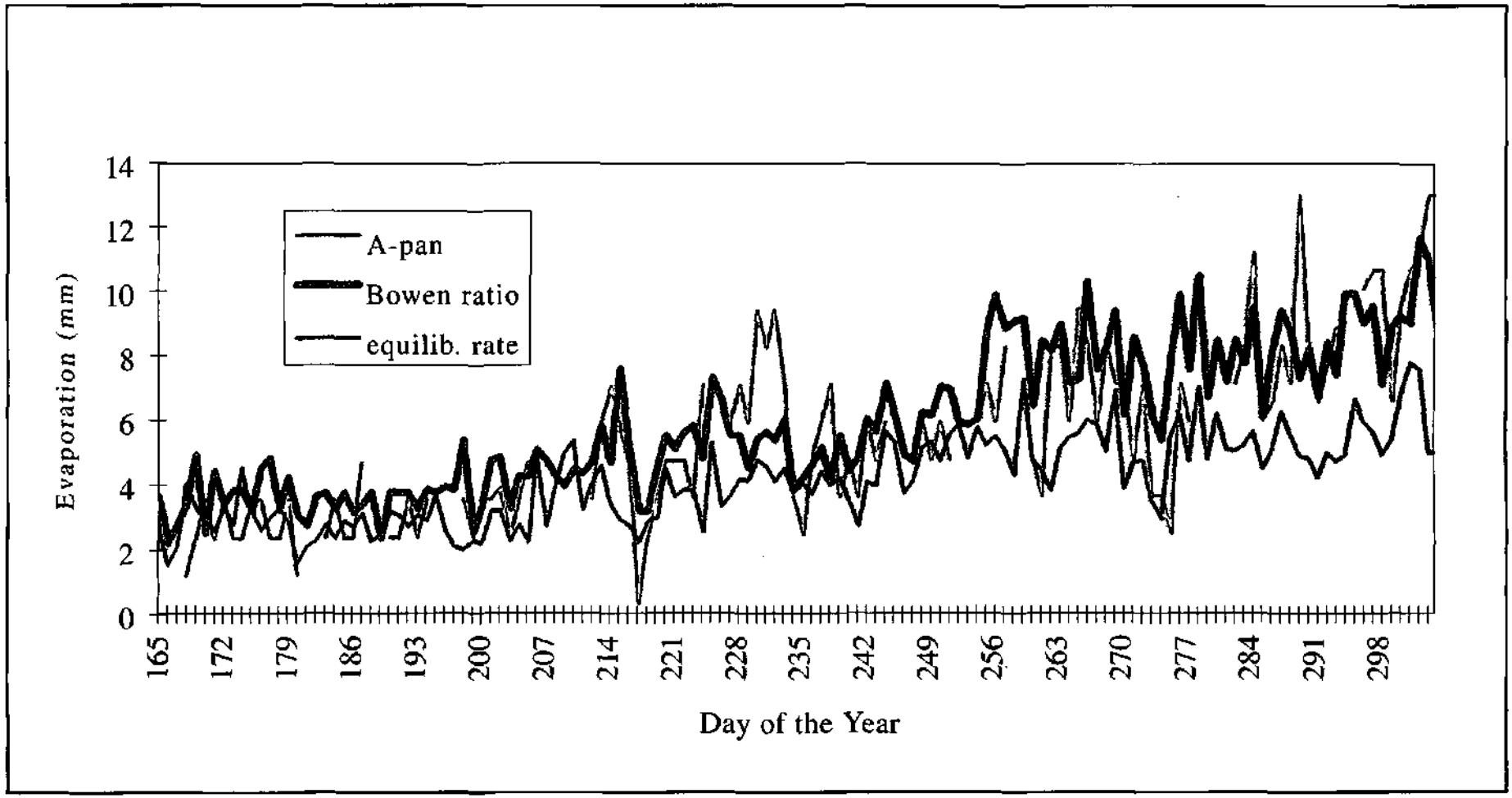

Figure 4.10. Daily evaporation totals (mm/day) for various techniques, Bowen ratio, equilibrium rate and A-pan evaporation, June to December 1995.

The regression analysis between the Bowen ratio and A-pan at the Agricultural research station showed a significant relationship between the two methods ($r=0.76$; $p= <0.0001$)(Table 4.3 and Figure 4.11). The fitted and 1:1 line showed good agreement, although there was a fairly large scatter in the data resulting in a standard error of $\pm$ 1.8 mm. This is a better fit than found during the pilot study in 1993 when the corrected A-pan for the Agricultural research station showed a poor fit to the data ($r=0.52$), and a 25% underestimate when compared to the Bowen ratio technique. The collection of data representative of the different seasons is therefore essential for reliable estimates of evaporation.

Variability between pan estimates of evaporation highlight the difficulties of using pan data to predict river evaporation. It is obvious that the choice of a particular A-pan site will have major effects on the final result. However, standardization of pans and observer accuracy could minimize these differences. Strict control measures are therefore necessary over all weather stations.

The findings of this study confirm those of Smith (1975), who stated that the extrapolation of evaporation pan data from its measurement site to other locations is a "very hazardous procedure". This study also shows that even if the A-pan is considered to be properly sited (i.e. the Gifkloof site in this study), it may still be seriously in error. Green (1985), also discusses large errors in A-pan extrapolation. In Zululand, a dense network of pans has yielded inexplicably variable results due to influences of local climate (Hope and Mulder, 1979).

Table 4.3 Regression analysis of the Bowen Ratio evaporation against the Agricultural Research station A-pan

Regression Statistics	
Multiple R	0.756
R Square	0.571
Adjusted R	0.568
Standard Error	1.807
Observations	112.000

Analysis of Variance

	df	*Sum of Squares*	*Mean Square*	*F*	*Significance*	
Regression	1.000	478.735	478.735	146.655	5.77E-22	
Residual	110.000	359.080	3.264			
Total	111.000	837.815				
	Coefficient	*Standard Error*	*t Statistic*	*P-value*	*Lower 95%*	*Upper 95%*
Intercept	-0.282	0.505	-0.558	0.578	-1.282	0.718
x 1	0.979	0.081	12.110	0.000	0.819	1.140

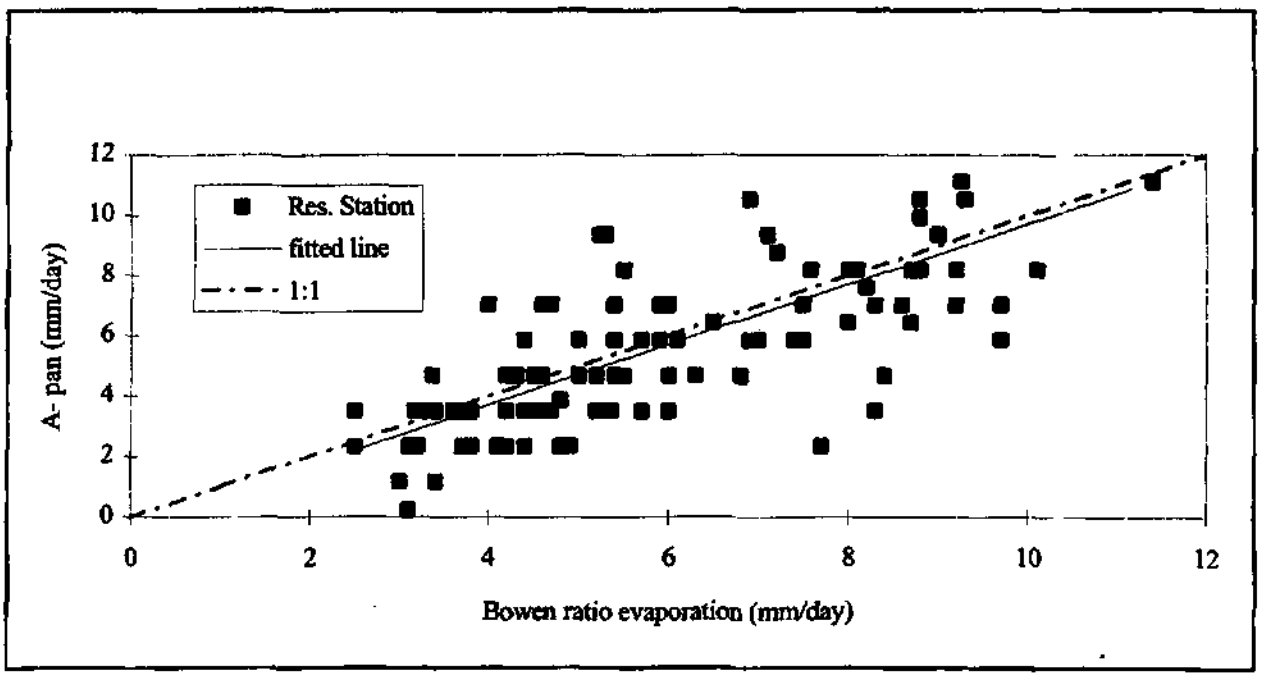

Figure 4.11. Regression of the Bowen ratio evaporation against the A-pan data.

4.3.2 *A comparison of the Bowen ratio with other measures of evaporation.*

4.3.2.1 Radiation Modeling

Solar radiation is the single most important component of the energy balance as it drives the process of evaporation and sensible heat exchange at the water surface. While most energy budgets require information on net radiation (the energy available at the surface), this is seldom routinely measured at standard weather stations in South Africa. Predictions of net radiation can be made by the relationship of the net radiation with solar radiation (solar radiation is estimated at most weather stations). This relationship can be improved with a knowledge of the dependence of the reflectivity of the water surface (albedo) on certain variables. For example, in the radiation model used in this study, it is essential to have prior knowledge of the absorptivity of water for solar radiation (i.e. 1 - albedo).

Mid-day values for the albedo and solar radiation between July and December 1994 showed a distinct seasonal relationship (Figure 4.12). Thus as the solar altitudes increased with summer (Solar radiation increasing) so the albedo decreased from approximately 0.1 in July (DOY 162) to 0.04 in December (DOY 365), while the radiation increased from 600 W m^{-2} in winter to 1000 W m^{-2} in summer. This inverse relationship is more clearly shown by the linear regression of solar radiation on albedo (Figure 4.13). The significant relationship developed here ($r=0.825$) can be used to predict the surface albedo of the river from mid-day values of solar radiation. These data confirm that the albedo of water is low, that solar angles have a major influence, and that water, as a poor reflector, serves as a good sink for solar energy. The values measured in this study are very similar to those measured by Oguntoyinbo (1974) on the Niger river, which varied between 0.06 and 0.12, depending on whether it was clear or dirty.

The relationship between the net radiation measured above water at the Bowen ratio station and the value predicted from this model using standard weather data was very good (Figure 4.14). An albedo of 0.15 gave the best fit. These data show that the net radiation can be modeled very

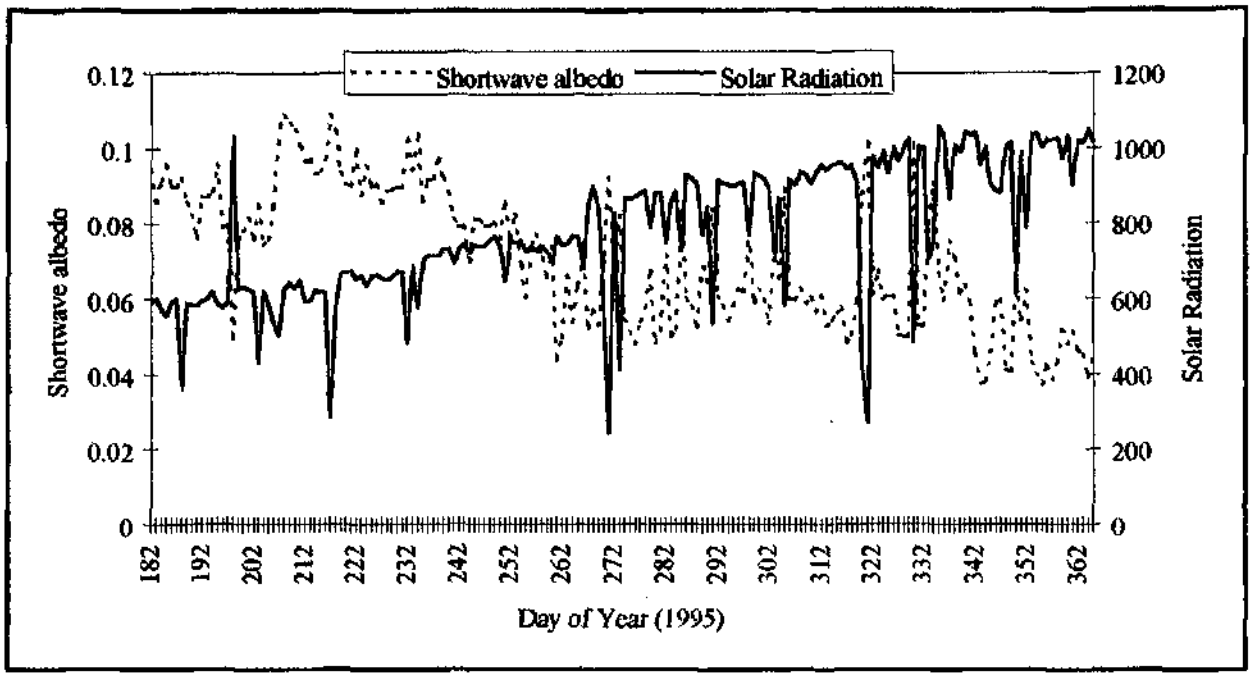

Figure 4.12. Seasonal trends in solar radiation (wm^2) and albedo during the study period.

Regression Statistics	
Multiple R	0.825
R Square	0.681
Adjusted R Square	0.680
Standard Error	0.010
Observations	184.000

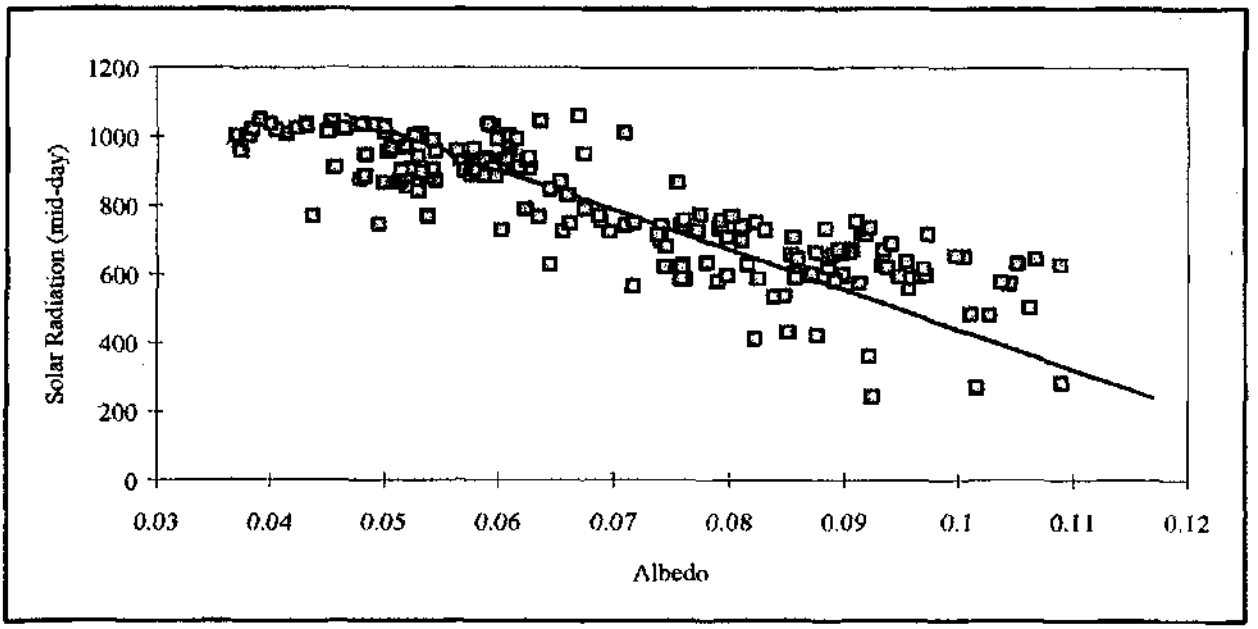

Figure 4.13. Regression analysis of the albedo versus the solar radiation.

accurately from standard weather station data. A limitation of this model is that it is complex. During the day, the ratio between the net and solar radiation was almost constant indicating a straight line was the best fit to the data (Figure 4.15):

$$R_n = -85.28 + 0.91 R_s \qquad (24)$$

where R_s is the solar radiation. Gay (1971), however, considers, that such simple regression models relating net and solar radiation are inadequate if they do not include a correction factor for longwave exchange as a function of shortwave exchange. This simple model should however provide a reasonable estimate of the net radiation. The effect of the sensitivity of the various evaporation formulations to equation 26 and the more detailed radiation model would make an interesting comparison.

4.3.3. *Bowen ratio, Penman, equilibrium and Priestley Taylor estimates of evaporation-(data from above the river)*

Meteorological data collected at the Gifkloof study site were used to calculate the river evaporation using the Penman, equilibrium and Preistley Taylor equations. These independent data could the be compared with the direct measurements made with the Bowen ratio technique. Solar radiation measured at the Gifkloof study site was used to estimate the hourly average of net radiation using the Campbell model. The 20 minute data were reduced to hourly data for these calculations. This was done to allow for later comparisons with the hourly land based data. In these calculations the available energy for evaporation was assumed to be equal to the net radiation since earlier measurements of G_s were found to be negligible for periods longer than one day.

The Penman derived techniques showed very similar trends to the Bowen ratio technique (Figure 4.16). The daily Bowen ratio evaporation increased from an average of approximately 4 mm in winter (DOY 182-242) to 10 mm by early November (DOY 305). The seasonal total (July to December) for the Bowen ratio technique was 1298 mm. The Priestley Taylor (1259 mm) and Penman (1207 mm) seasonal totals differed by only -3% and -9% respectively. The equilibrium

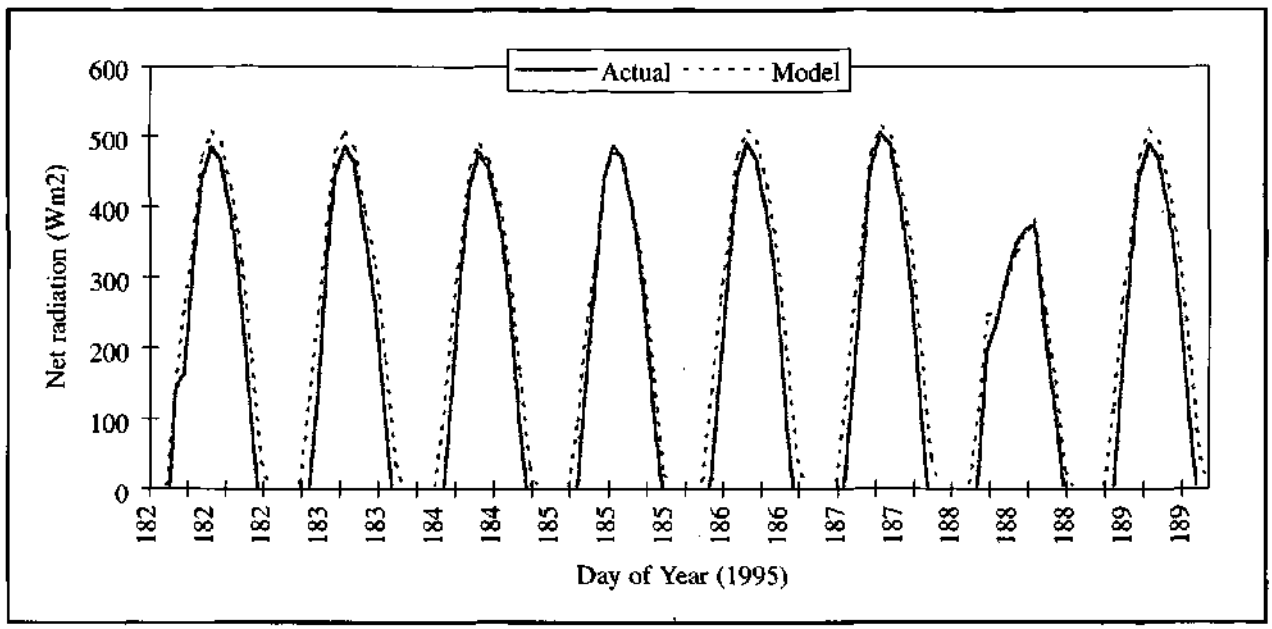

Figure 4.14. Comparison of modeled and measured net radiation over a 7 day period, July 1995.

Regression Statistics

Multiple R	0.986
R Square	0.973
Adjusted R Square	0.973
Standard Error	42.068
Observations	999.000

Analysis of Variance

	df	*Sum of Squares*	*Mean Square*	*F*	*Significance F*
Regression	1.0	62658114.5	62658114.5	35405.7	0.0
Residual	997.0	1764407.1	1769.7		
Total	998.0	64422521.6			

	Coefficients	*Standard Error*	*t Statistic*	*P-value*	*Lower 95%*	*Upper 95%*
Intercept	-85.282	2.066	-41.265	0.000	-89.336	-81.229
x 1	0.906	0.005	188.164	0.000	0.897	0.916

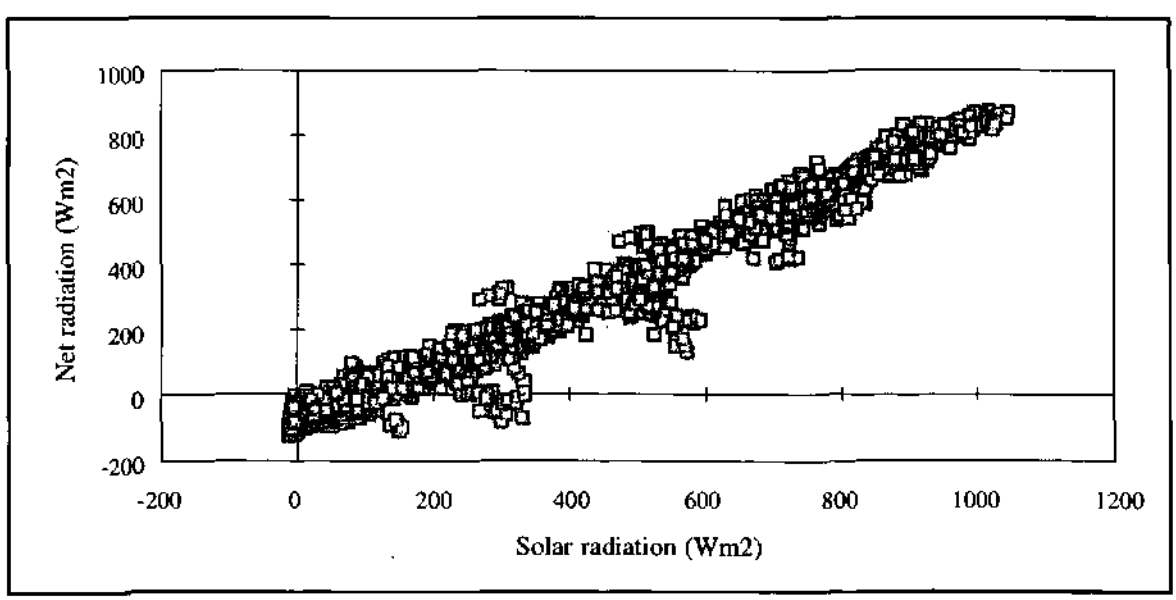

Figure 4.15. The relationship between hourly average values of solar and net radiation measured at the Gifkloof study site on the Orange river.

evaporation rate (999 mm) underestimated the Bowen ratio seasonal total by 23%. E_α (equation 13) gave data that were completely unrealistic due to the sensitivity of the method to the value of α . For this reason the results are not presented and no further analysis was attempted using this equation.

Figure 4.17 shows the Bowen ratio evaporation measurements plotted against the equilibrium evaporation rate. A regression analysis suggested that for the Orange River, the coefficient α has a value of about 1.21, which is similar to the 1.26 proposed by Priestley and Taylor. However, individual daily values showed a standard error of 1.3 mm, which suggests that, on a daily basis, the Priestley Taylor equation does not give an adequate description of the evaporation process. The implication of these results is that the aerodynamic term of the Penman formula is too variable to be represented as a constant proportion of the total evaporation. However, the results of this study show that for periods of a day or longer, both the Penman and Priestly Taylor equations give reasonable estimates (better than 10%) of the open water evaporation of the Orange River.

4.3.4 *Land based measurements*

Investigations were made into the relationship between meteorological measurements made over the water at Gifkloof to standard data measured at the Upington Weather Bureau (WB) station. All the data obtained from the WB were in tables and special programs had to be written to reformat the data into comma delineated ascii. The AWK software on the CCWR was used for this purpose.

4.3.4.1 Solar Radiation.

Very little difference was expected between the solar radiation of the two sites which were in close proximity to each other. Figure 4.18 showed, however, that this assumption was not correct. Although the slope of the lines were identical, there was an offset difference of approximately 100 Wm^{-2}. One of the sensors was presumably not calibrated or installed correctly (i.e. wrong offset but correct multiplier). For the purposes of modelling the evaporation from the land the WB sensor was presumed to be correct and no adjustments were made to the data.

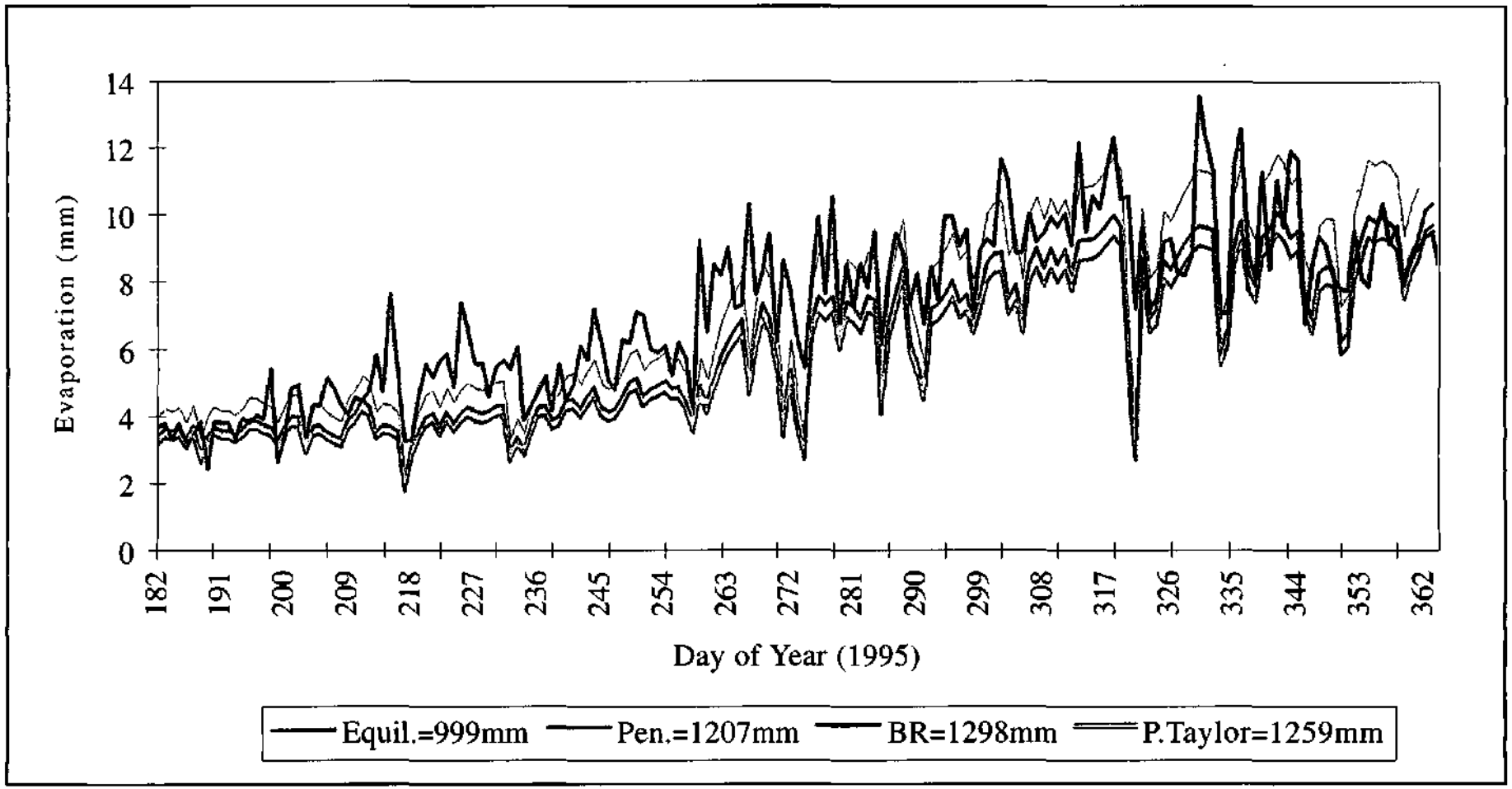

Figure 4.16. Daily estimates of evaporation from the Orange River using the Bowen ratio, Priestly Taylor, Penman and equilibrium techniques. Data obtained from the Gifkloof study site situated in the Orange river.

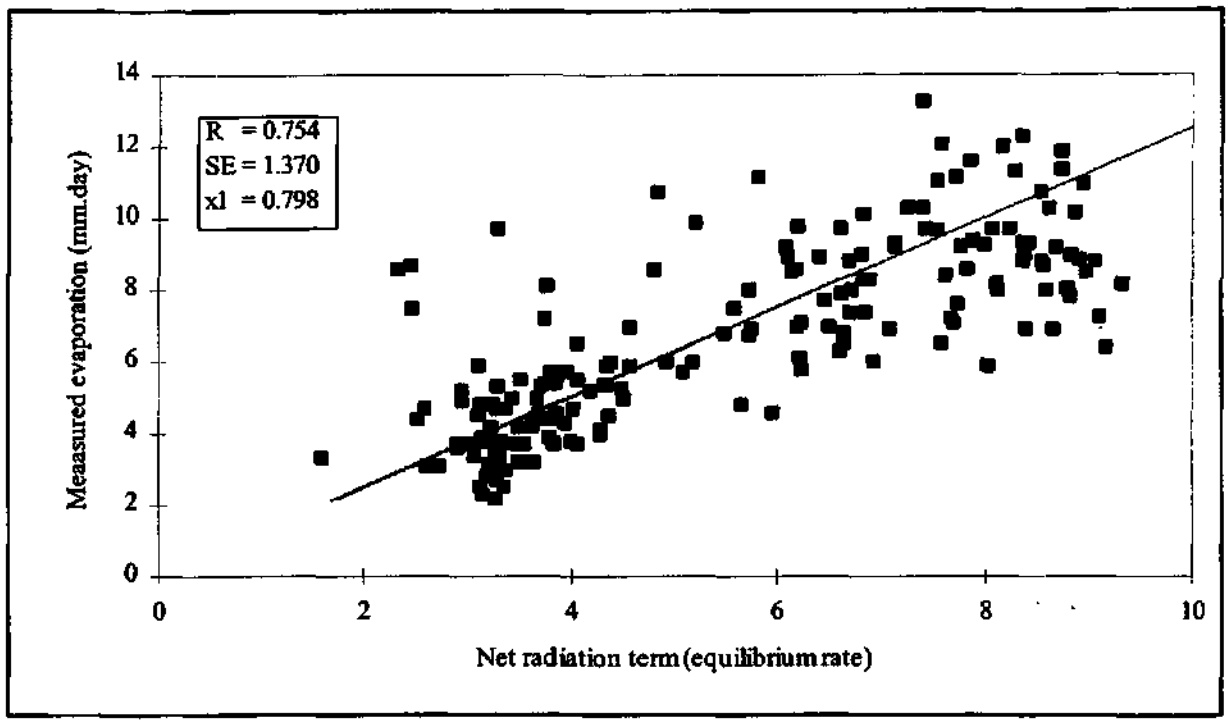

Figure 4.17. Daily total Bowen ratio evaporation measurements plotted against the daily equilibrium rate.

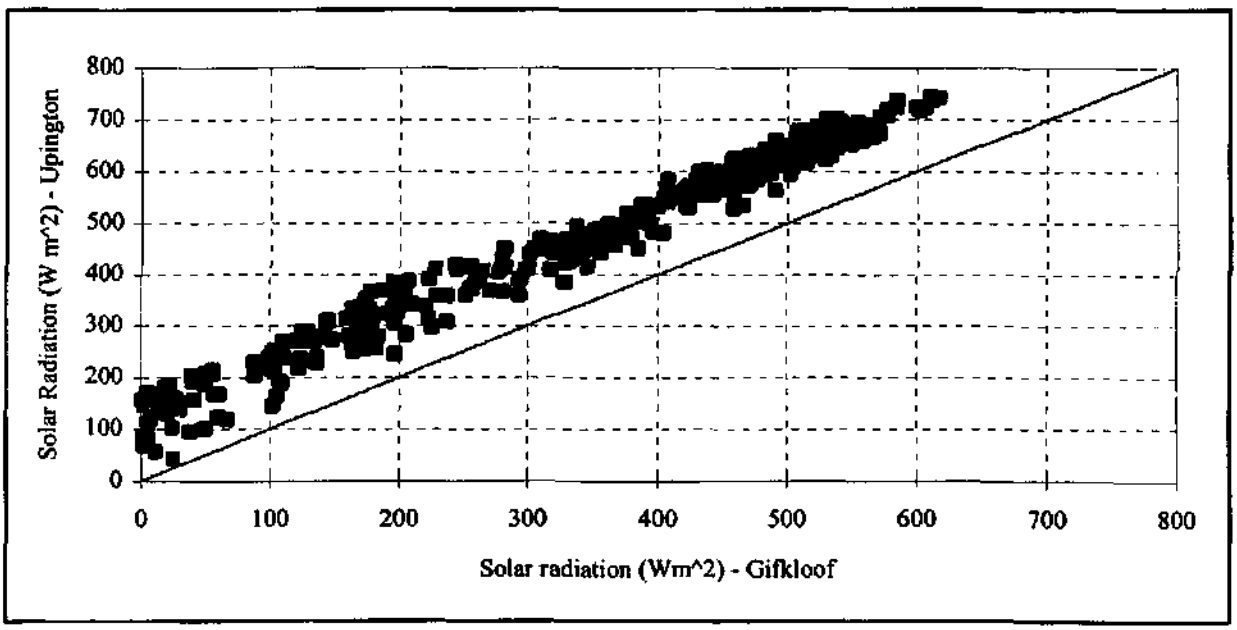

Figure 4.18. The relationship between solar radiation measured at the Gifkloof study site and at the Upington weather station.

4.3.4.2 Temperature.

The trend in the hourly changes in ambient air temperature above the river and over the land surface were very similar. A linear regression on these data resulted in a r^2=0.96, a slope of 0.89 and intercept of 1.52°C (Figure 4.19). This would imply that the temperature over the land was marginally warmer than over the river. For example a temperature of 30°C translates into 28.3°C at the river. The hourly weather data were all adjusted using this relationship.

4.3.4.3 Relative Humidity.

Although the trend in the hourly changes in relative humidity above the river and over the land surface were similar, the extremes were greater over the land. This implies that the conditions were more stable over the water. A plot of the relative humidity from the Orange River and Upington revealed a cloud of data points with a rather unusual shape (Figure 4.20). These data showed quite clearly that the relative humidity at Gifkloof never dropped below 10%, while this was often the case at Upington. Because the relative humidity is not a unique value, the vapour pressure obtained directly from the PC207 probe and a vapour pressure calculated from the RH at Upington (Figure 4.20) were used in subsequent analyses. By manipulating the data it was found that there is a distinct seasonal relationship between the vapour pressure at the river and over the land. Three distinct groups were identified which corresponded with the seasons winter, spring and summer (Figure 4.21 a-c). In winter the relationship is linear, becoming exponential as the season progresses. This relationship is strongest in November and December. The best non-linear fit was found by using a first order exponential of the form :

$$y = B_1 * EXP(B_2 * X)$$

The regression statistics are included in Figure 4.21. Coefficients of determination of 0.96, 0.62 and 0.76 were obtained for winter, spring and summer respectively. The coefficients determined in this way were used to correct the Upington data.

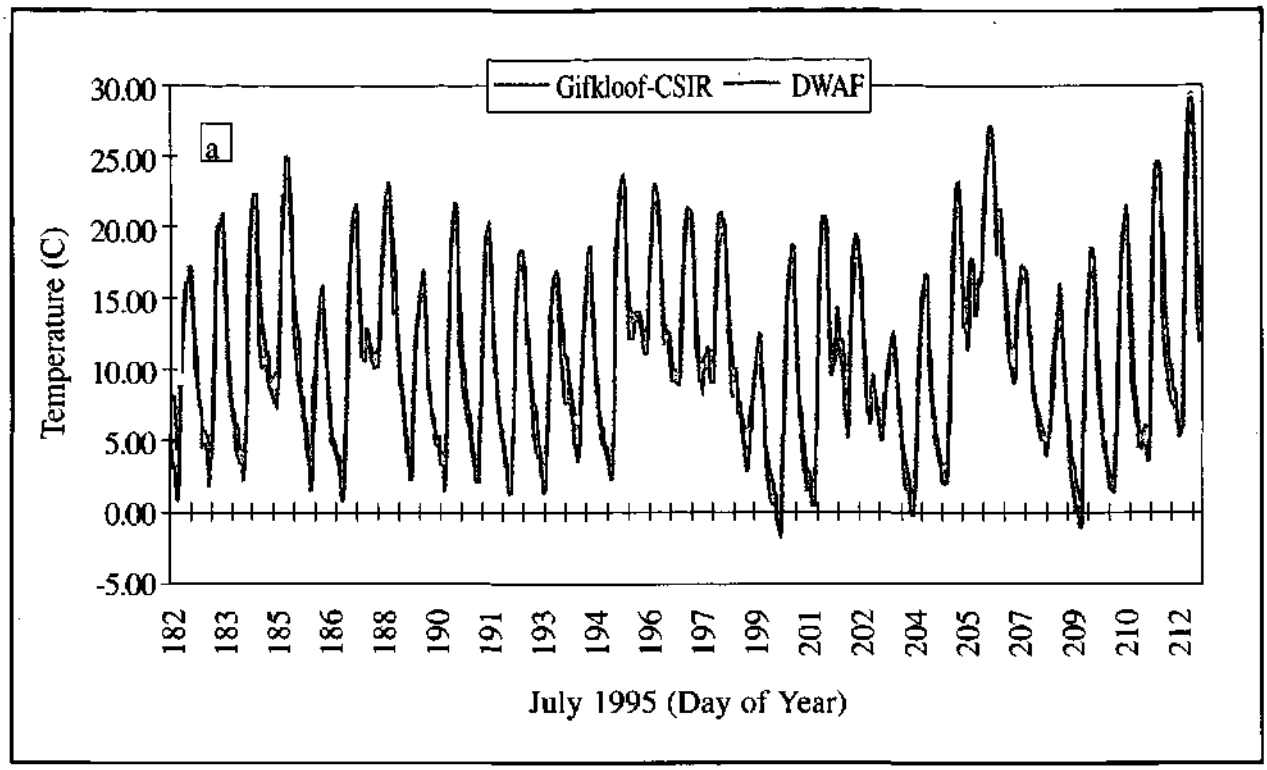

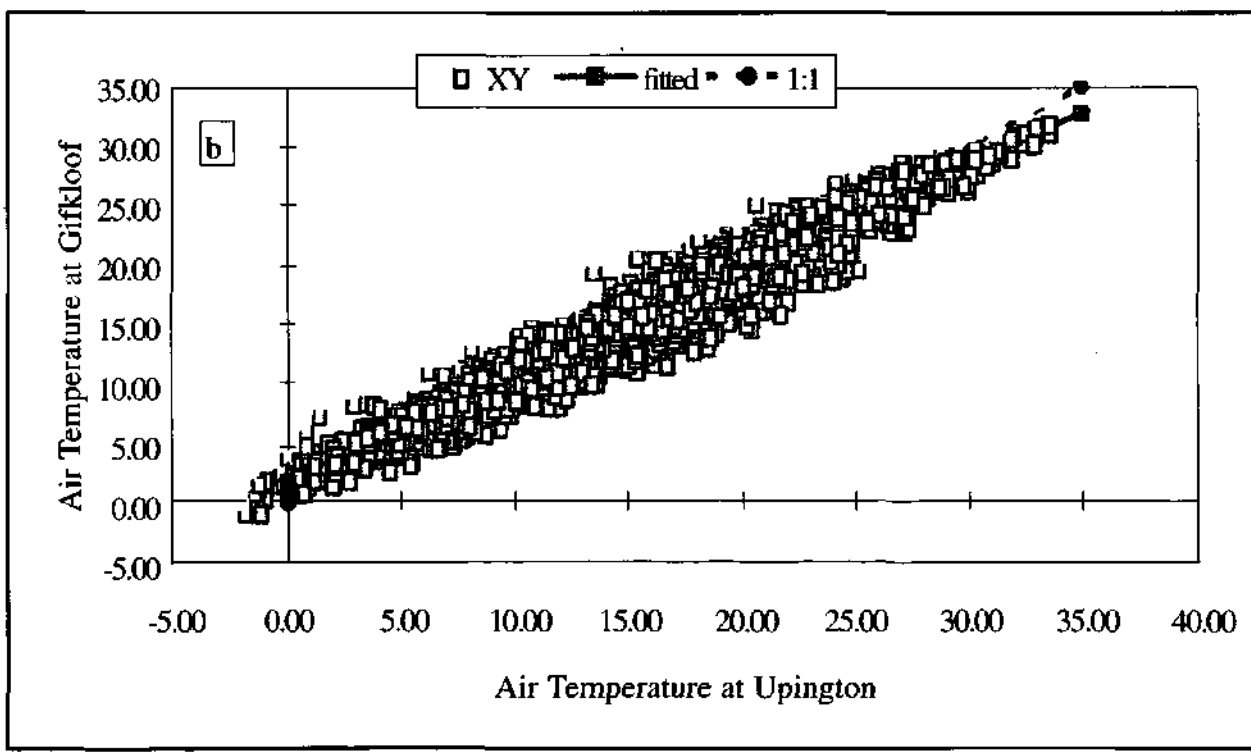

Figure 4.19. (a) The hourly course of temperature at Gifkloof-CSIR and Upington-DWAF during July 1995. (b) The relationship between the river (Gifkloof) and land based (Upington) measurements.

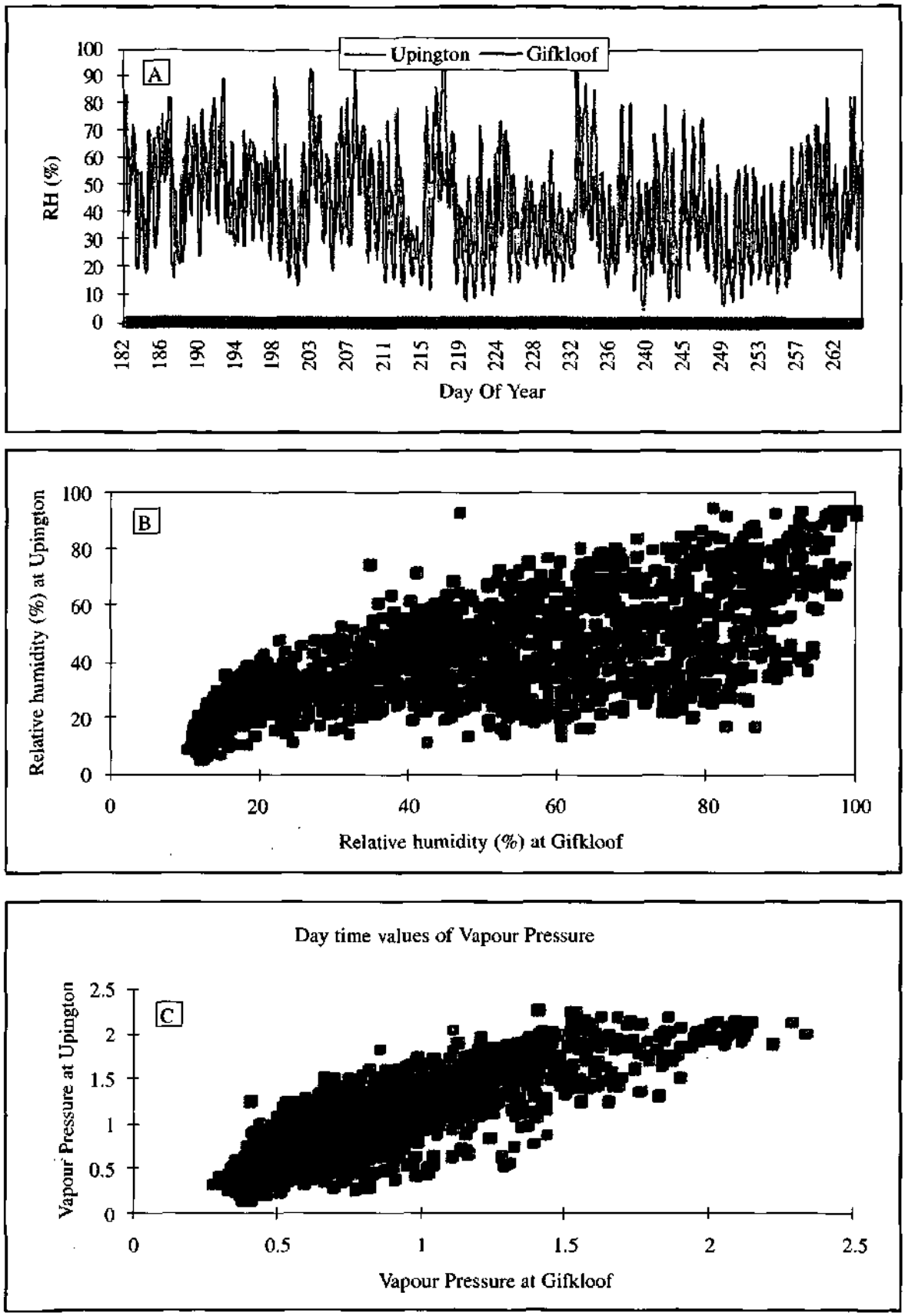

Figure 4.20. (A) The hourly course of relative humidity at Gifkloof and Upinton. (B) the relationship between RH at Gifkloof (river) and Upington (land). (C) The relationship between vapour pressure (kPa) at Gifkloof and Upington.

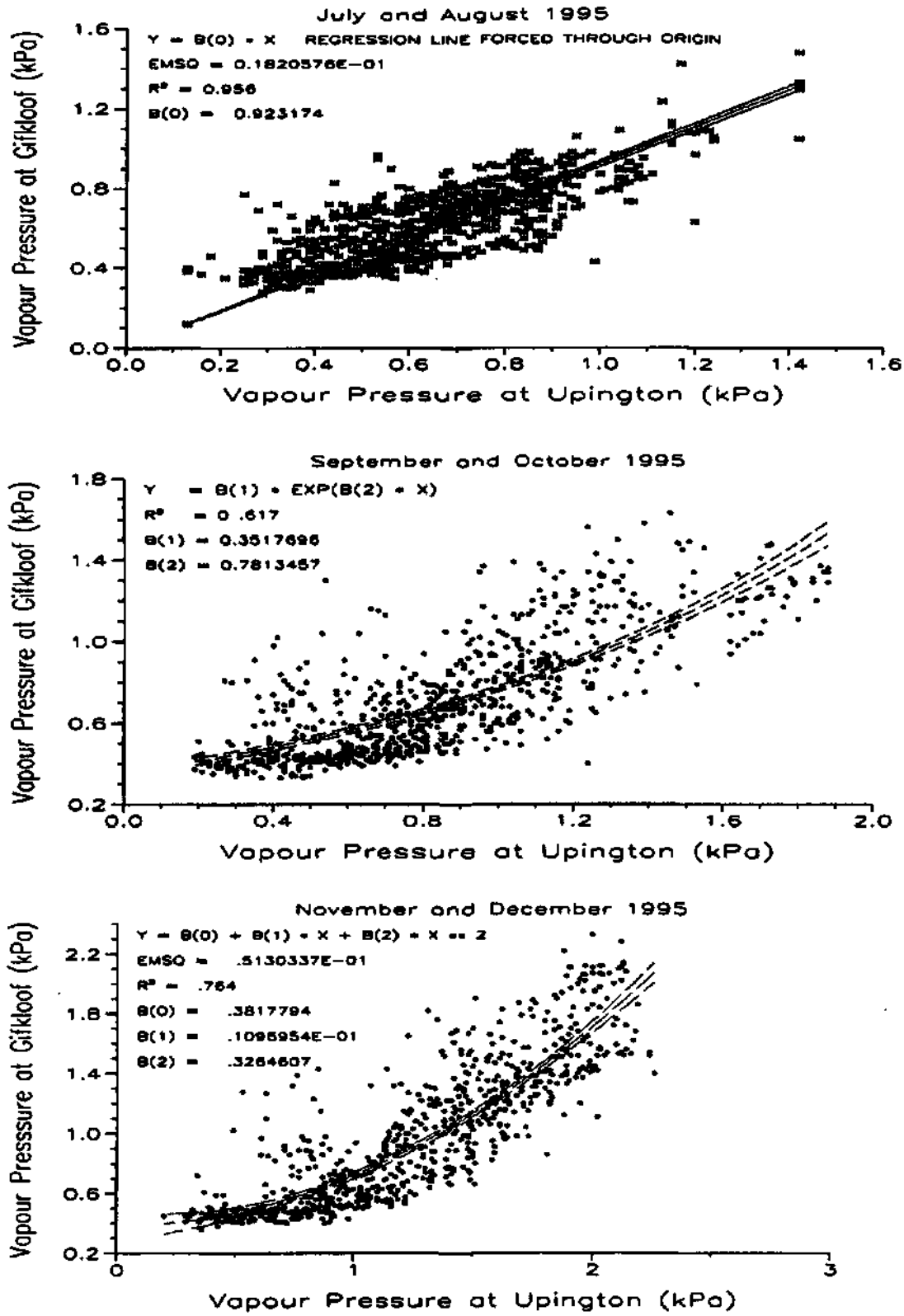

Figure 4.21 a-c. The seasonal trend in the relationship between the vapour pressure (kPa) at Gifkloof (river) and Upington (land).

The Penman evaporation estimated over the period July to December (DOY 182 - 365) on unadjusted (1072 mm) and adjusted (1057 mm) Upington weather station data showed little difference in the daily evaporation (Figure 4.22). This indicates that adjusting the data is not necessary.

The Penman evaporation calculated for the same period using the Gifkloof river data (1082 mm) was only 10 mm higher than the Upington data. An exception to this was the period from DOY 220 to DOY 262 when the Gifkloof data exceed the other estimates by about 1mm per day. These data show that land based weather data can be successfully used to predict the climate of the Orange River.

4.3.5 *Evaporation along the Orange River*

Meteorological data from the three stations representing the upper, middle and lower reaches of the Orange River were used to investigate the differences in evaporation along the Orange River. The weather variables required to run the evaporation model were solar radiation, air temperature, a measure of atmospheric humidity (relative humidity, wet bulb temperature or vapour pressure), and wind speed. Data from 1994 and 1995 were used in the analysis.

4.3.5.1. Rainfall

Rainfall along the river in 1994 decreased from 238 mm at Bleskop, to 156 mm at Upington and to only 32 mm at Vioolsdrif (Figure 4.23 a & b). A similar trend was shown in 1995 (276:116:60 mm). Rainfall in the lower reaches is therefore not an important factor affecting the evaporation process since it is a small amount in terms of the total amount evaporated.

4.3.5.2. Solar radiation

The seasonal trend in solar radiation was similar at all three sites for both 1994 and 1995. For example in 1995 the total radiation was 7300, 7677 and 7862 MJ for Bleskop, Upington and Vioolsdrif respectively (Figure 4.24). The lower radiation in the upper reaches is probably a result of the increased cloud cover in this area. The fact that the daily totals are very similar on cloudless days is not surprising as the entire Orange River lies roughly along the same line of

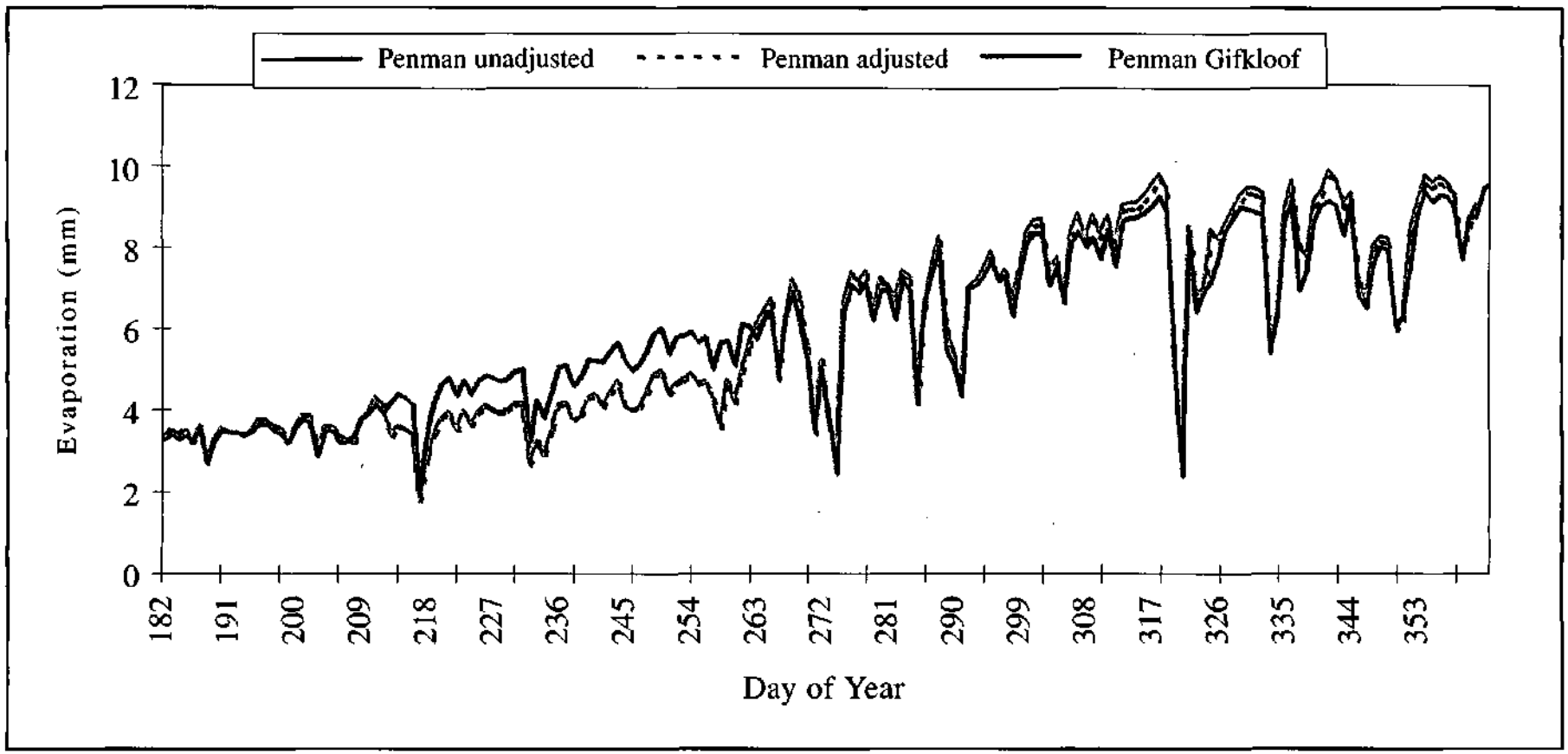

Figure 4.22. The Penman equation calculated using river data (Gifkloof) and land based weather data (unadjusted and adjusted).

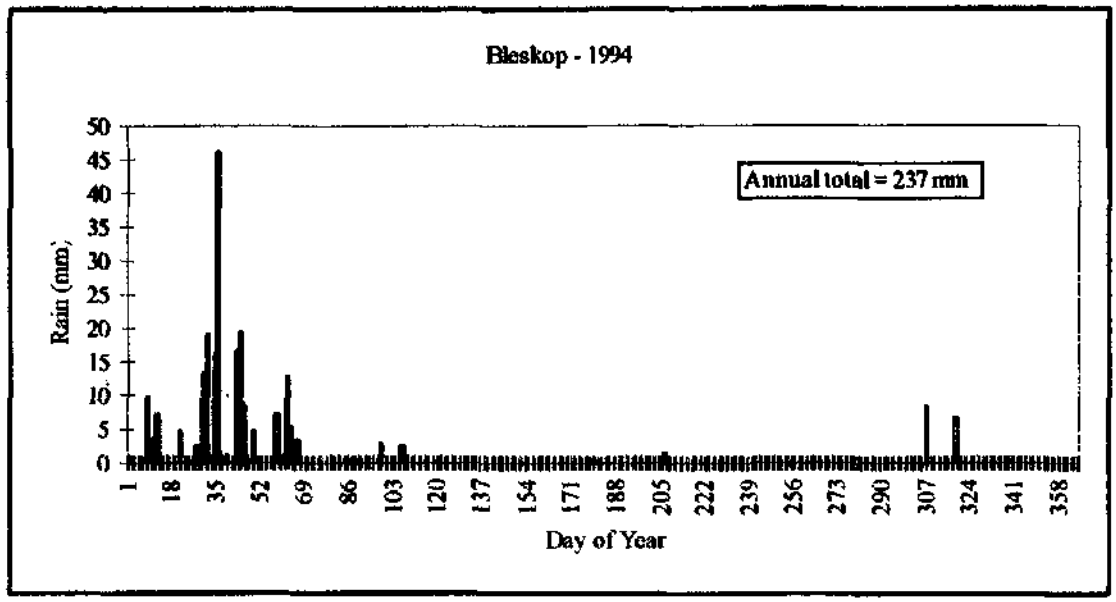

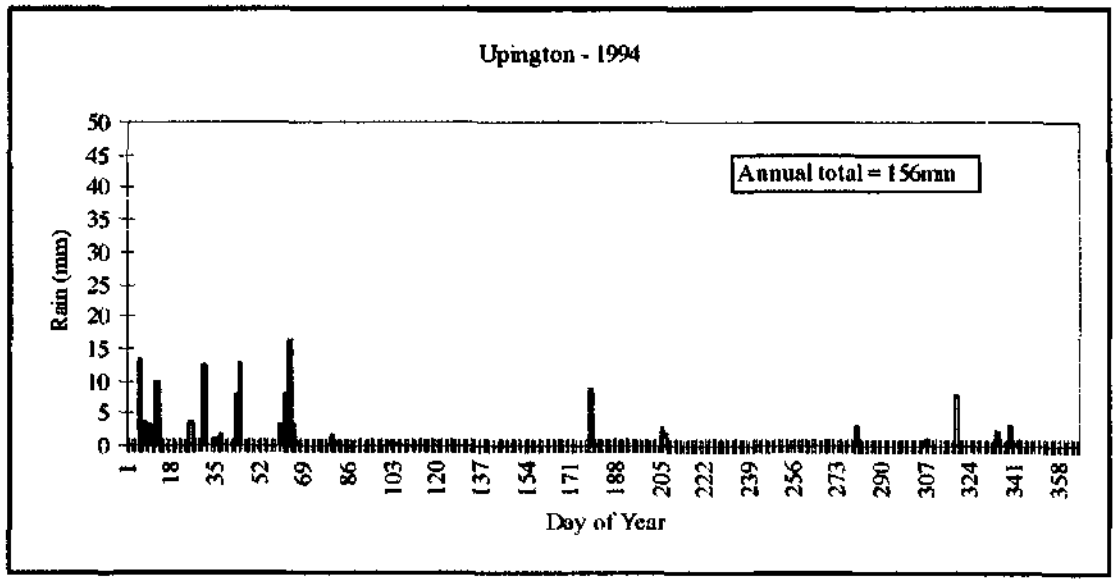

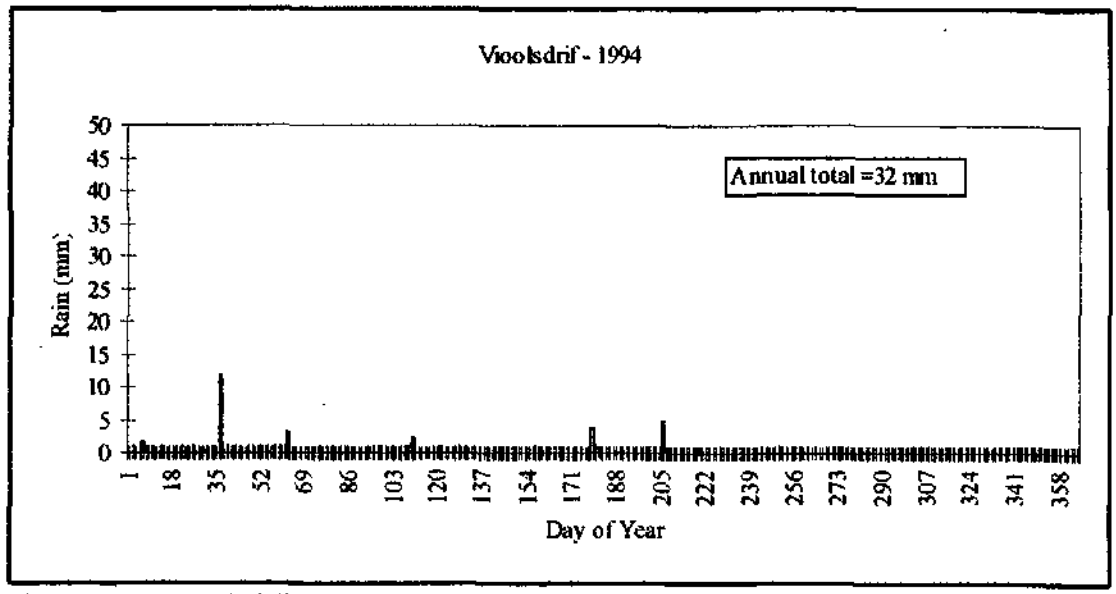

Figure 4.23 a. Rainfall at three sites along the Orange river during 1994.

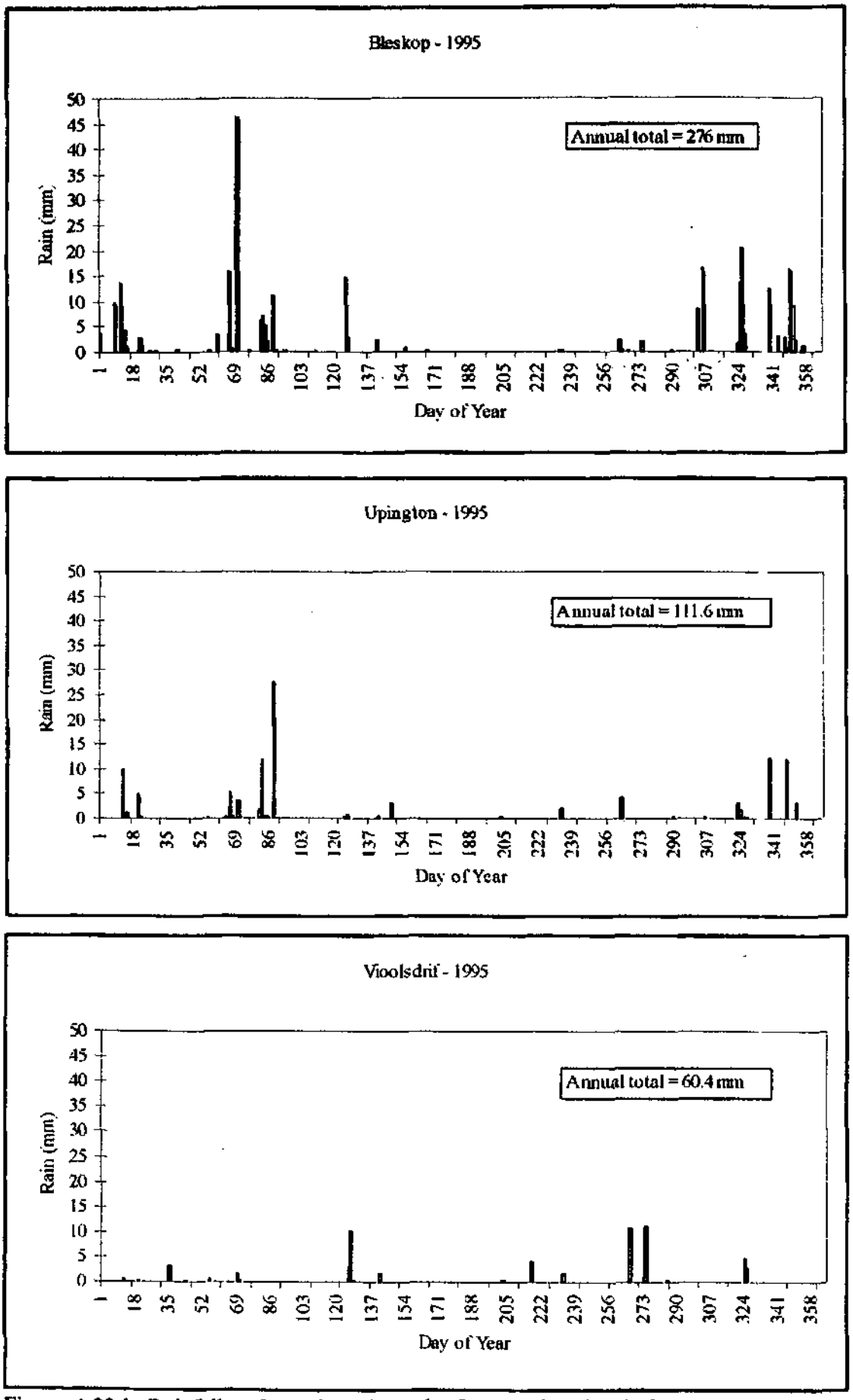

Figure 4.23 b. Rainfall at three sites along the Orange river in 1995.

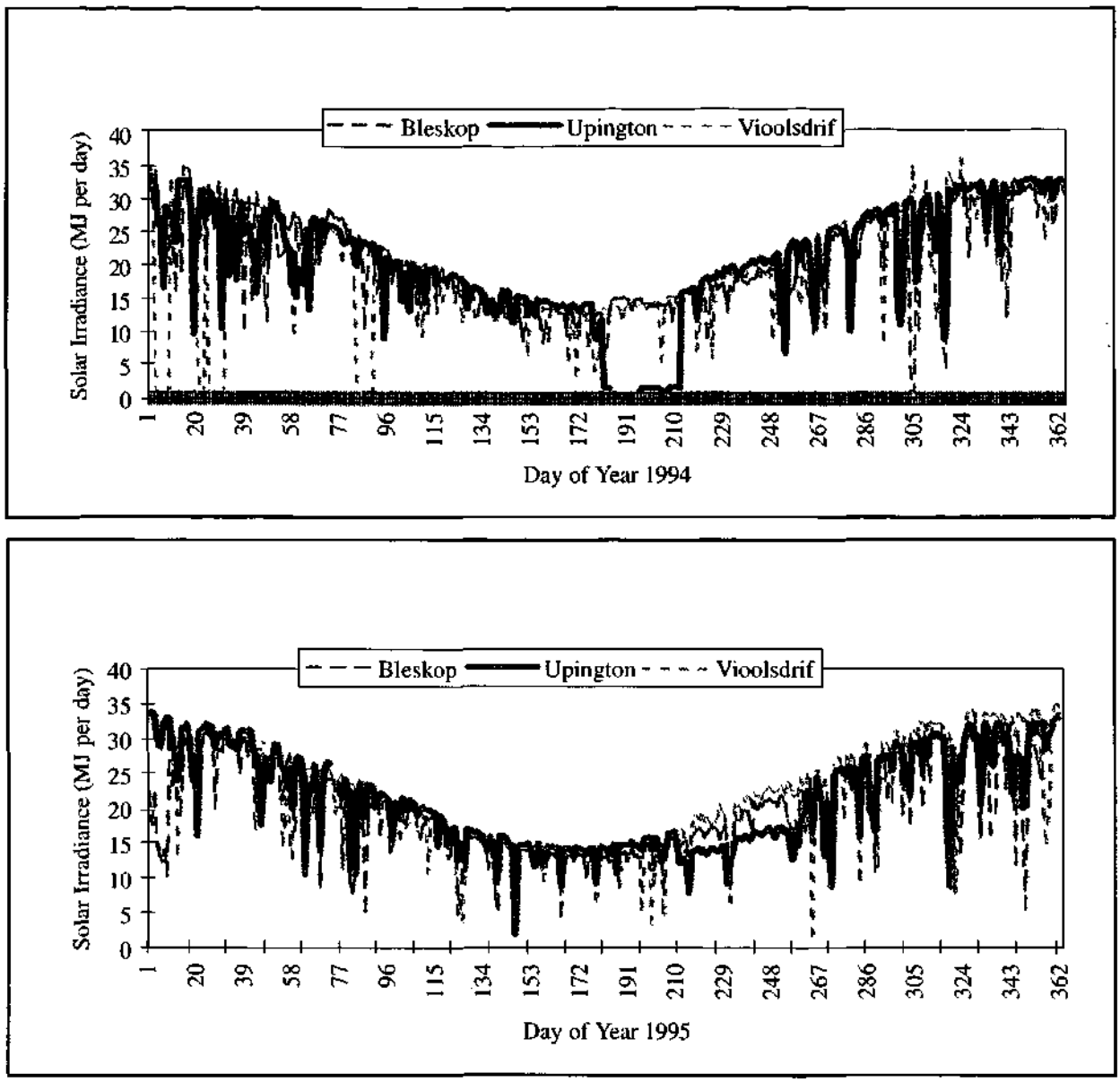

Figure 4.24. Solar radiation (MJ per day) at three sites along the Orange river during 1994 and 1995.

latitude. Daily totals varied from approximately 35 MJ day^{-1} in mid summer to 15 MJ day^{-1} in winter. Although radiation is not measured at all the weather stations along the river, these results show that it would be possible to estimate solar radiation accurately from neighbouring stations.

4.3.5.3. Wind

Wind speeds along the river were very variable during both 1994 and 1995 with daily average windspeeds varying between 0 and 9 ms^{-1} (Figures 4.25). Upington (1994: $\bar{x}$=3.9 ms^{-1}; 1995: $\bar{x}$ = 4.1 ms^{-1}) was much windier than either Bleskop (1994: $\bar{x}$=1.9 ms^{-1}; 1995: $\bar{x}$ = 2.0 ms^{-1}) or Vioolsdrif (1994: $\bar{x}$=2.0 ms^{-1}; 1995: $\bar{x}$ = 2.4 ms^{-1}). There could be many reasons why the Upington area is twice as windy as either Bleskop or Vioolsdrif, although the most likely is the way different pressure cells or frontal systems develop over the western portion of southern Africa.

4.3.4.4. Temperature

All three sites followed similar cycles in daily temperatures with summer highs of 30-35 °C and winter lows between 5 - 15°C (Figure 4.26). There is very strong temperature gradient along the river with annual means of 18.2, 20.7 and 22.5 °C for Bleskop, Upington and Vioolsdrif respectively. Large differences were observed in the daily mean temperature with Vioolsdrif being up to 20 °C hotter than Bleskop and 7 °C hotter than Upington (Figure 4.26).

4.3.4.5. Relative Humidity

Mean daily relative humidity varied widely with no clear seasonal trend in the data (Figure 4.27). An analysis of the differences between the various sites indicated that Upington is generally drier (less humid) than Vioolsdrif or Bleskop. Surprisingly Vioolsdrif is also on average more humid than Bleskop.

4.3.4.6. Evaporation

The 1994 and 1955 meteorological data for the Bleskop, Upington and Vioolsdrif weather stations was used to calculate the Priestley Taylor hourly evaporation. In the model the land based data were adjusted to conditions at the river using the relationships developed between the

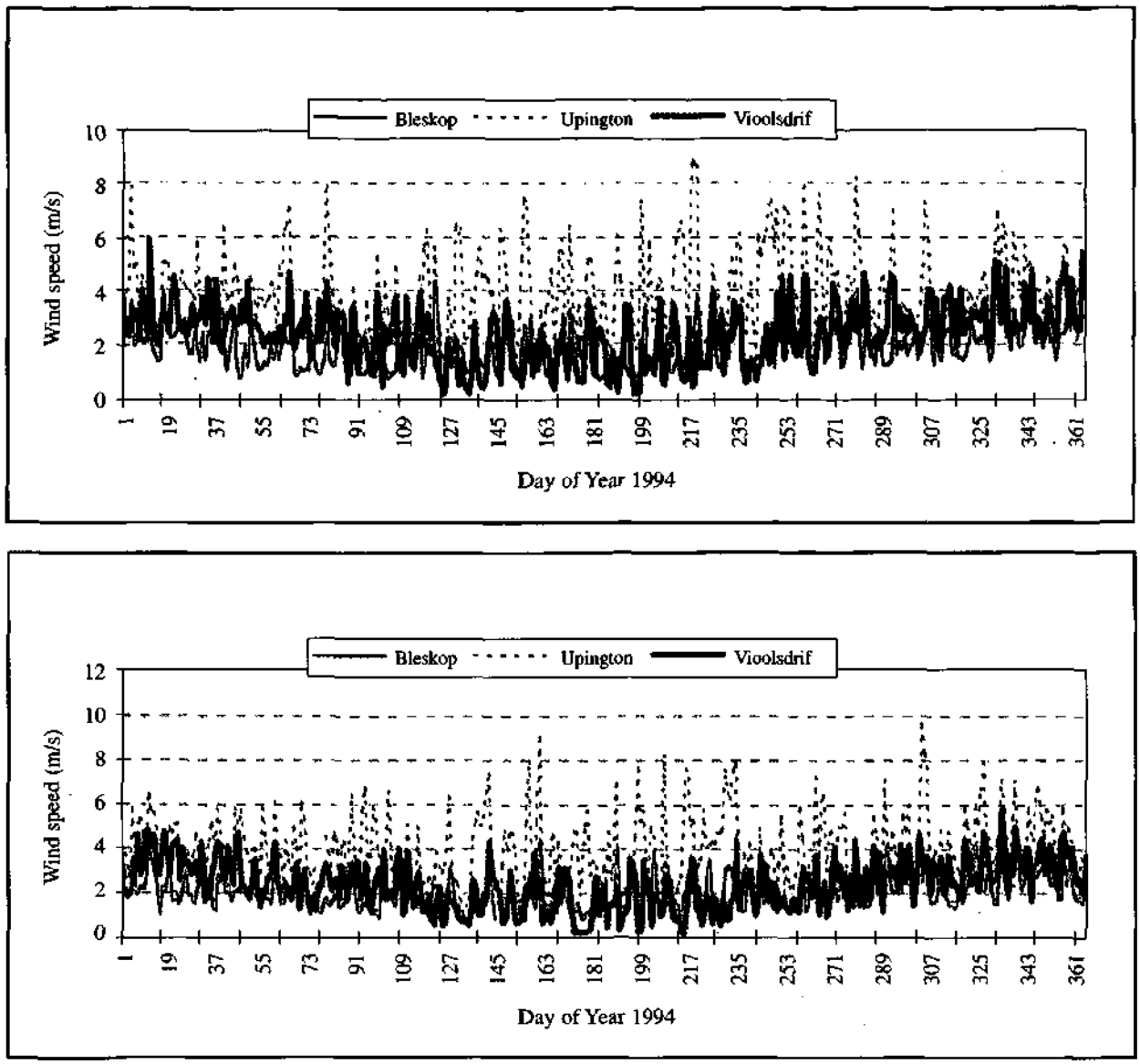

Figure 4.25. Average wind speed at three sites along the Orange River during 1994 and 1995.

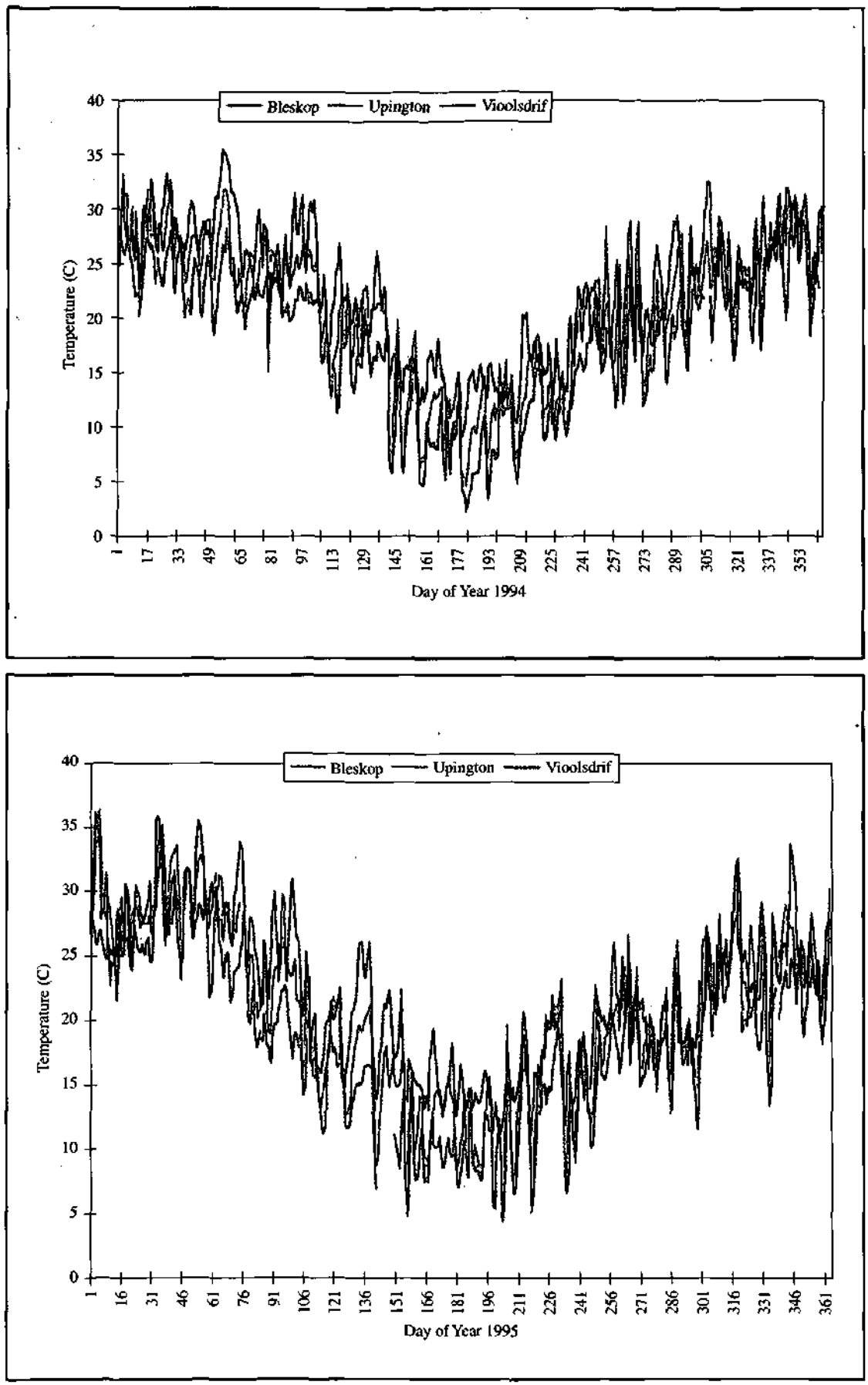

Figure 4.26. Daily average temperature at three sites along the Orange river during 1994 and 1995

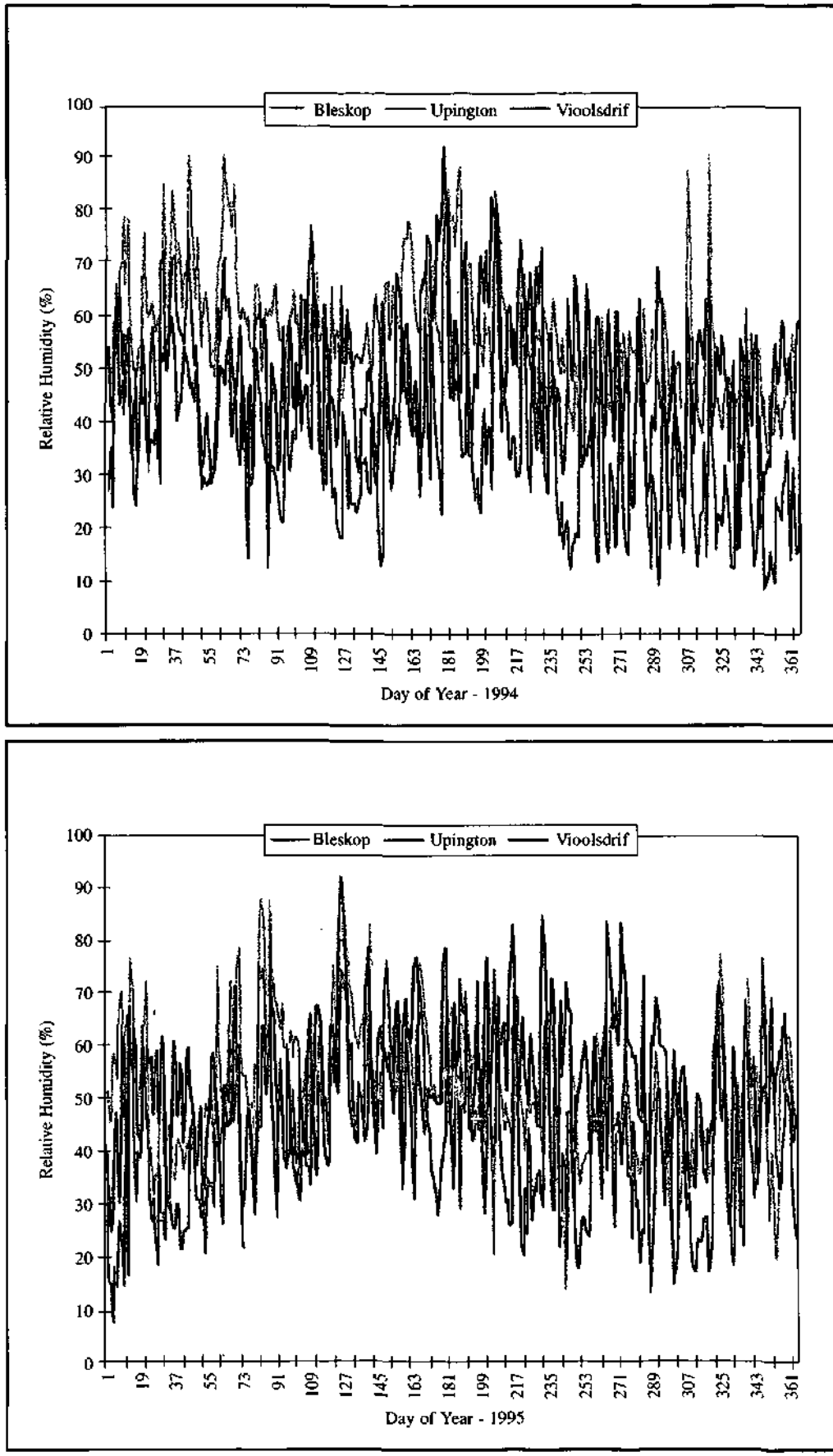

Figure 4.27. Daily average relative humidity at three sites along the Orange river during 1994 and 1995.

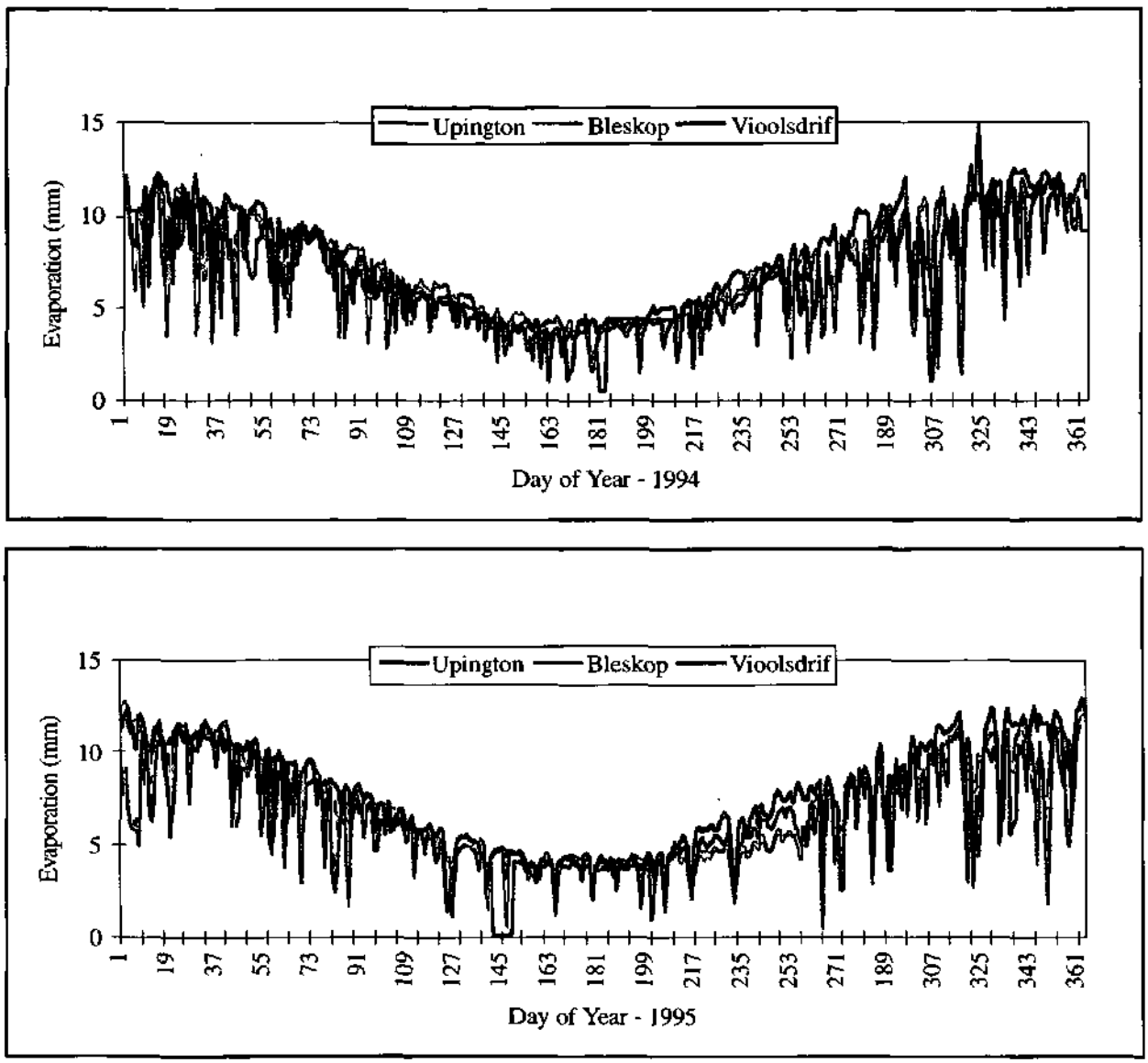

Figure 4.28. Priestly Taylor evaporation at three sites along the Orange river during 1994 and 1995.

river at Gifkloof and the Upington weather station. These data were then summed into daily totals (*Figure 4.28*). *Daily evaporation along the river in 1994 and 1995 was very high in summer*, estimates on cloudless days being greater than 10 mm day^{-1} for about four months of the year. During the winter months the daily evaporation dropped to approximately 5 mm/day. The trends in 1994 and 1995 were very similar. Differences between the stations are not easily distinguishable from the graphs, but become clear by examining the annual totals (Table 4.4). In 1994 the annual totals at Upington and Vioolsdrif were very similar (2541 and 2539 mm respectively), while at Bleskop the evaporation was approximately 200 mm lower (2351 mm). During 1995 there was a trend of increasing evaporation along the river, Vioolsdrif being 377 mm higher than Bleskop and 115 mm higher than Upington.

Table 4.4 Annual totals of evaporation (mm) at three sites along the Orange River.

Station	1994		1995	
	P- Taylor	Penman	P- Taylor	Penman
Bleskop	2351	1987	2332	1958
Upington	2541	2115	2593	2208
Vioolsdrif	2539	2222	2705	2308

The Priestley Taylor evaporation data for 1994 and 1995 were used to estimate the river losses for various flow rates using the most recent surface areas calculated by BKS Inc (Table 4.5 a & b, McKenzie and Craig, *in press*). As evaporation data were not available for each reach of the river the values for Bleskop, Upington and Vioolsdrif were simply extended to neighbouring reaches. River losses varied between 516 and 815 million m^3 $annum^{-1}$ in 1994 for the lowest (60 m^3 s^{-1}) and highest (400 m^3 s^{-1}) flows respectively. In 1995 the higher evaporation increased the losses to 532 and 841 million m^3 $annum^{-1}$. McKenzie and Craig (in press) using the same areas and flow rates and an evaporation estimate based on corrected A-pan data (+8%), found corresponding values of 595 and 939 million m^3 $annum^{-1}$. Since their data are based on a long term average, it is possible that the low values of this study are a result of 1994 and 1995 being cooler years than the long term average. It is very encouraging that both sets of independently collected data are of the same order of magnitude. The main finding of this study is that irrespective of the method used, transmission losses along the Orange River are very high. A complete analysis of the historical weather data along the Orange River would provide valuable insights into the annual variation in river losses.

Table 4.5.a. Estimates of Orange river transmission losses per reach for different flow rates (surface areas) using the 1994 Priestley Taylor evaporation data.

NReach	From	To	Gross Evap	Rainfall (mm)	FLOW (m3/s)				AREA (Ha)				AREA (Ha)		LOSSES (Mm3/a)		
					LOW	LMED	HMED	HIGH	LOW	LMED	HMED	HIGH	REEDS	TREES	LMED	HMED	HIGH
1	Vanderkloof	Marksdrift	2351	238	20	58	120	400	1,400	1,868	2,270	3,135	50	772	45.63	54.13	71.14
2a	Marksdrift	Prieska	2351	200	19	52	107	385	1,860	2,440	2,940	3,918	120	842	61.02	71.77	89.71
2b	Prieska	Boegoberg	2451	170	18	47	99	380	1,180	1,500	1,800	2,380	100	348	39.34	46.18	56.67
3a	Boegoberg	Gifkloof	2541	156	16	39	84	365	2,050	2,500	2,950	4,000	133	993	70.54	81.27	102.51
3b	Gifkloof	Neusberg	2541	156	14	31	72	352	980	1,250	1,620	2,600	171	604	39.01	47.84	66.33
4	Neusberg	20°E	2541	120	12	23	58	340	770	900	1,100	1,626	150	506	29.82	34.66	43.04
5a	20°E	Pella	2541	90	11	21	53	335	1,580	1,850	2,300	3,500	144	597	53.97	65.00	90.17
5b	Pella	Vlooisdrift	2539	32	9	18	48	330	1,950	2,300	2,900	4,350	242	740	70.51	85.55	114.62
6	Vlooisdrift	Fish	2539	30	7	14	42	325	1,200	1,400	1,850	3,050	309	468	47.96	59.25	80.05
7	Fish	Mouth	2539	30	7	12	39	320	1,370	1,600	2,150	3,750	375	949	58.57	72.37	101.23
Total	Vanderkloof	Mouth	2493.4	122.2	20	58	120	400	14,340	17,608	21,880	32,309	1,794	6,819	516.36	618.01	815.46
													Reed Factor	Tree Factor			
													1.2	0.3			

Table 4.5.b. Estimates of Orange river transmission losses per reach for different flow rates (surface areas) using the 1995 Priestley Taylor evaporation data.

NReach	From	To	Gross Evap	Rainfall (mm)	FLOW (m3/s)				AREA (Ha)				AREA (Ha)		LOSSES (Mm3/a)		
					LOW	LMED	HMED	HIGH	LOW	LMED	HMED	HIGH	REEDS	TREES	LMED	HMED	HIGH
1	Vanderkloof	Marksdrift	2332	276	20	58	120	400	1,400	1,868	2,270	3,135	50	772	44.40	52.67	69.22
2a	Marksdrift	Prieska	2332	200	19	52	107	385	1,860	2,440	2,940	3,918	120	842	60.48	71.14	88.92
2b	Prieska	Boegoberg	2500	170	18	47	99	380	1,180	1,500	1,800	2,380	100	348	40.18	47.17	57.89
3a	Boegoberg	Gifkloof	2593	112	16	39	84	365	2,050	2,500	2,950	4,000	133	993	73.38	84.54	106.63
3b	Gifkloof	Neusberg	2593	112	14	31	72	352	980	1,250	1,620	2,600	171	604	40.58	49.76	69.00
4	Neusberg	20°E	2593	90	12	23	58	340	770	900	1,100	1,626	150	506	30.83	35.84	44.50
5a	20°E	Pella	2593	60	11	21	53	335	1,580	1,850	2,300	3,500	144	597	55.77	67.17	93.19
5b	Pella	Vlooisdrift	2705	60	9	18	48	330	1,950	2,300	2,900	4,350	242	740	74.39	90.26	120.93
6	Vlooisdrift	Fish	2705	60	7	14	42	325	1,200	1,400	1,850	3,050	309	468	50.56	62.46	84.39
7	Fish	Mouth	2705	60	7	12	39	320	1,370	1,600	2,150	3,750	375	949	61.74	76.29	106.72
Total	Vanderkloof	Mouth	2565.1	120	20	58	120	400	14,340	17,608	21,880	32,309	1,794	6,819	532.32	637.30	841.37
													Reed Factor	Tree Factor			
													1.2	0.3			

Note: The areas and algorithms used to calculate the losses were kindly supplied by Andrew Craig of BKS Inc.

CHAPTER 5

Conclusions

This study is the first of its kind in South Africa whereby detailed energy balance estimates of evaporation have been performed for a flowing river. The Bowen ratio technique has provided valuable insights into the surface energy budget of the Orange River.

Comparison between evaporation data collected from the Bowen ratio above the Orange River and A-pan evaporation indicate that pan data are approximately 8% lower than the energy balance technique. Regression analysis between the A-pan and Bowen ratio showed that the A-pan can be used to predict transmission losses from the Orange River. However, the large scatter found in pan data, associated with the inherent problems that arise from poor installation and maintenance, make pan data potentially unreliable. If pan data are used they should be obtained from organisations which maintain high standards of meteorological observation, such as the South African Weather Bureau.

Evaporation from the Orange River was modelled using the energy balance approach (Priestley Taylor and Penman formulations) from standard weather data measured along the extent of the river. The measurements used are dry bulb temperature, relative humidity (2 m height), wind speed and solar radiation. Comparison of the Priestley Taylor equation with direct measurements using the Bowen ratio energy balance approach showed small errors (approximately 3% or 0.2 mm day^{-1}). This close agreement substantiates the finding of Priestley Taylor (1972) and Stewart and Rouse (1977) that the aerodynamic term $\propto$ can be represented by a factor of 1.26. Their results are normally applicable to small lakes ($\approx$ 0.1-35 km^2). This study has shown that the Priestley Taylor model is also applicable to a large river running through an arid region where advective conditions are extreme. Strictly speaking this conclusion is contrary to the original concept they proposed as they restricted themselves to advection free conditions.

The Penman equation underestimated the river evaporation by about 9% (0.6 mm day^{-1}), while the equilibrium evaporation rate underestimated the Bowen ratio seasonal total by 23%.

Algorithms developed for adjusting the land based weather data to approximate the river conditions had little effect on the overall evaporation loss. Therefore adjusting the land based weather data to river conditions is not necessary. It was shown that the net radiation can be modelled very accurately from standard weather station data, an essential requirement when using the energy balance approach. Simple linear models are also proposed for predicting the surface albedo and net radiation.

There is a climatic gradient down the Orange River which results in a increase in the evaporation by as much as 380 mm or 0.3 mm km^{-1} between Bleskop and Vioolsdrif. The high annual evaporation measured from the Orange River (2500-2700 mm) in this study confirm that transmission losses are a major component of the water balance. These evaporation data translate into river losses that vary between 516 and 841 million m^3 $annum^{-1}$ for the low (60 m^3 s^{-1}) and high (400 m^3 s^{-1}) flows respectively. These findings are in agreement with A-pan based estimates of river losses determined by McKenzie and Craig (1977, in press).

5.1 Acknowledgements

The Water Research Commission are gratefully acknowledged for their financial support of the project and the Department of Water Affairs (particularly Stanley Chamberlain and Kraai Luus) for their help with the field studies. Ronnie McKenzie and Andrew Craig of BKS are thanked for their assistance in providing the weather data and other information.

Members of the steering committee are thanked for their support and guidance during the study.

5.2 References

Anderson, E. R., (1972). Energy-budget studies. In: Water-Loss Investigations: Lake Hefner Studies. Tech. Rep., U.S. Geol. Surv., Prof. Pap., **269**, 17-34.

Ficke, J.F., (1972). Comparison of evaporation computation methods, Pretty Lake, La Grange Country, northeastern Indiana. U.S. Geol. Surv., Prof. Pap., **686-A**, 49pp.

Gay, L.W., (1971). The regression of net radiation upon solar radiation. *Agric. Meteorol.* **8**: 39-50

Green, G. C. (1985). (ed.) Estimated irrigation requirements of crops in South Africa. Department of Agriculture and Water Supply, *Memoirs on the Agricultural Natural Resources of South Africa*, Soil and Irrigation Research Institute, Pretoria. **2**, pp857.

Hope, A. S. and Mulder, G. J. (1979). Hydrological investigations of small catchments in the Natal coastal belt and the role of physiography and landuse in the rainfall-runoff process. University of Zululand, Kwa Dlangeza. Series B. No.2.

Keijman, J.Q., (1974). The estimation of the energy balance of a lake from simple weather data. *Boundary-Layer Meteorology* 7: 399-407.

McKenzie and Craig (1977, in press). The application of hydraulic modelling in calculating evaporation losses from South African rivers. Paper submitted to the International Conference on River Flood Hydraulics, November 1997.

Mckenzie, R.S. & Roth, C., (1994). The evaluation of river losses from the Orange River downstream of the PK Le Roux dam. WRC Report No. 510/1/94.

McKenzie, R. S., Roth, C. and Stoffberg (1993). Orange River losses. Sixth South African National Hydrological Symposium, Pietermaritzburg.

Oguntoyinbo, J. S. (1974). Land use and reflection coefficient (albedo) map for southern parts of Nigeria. *Agric. Meteorol.* 13: 277-237.

Priestley, C. H. B. and Taylor, R. J. (1972). On the assessment of surface heat flux and evaporation using large-scale parameters. *Mon. Wea. Rev.*, **100**, 81-92.

Rosenberg, N.J., Blad, B.L. and Verma, S.B., (1983). Microclimate the biological environment. John Wiley & Sons, New York, pp 495.

Ryan, P.J., Harleman, D. R. F. and Stolzenbach, K. D. (1974). Surface heat loss from cooling

ponds. *Water Resour. Res.*, **10**, 930-938.

Schulze, R. E. (1989). ACRU: Background. Concepts and Theory. WRC Report No 154/1/89.

Smith, L. P. (1985). Methods in agricultural meteorology. Directions in Atmospheric Science, 3, Elsevier, Amsterdam.

Stewart, R. B. and Rouse, W.R. (1976). A Simple method for determining the evaporation from shallow lakes and ponds. *Water Res. Res.*, **12**, 623-628.

Wiesner, C.J. (1970). Hydrometeorology. Chapman and Hall Ltd, London EC4.

Appendix 1: Sample Output Data from the Orange River Evaporation Project.

The data were output at 20 minute intervals. Sampling rate for array 116 was 1 second and array 252 10 seconds. Each data point is
therefore the mean of either 1200 (array 116) or 120 (array 252) samples. Twelve hours data are shown in the example.
Key: id=array identifier, doy=day of year, Pt=panel temperature, Tlo=temperature of lower arm, Δt= average temperature difference
between upper and lower arms, Tdlo=dew point temperature lower arm, elo=vapour pressure lower arm, TdH= dew point temperature
upper arm, eH=vapour pressure upper arm , Tmet=air temperature from met station, emet=vapour pressure from the met station, Is=
solar radiation, Rn=Net irradiance, Fs=heat flux at 0.1m, H20T=spatial average of water temperature (0-0.1m), T=change from previous soil temp., Pn=rain, Wm/s= wind speed , Wd=wind direction, T50=water temp. 0.5m below surface, T0=water temp. at the surface, HFs= heat flux at the sediment surface.

id ,doy,tod,Pt, Tlo , Δt, Tdlo , elo ,TdH , eH , Tmet,emet, Is
116,230,0,12.97,10.29,.171,4.869,.864,4.23,.825,9.97,.748,0
id ,doy,tod,Rn ,Fs1 , Fs2 , H20T, T , Pn, Wm/s,Wd, T50 , T50, T50, T0, T0, T0, T0, T0 , T0 , HFs1,HFs2, HFs3
252,230,0,-96,-.168,-.361,15.29,-.173,0,1.129,125.7,15.24,15.24,15.15,15.13,15.19,15.1,15.06,14.22,15.07,-.157,-.129,-.118
116,230,20,12.61,10.2,.182,3.856,.805,3.571,.789,9.92,.682,-.013
252,230,20,-97.6,-.53,-.706,15.36,.071,0,.878,97.7,15.3,15.28,15.24,15.2,15.23,15.14,15.17,14.29,15.12,-.125,-.122,-.115
116,230,40,12.27,9.9,.145,3.681,.795,3.218,.769,9.57,.671,0
252,230,40,-98,-.762,-.375,15.33,-.024,0,.713,110.1,15.29,15.29,15.24,15.18,15.23,15.13,15.12,14.29,15.09,-.109,-.103,-.102
116,230,100,12,10.1,.185,2.96,.755,2.338,.723,9.75,.612,0
252,230,100,-97.6,-.713,-.553,15.28,-.054,0,.73,78,15.24,15.21,15.17,15.07,15.17,15.05,15.07,14.26,14.9,-.112,-.105,-.1
116,230,120,11.73,9.74,.118,2.268,.719,1.52,.682,9.59,.573,0
252,230,120,-98.3,-.815,-.471,15.23,-.05,0,.33,83.1,15.18,15.17,15.12,15.05,15.12,15.15,15.02,14.23,14.98,-.114,-.105,-.099
116,230,140,11.55,10.28,.08,.297,.625,-.002,.612,9.83,.502,0
252,230,140,-97.1,-.567,-.497,15.19,-.036,0,.953,100.9,15.14,15.13,15.1,15.03,15.09,15.03,14.98,14.15,14.99,-.118,-.109,-.1
116,230,200,11.39,10.17,.124,.378,.629,-.573,.586,9.93,.516,0
252,230,200,-97.2,-.111,-.549,15.08,-.117,0,.918,109.6,14.96,14.99,14.94,14.93,15.01,14.86,14.93,14.11,14.85,-.132,-.121,-.104
116,230,220,11.29,10.54,.136,.173,.619,-.315,.598,10.11,.494,0
252,230,220,-95.8,-.29,-.644,15.04,-.04,0,1.078,107,14.9,14.9,14.88,14.82,14.93,14.78,14.85,14.03,14.78,-.128,-.122,-.103
116,230,240,11.19,9.53,.171,1.256,.669,.163,.619,9.76,.54,0
252,230,240,-98.1,-.639,-.599,14.97,-.066,0,.438,88.3,14.85,14.85,14.84,14.72,14.84,14.74,14.74,14.74,13.97,14.7,-.133,-.124,-.1
116,230,300,10.97,9.16,.15,1.307,.671,.71,.643,9,.528,0
252,230,300,-97.6,-.594,-.698,14.93,-.046,0,.603,97.1,14.85,14.84,14.8,14.7,14.8,14.75,14.7,13.97,14.67,-.132,-.125,-.099
116,230,320,10.76,9.22,.153,.677,.642,-.041,.609,8.91,.511,0
252,230,320,-97.5,-.616,-.541,14.85,-.072,0,.715,98.7,14.8,14.78,14.74,14.66,14.77,14.68,14.62,13.92,14.63,-.139,-.135,-.106
116,230,340,10.6,9.52,.151,.324,.626,-.307,.597,9.11,.494,0
252,230,340,-95.8,-.284,-.323,14.8,-.052,0,1.083,105.4,14.72,14.69,14.64,14.64,14.66,14.59,14.61,13.81,14.57,-.144,-.135,-.11
116,230,400,10.49,9.17,.123,-.783,.577,-1.583,.544,9.09,.467,0
252,230,400,-96.3,-.319,-.248,14.72,-.087,0,.978,101.1,14.63,14.6,14.55,14.51,14.57,14.5,14.46,13.77,14.44,-.148,-.147,-.115
116,230,420,10.34,8.57,.105,-.256,.6,-1.333,.554,8.62,.473,0
252,230,420,-96.3,-.609,-.342,14.68,-.032,0,.667,92.5,14.63,14.6,14.56,14.5,14.56,14.45,14.5,14.5,13.77,-.154,-.158,-.118
116,230,440,10.17,8.92,.102,-.01,.611,-.961,.57,8.52,.471,0
252,230,440,-95.9,-.469,-.321,14.63,-.053,0,.853,98.8,14.54,14.57,14.53,14.41,14.5,14.47,14.43,13.69,14.42,-.157,-.156,-.122
116,230,500,10.04,8.64,.151,-.929,.571,-1.769,.537,8.58,.457,0
252,230,500,-96.1,-.27,-.29,14.53,-.097,0,.926,102.8,14.45,14.42,14.41,14.35,14.37,14.24,14.35,13.63,14.3,-.166,-.16,-.123
116,230,520,9.87,8.04,.224,-.685,.581,-1.671,.541,8.01,.461,0
252,230,520,-96.5,-.593,-.419,14.46,-.072,0,1.115,94.1,14.4,14.36,14.34,14.3,14.28,14.23,14.27,13.55,14.21,-.17,-.171,-.129
116,230,540,9.67,8.16,.252,.966,.655,-.169,.603,7.68,.501,0
252,230,540,-95.6,-.226,-.371,14.36,-.101,0,1.632,118.2,14.33,14.34,14.28,14.24,14.24,14.22,14.19,13.54,14.14,-.186,-.184,-.136
116,230,600,9.54,8.47,.169,.089,.615,-.811,.576,8.22,.47,0
252,230,600,-97.2,-.553,-.565,14.27,-.087,0,.686,116.3,14.23,14.18,14.18,14.06,14.15,14.01,14.13,13.37,14.08,-.199,-.195,-.145
116,230,620,9.38,7.6,.15,.745,.645,-.075,.608,7.63,.52,0
252,230,620,-99.2,-1.003,-.32,14.26,-.017,0,.102,113.7,14.15,14.16,14.12,13.94,14.08,14.03,14.01,13.41,13.99,-.187,-.193,-.144
116,230,640,9.16,7.23,.184,1.952,.703,1.061,.66,7.1,.584,0
252,230,640,-98.3,-.491,-.327,14.2,-.054,0,.873,123.1,14.14,14.05,14.02,13.98,13.98,13.95,13.98,13.29,13.9,-.193,-.195,-.145
116,230,700,8.92,6.805,.194,2.273,.719,1.677,.689,6.627,.624,.408
252,230,700,-97.5,-.657,-.596,14.16,-.042,0,.65,120.3,14.11,14.09,14.05,13.99,14.01,13.9,13.89,13.33,13.9,-.198,-.204,-.152
116,230,720,8.7,7.09,.179,.632,.639,.573,.637,6.603,.532,10.53

Appendix 2. The diurnal course of ambient air and surface water temperature during the study period.

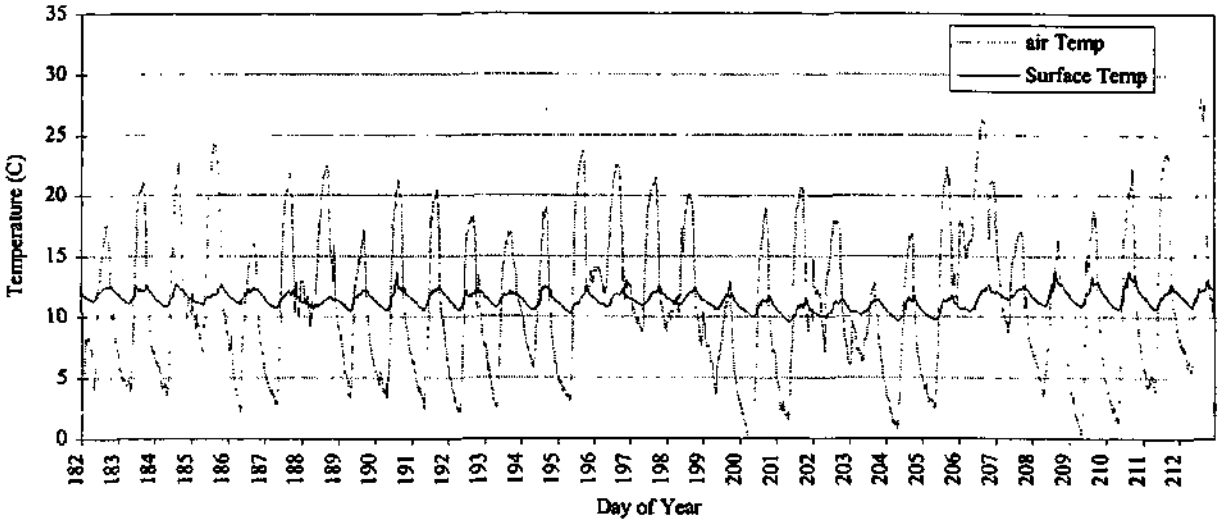

Appendix 2a. Diurnal course of ambient air and surface water temperature - July 1995

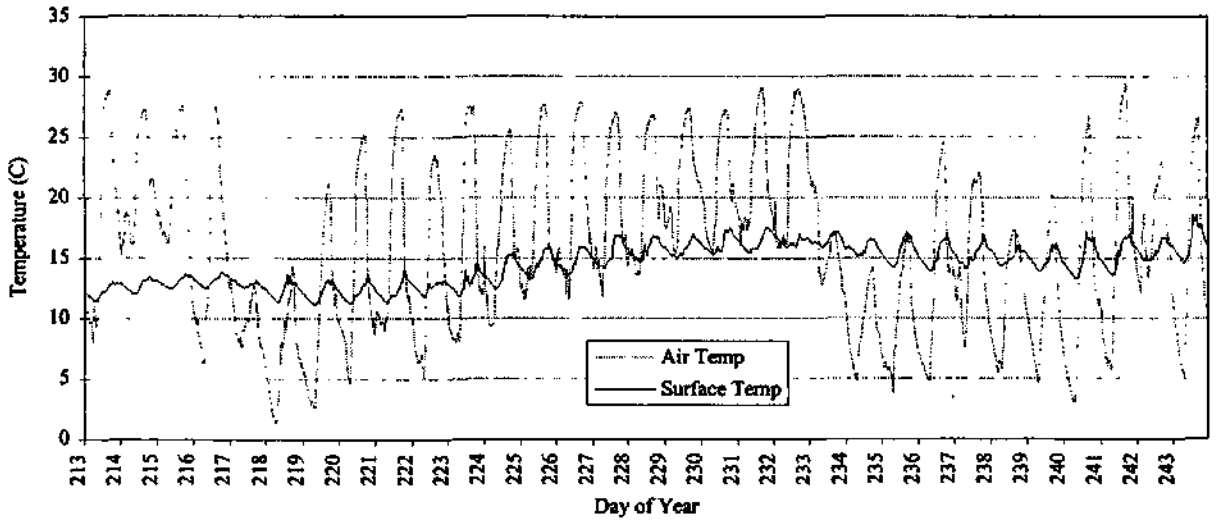

Appendix 2b. Diurnal course of ambient air and surface water temperature - August 1995

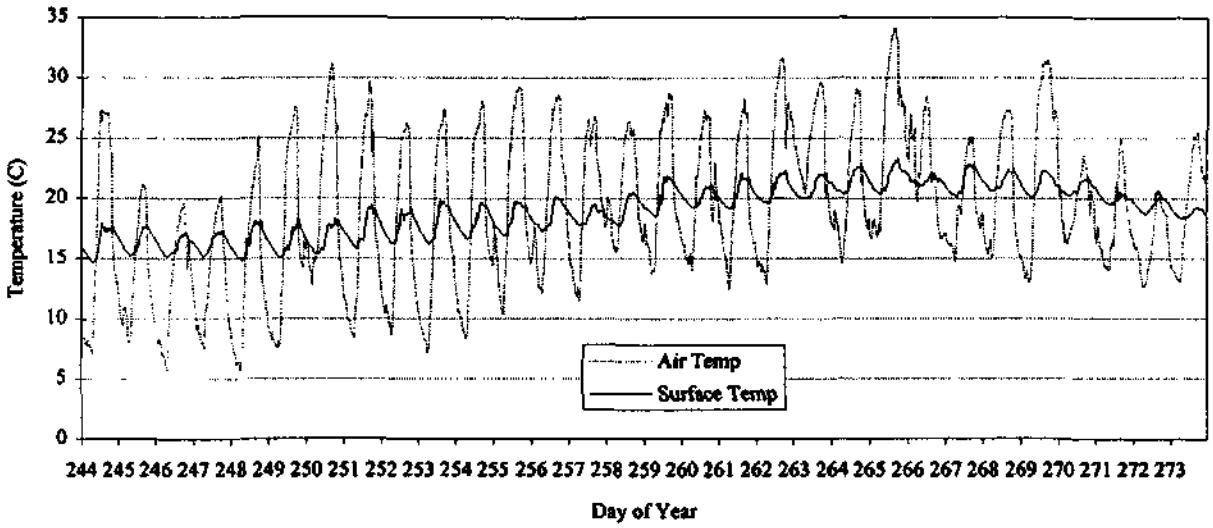

Appendix 2c. Diurnal course of ambient air and surface water temperature - September 1995

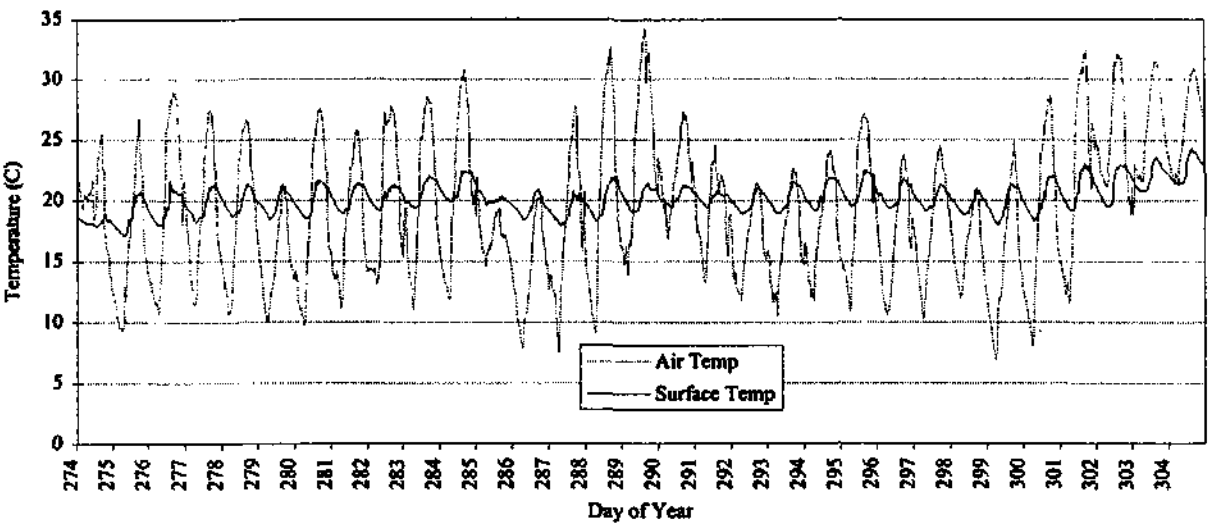

Appendix 2d. Diurnal course of ambient air and surface water temperature - October 1995

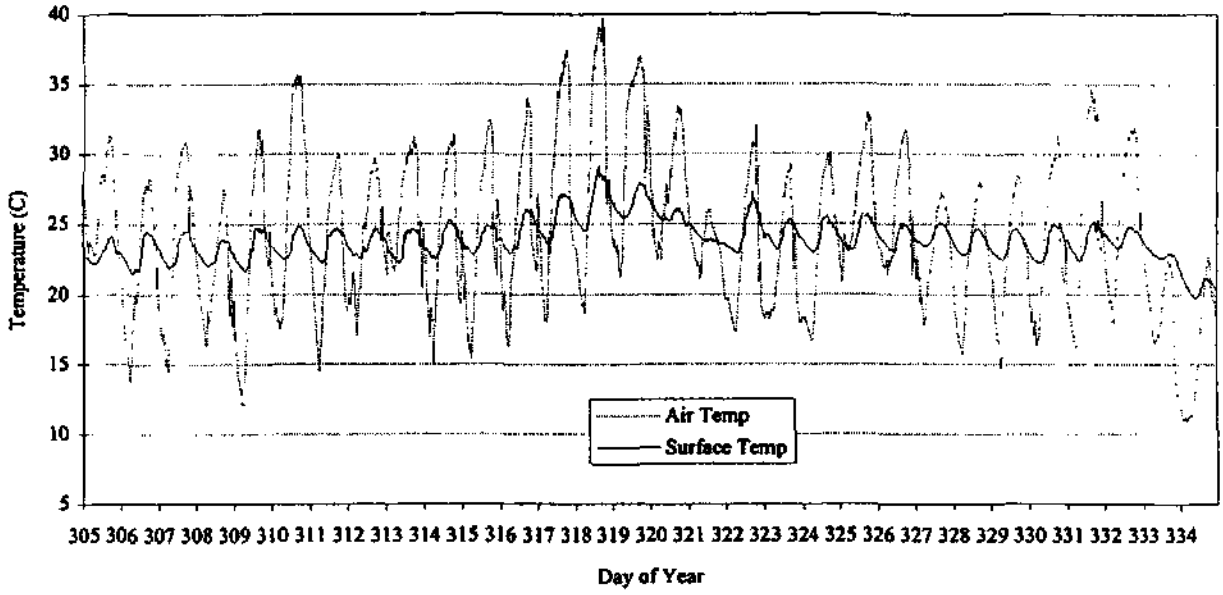

Appendix 2e. Diurnal course of ambient air and surface water temperature - November 1995

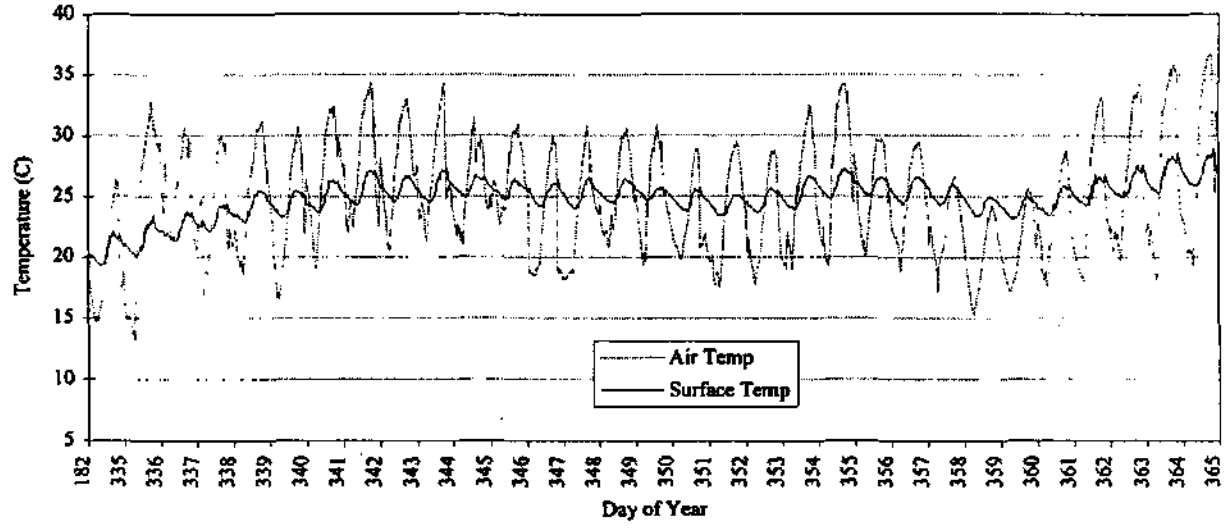

Appendix 2f. Diurnal course of ambient air and surface water temperature - December 1995

Appendix 3. The diurnal course of the energy balance during the study period.

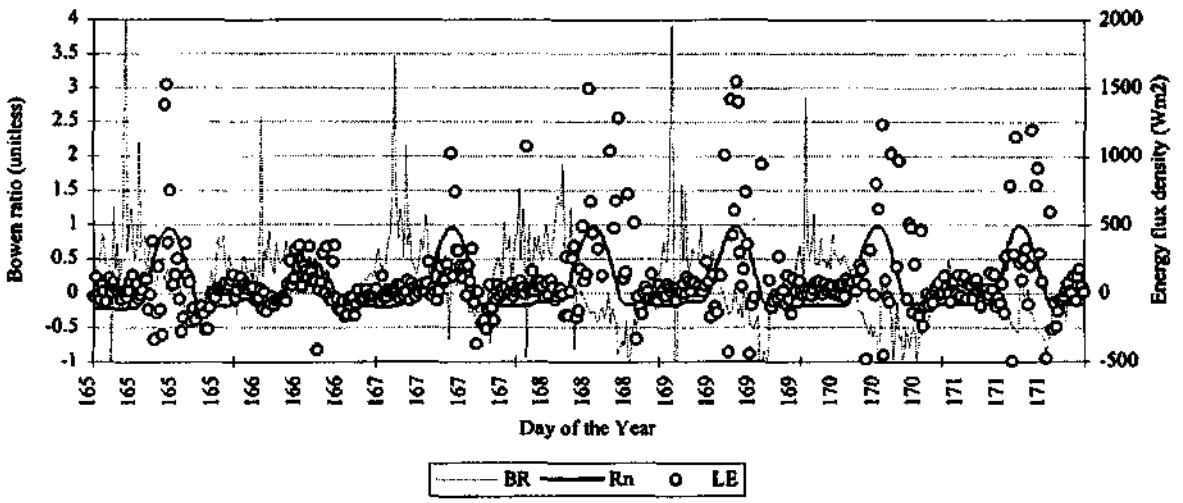

Appendix3a. Diurnal variation in the net radiation, latent heat flux density and Bowen ratio for DOY 165 -171 (June 1995).

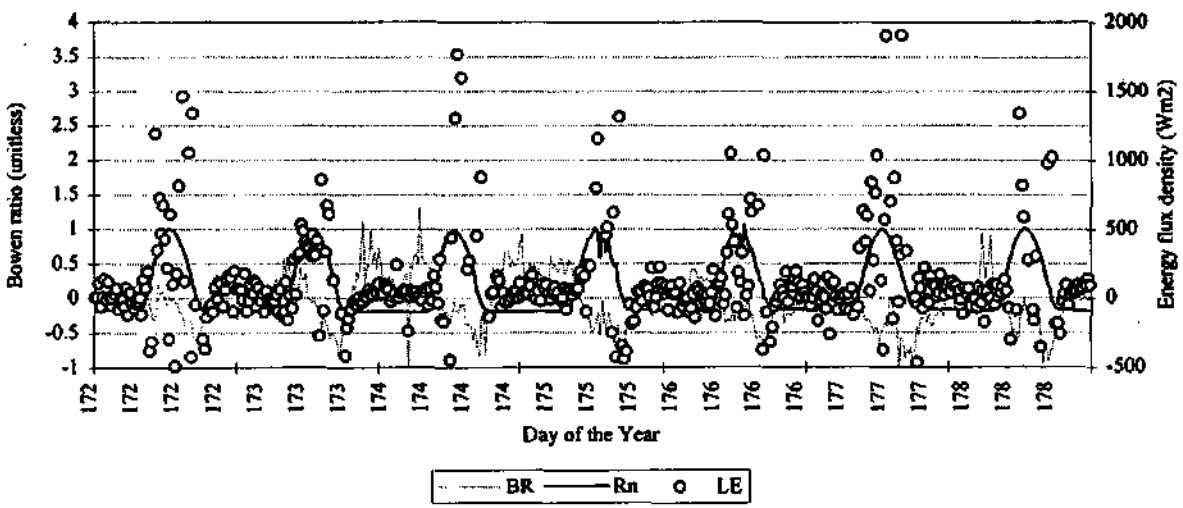

Appendix 3b. Diurnal variation in the net radiation, latent heat flux density and Bowen ratio for DOY 172 -178 (June 1995). Winter.

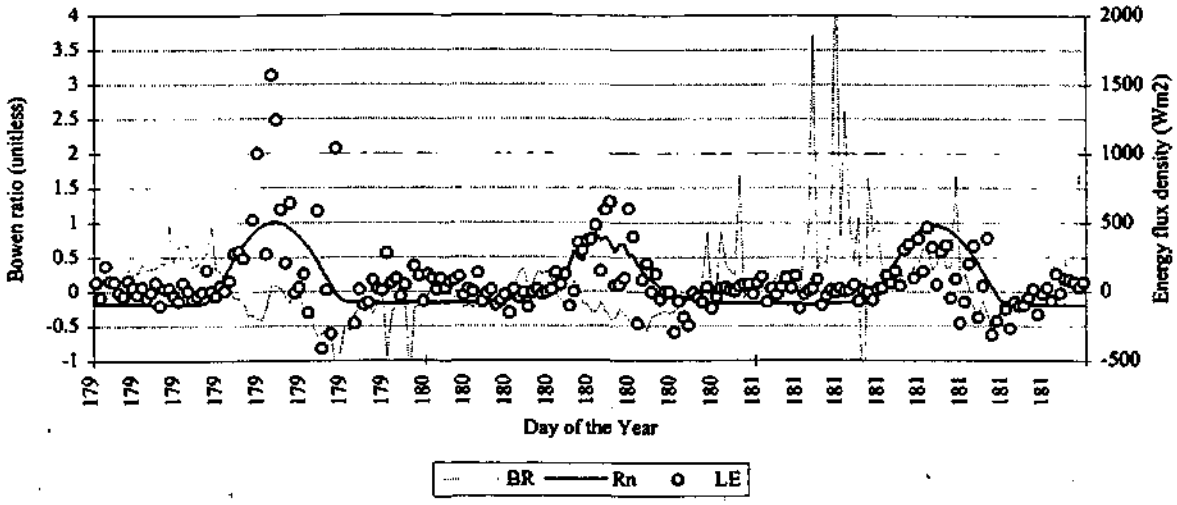

Appendix 3c. Diurnal variation in the net radiation, latent heat flux density and Bowen ratio for DOY 179 - 181 (June 1995)

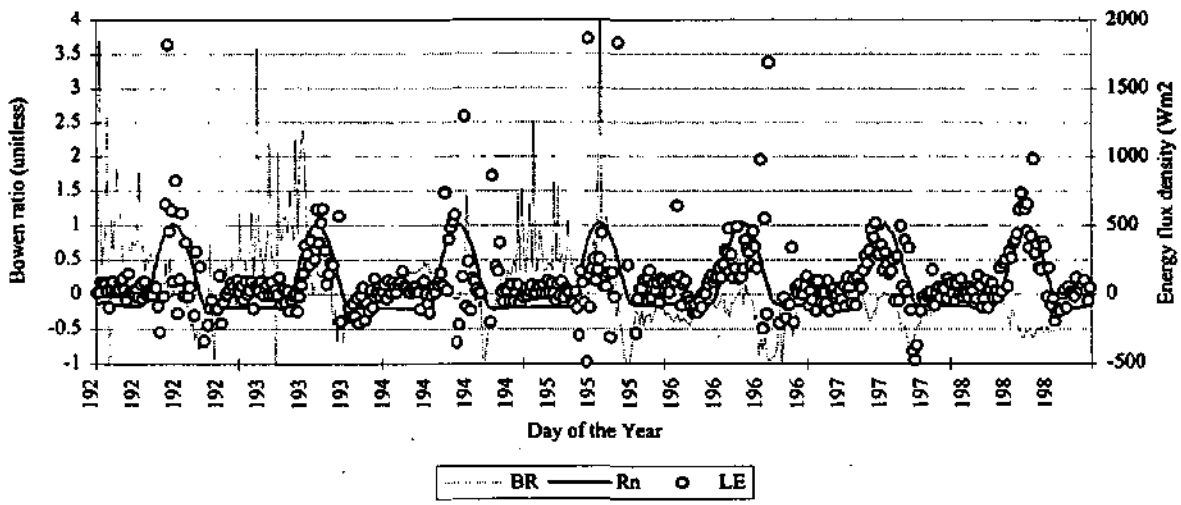

Appendix 3d. Diurnal variation in the net radiation, latent heat flux density and Bowen ratio for DOY 192 - 198 (July 1995)

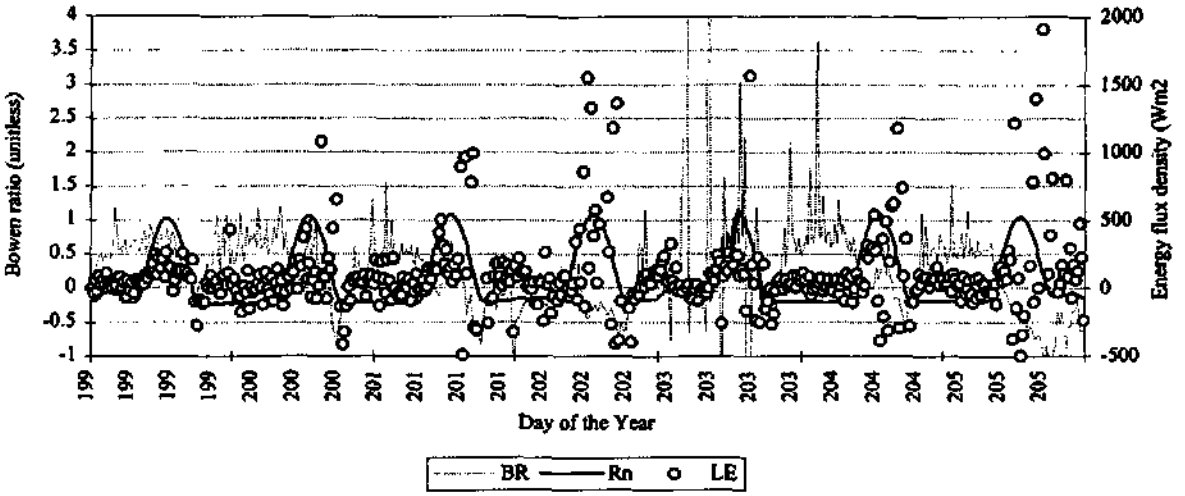

Appendix 3e. Diurnal variationin the net radiation, latent heat flux density and Bowen ratio for DOY 199 - 205 (July 1995)

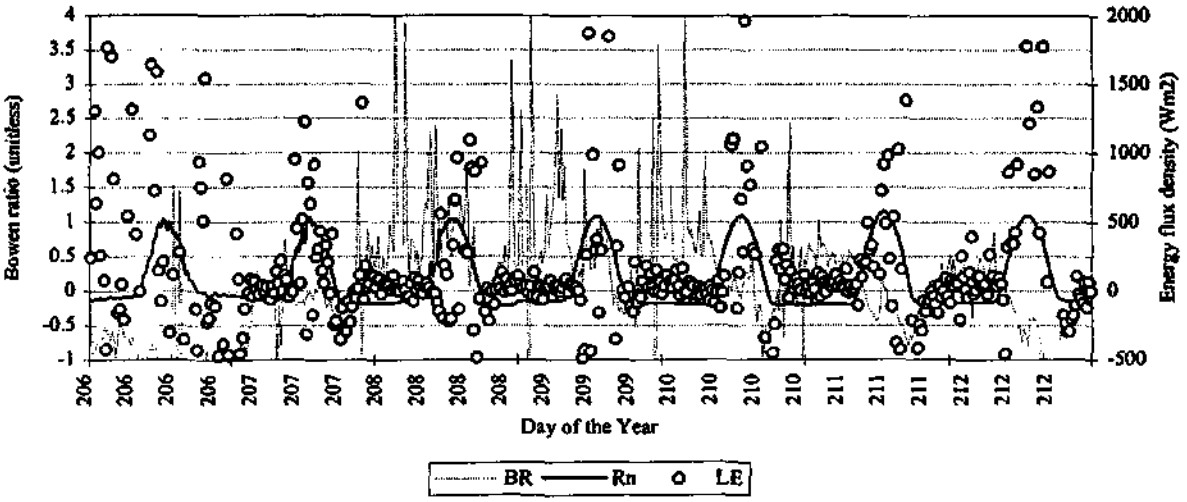

Appendix 3f. Diurnal variation in the net radiation, latent heat flux density and Bowen ratio for DOY 206 -212 (July 1995)

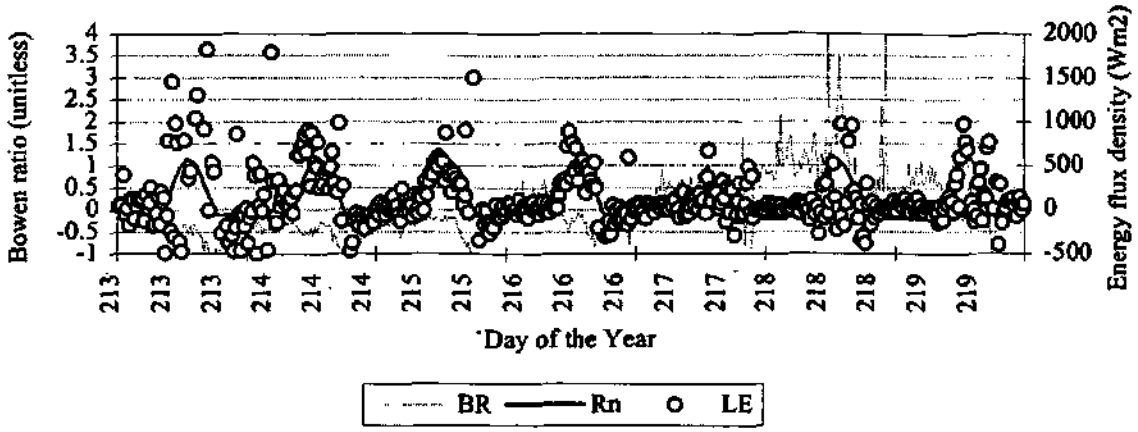

Appendix 3g. Diurnal variation in the net radiation, latent heat flux density and Bowen ratio for DOY 213 - 219 (August 1995).

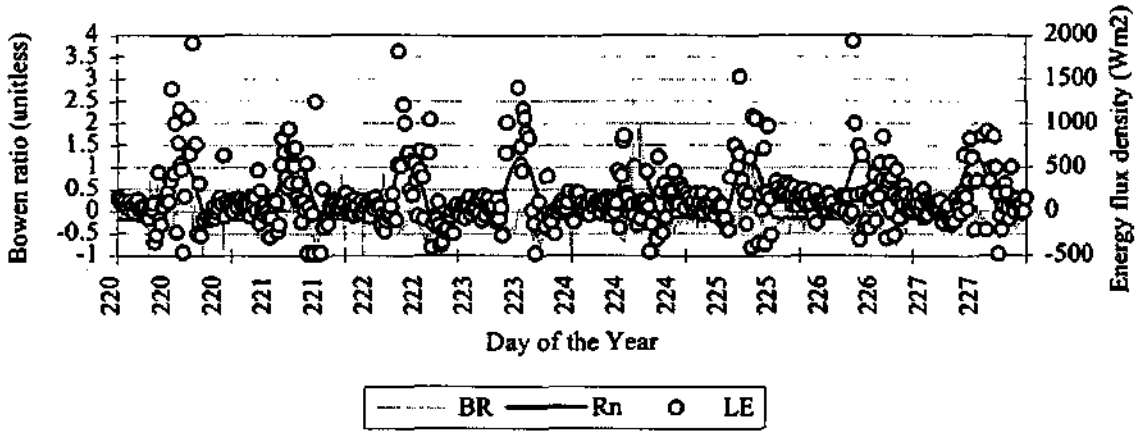

Appendix 3h. Diurnal variation in the net radiation, latent heat flux density and Bowen ratio for DOY 220 - 227 (August 1995).

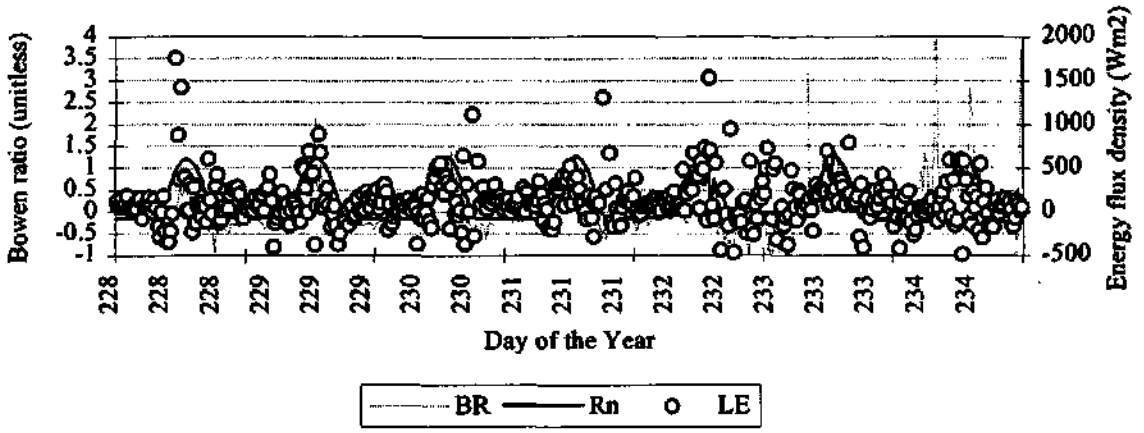

Appendix 3i. Diurnal variation in the net radiation, latent heat flux density and Bowen ratio for DOY 228 - 234 (August 1995).

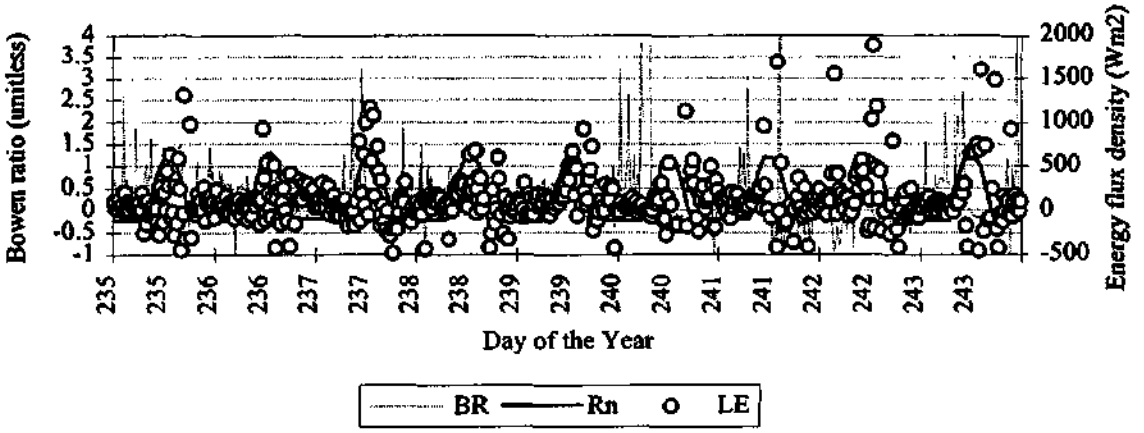

Appendix 3j. Diurnal variation in the net radiation, latent heat flux density and Bowen ratio for DOY 235 - 243 (August 1995).

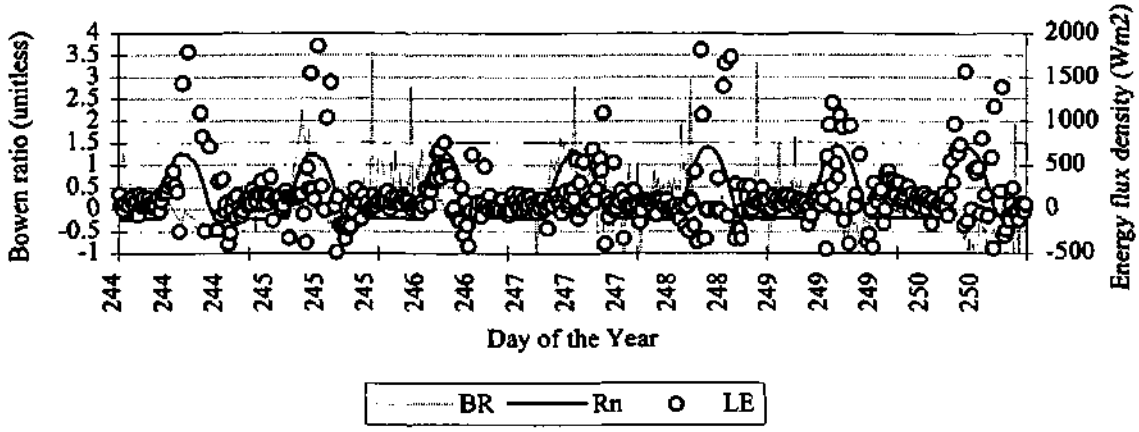

Appendix 3k. Diurnal variation in the net radiation, latent heat flux density and Bowen ratio for DOY 244 - 250 (September 1995).

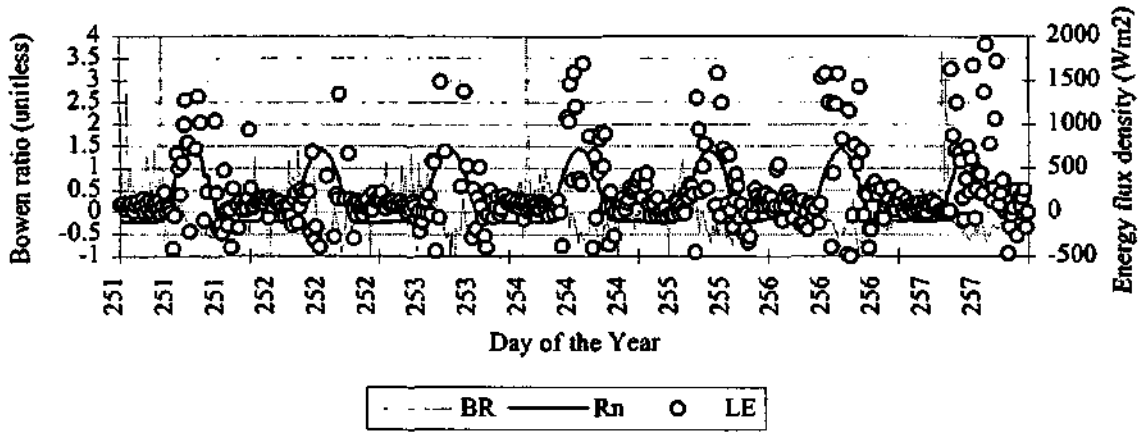

Appendix 3l. Diurnal variation in the net radiation, latent heat flux density and Bowen ratio for DOY 251 - 257 (September 1995).

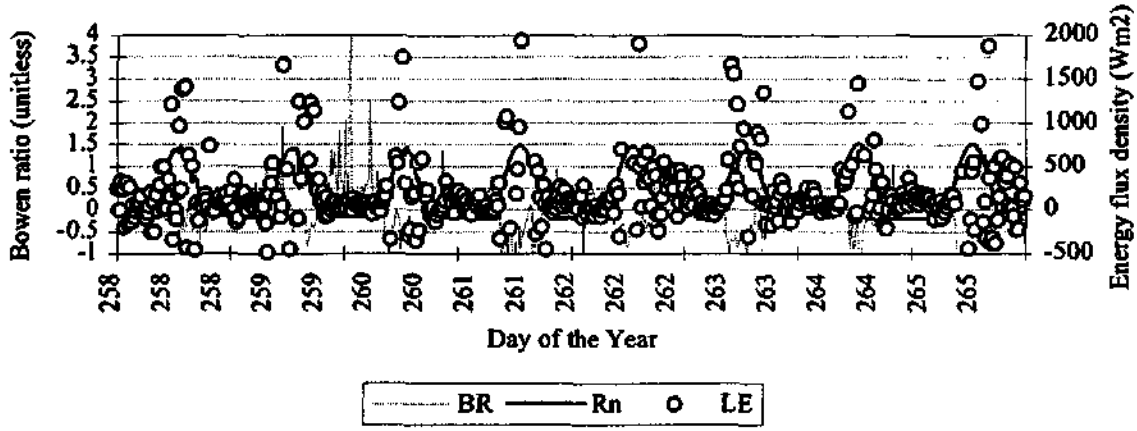

Appendix 3m. Diurnal variation in the net radiation, latent heat flux density and Bowen ratio for DOY 258 - 265 (September 1995).

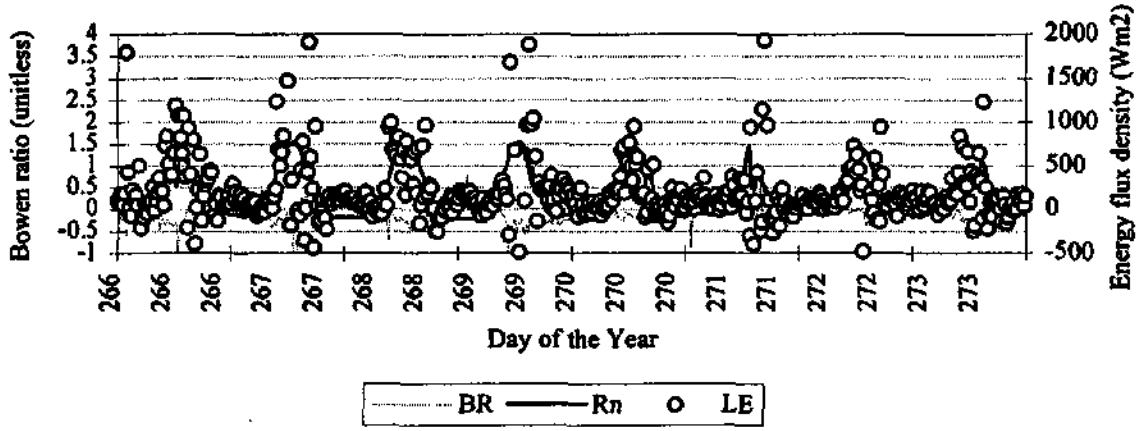

Appendix 3n . Diurnal variation in the net radiation, latent heat flux density and Bowen ratio for DOY 266 - 273 (September 1995).

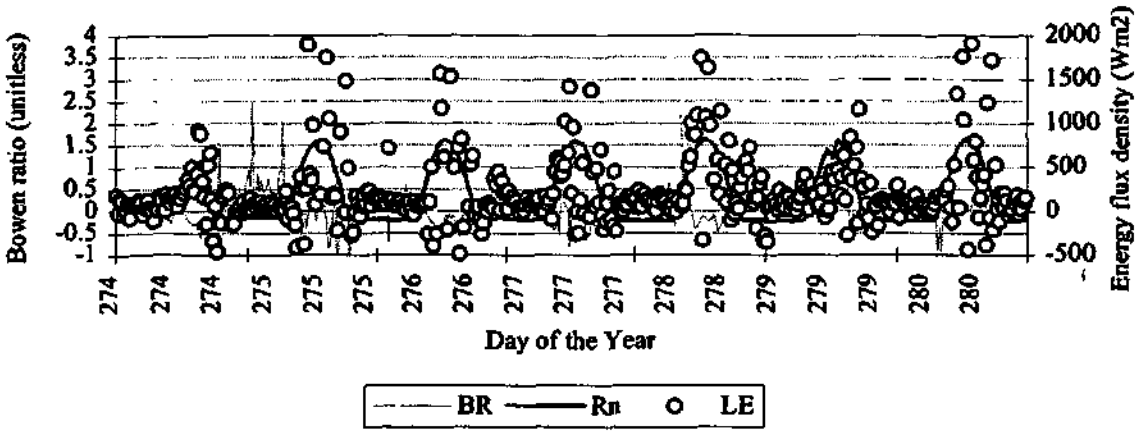

Appendix 3o. Diurnal variation in the net radiation, latent heat flux density and Bowen ratio for DOY 274 - 280 (October 1995).

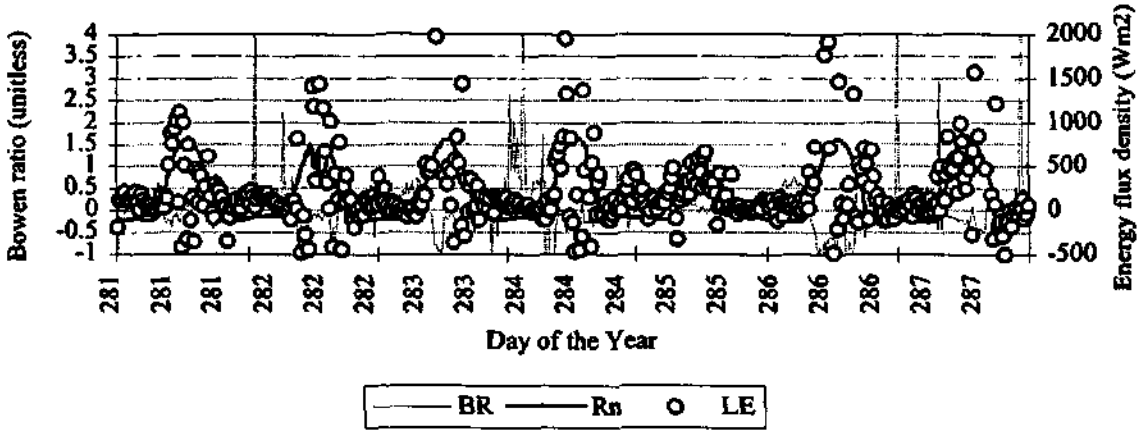

Appendix 3p. Diurnal variation in the net radiation, latent heat flux density and Bowen ratio for DOY 281 - 287 (October 1995).

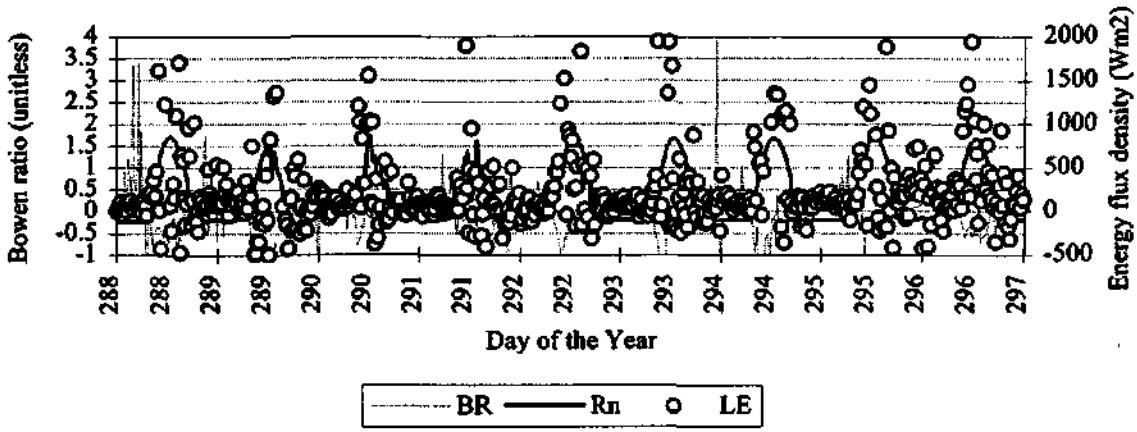

Appendix 3q. Diurnal variation in the net radiation, latent heat flux density and Bowen ratio for DOY 288 - 296 (October 1995).

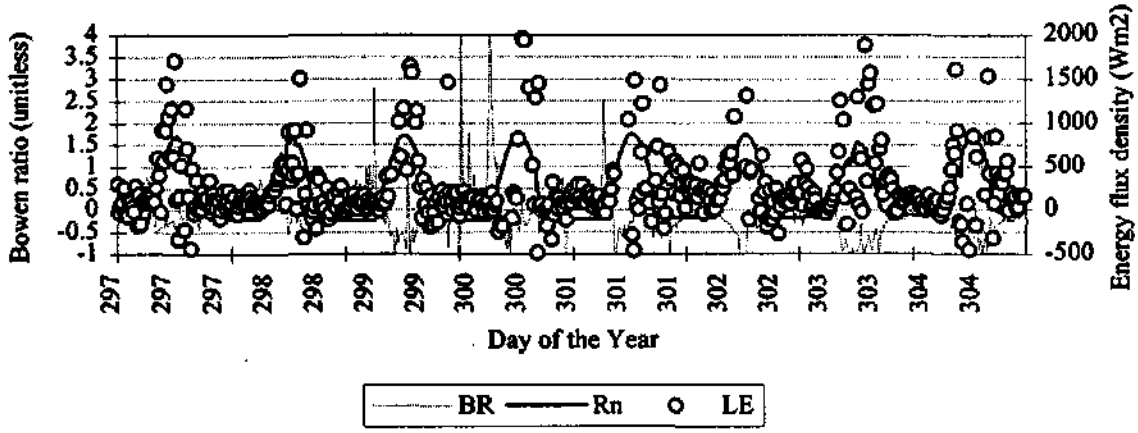

Appendix 3r. Diurnal variation in the net radiation, latent heat flux density and Bowen ratio for DOY 297 - 304 (October 1995).

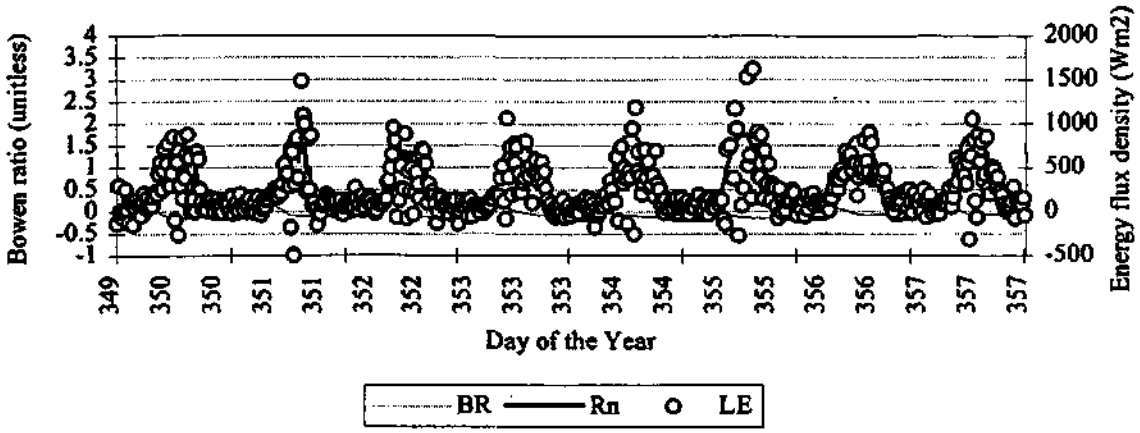

Appendix 3s. Diurnal variation in the net radiation, latent heat flux density and Bowen ratio for DOY 350 - 357 (December 1995).

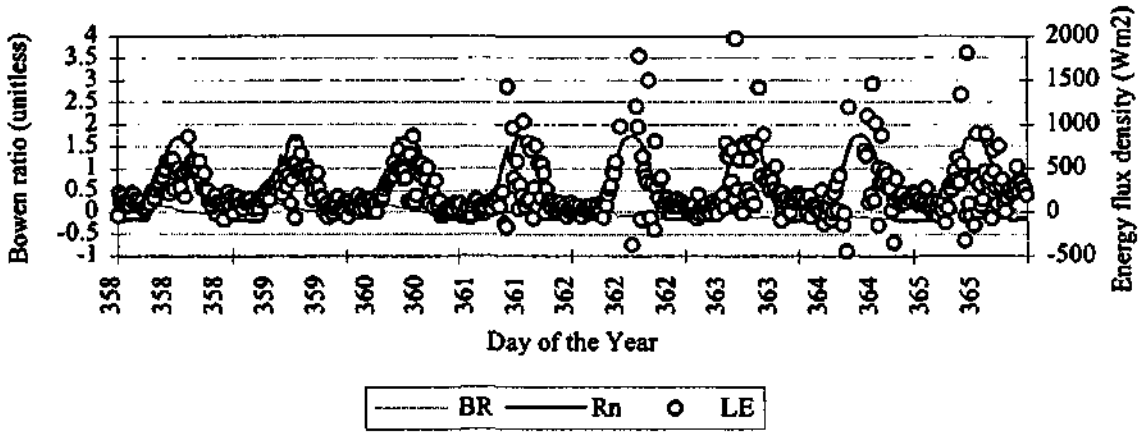

Appendix 3t. Diurnal variation in the net radiation, latent heat flux density and Bowen ratio for DOY 358 - 365 (December 1995). Summer.

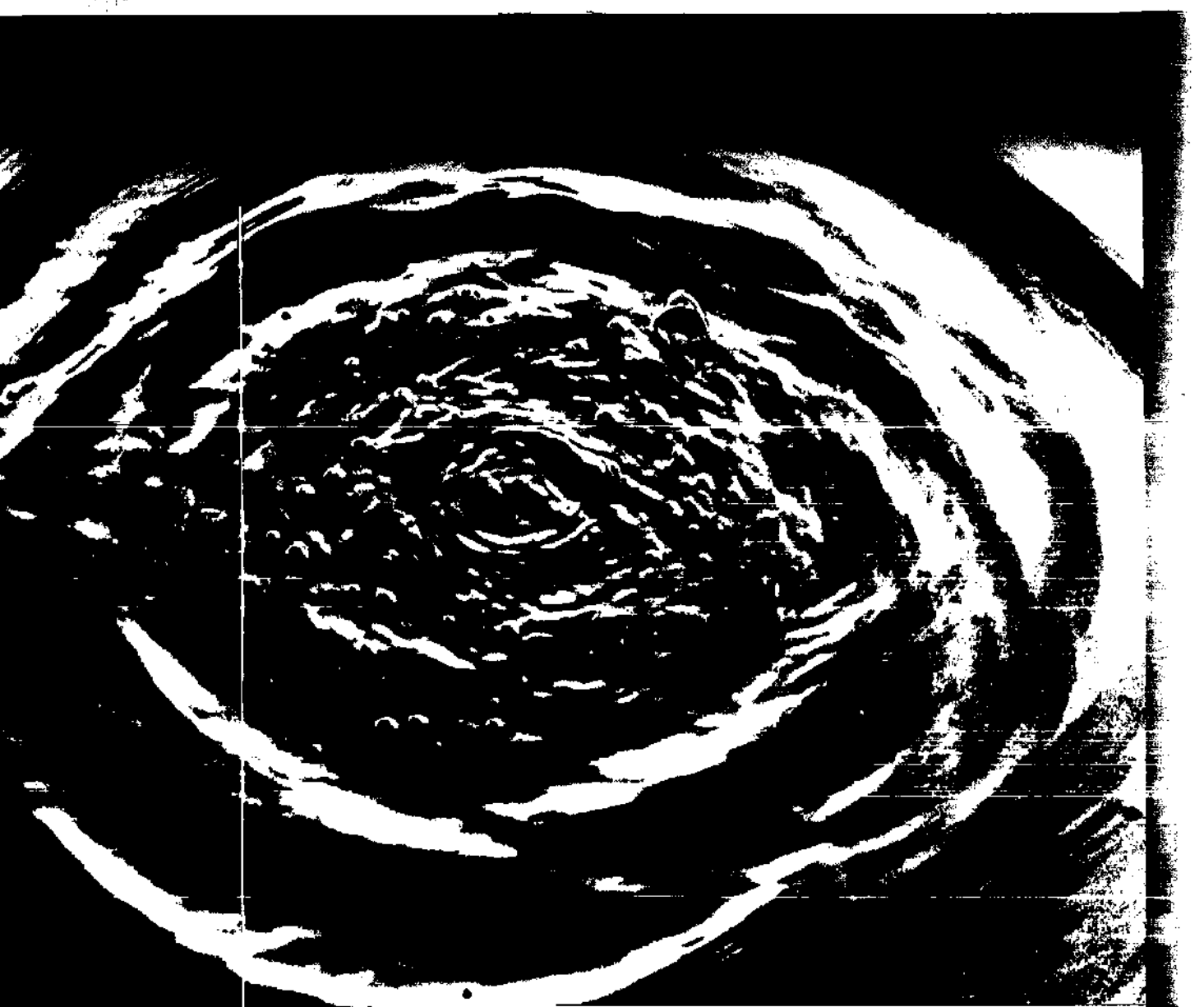

Water Research Commission
PO Box 824, Pretoria, 0001, South Africa
Tel: +27 12 330 0340, Fax: +27 12 331 2565
Web: http://www.wrc.org.za